2009:055 CIV

MASTER'S THESIS

Stress Concentration at the Door Opening of Steel Towers for Wind Turbines

Stefan Golling

Luleå University of Technology

MSc Programmes in Engineering
Civil Engineering
Department of Civil and Environmental Engineering
Division of Structural Engineering

2009:055 CIV - ISSN: 1402-1617 - ISRN: LTU-EX--09/055--SE

LULEÅ UNIVERSITY OF TECHNOLOGY

Stress concentration at the door opening of steel towers for wind turbines

Stefan Golling

Luleå University of Technology
Dept. of Civil, Mining and Environmental Engineering
Division of Structural Engineering – Steel Structures
Luleå, March 2009

Cover picture:
The MM92 wind turbine of REpower
http://www.repower.de/fileadmin/download/produkte/PP_MM92_de.pdf
Accessed: 27.01.2009

Acknowledgement

I want to thank Wylliam (Wylliam Husson, PhD-student) who was my teacher in applied FEM in my study abroad year at the Luleå University of Technology and who offered me the possibility to stay for an internship.

Thank you Milan (Milan Veljkovic, professor at Luleå University of Technology) for accepting me at the department of steel structures and guiding me through the project.

Also, I want to thank all the people who made my time in Sweden to an unforgettable period of my life.

Tack så mycket!

Abstract

This document will be public domain after 2010.01.01 when the RFCS project HISTWIN, RFSC-CT200600031, is completed, before that date the report is property of the project partners and cannot be used without priory given permission by the coordinator for its use.

Due to increasing energy prices and the growing consciousness of saving natural resources, it is necessary to find new alternatives for nowadays energy need. The electric energy generated by wind became the last years more and more popular in many countries with regions of constant wind. The increasing interest in wind energy leads to higher demands of wind turbines. Higher production rates caused by the demand make it essential to develop wind turbines in a way that cost savings in the whole production and assembly line are realised. To compete in the market it is an important factor to produce wind turbines in a competitive way. The steel tower used to support the nacelle causes around 20% of the total costs of the wind turbine.

The aim is to reach material or assembly time reductions and it could be reached with an optimisation of the tower and its details. A European research project called HISTWIN has the aim to improve the competitiveness of steel towers for wind turbines. Steel towers for multi megawatt turbines usually consist of several conical steel segments which are welded together to sections. These sections are connected by bolted flange connections. Part of the HISTWIN project is to investigate new flange connections between the tower sections. The change to the friction connection between the sections creates the possibility to allow higher stresses in the tower shell. Allowing higher stresses in the tower shell leads to lower safety factors while using the state of the art steel. As an alternative of reducing safety factors a change to steel with higher yield strength is possible. A change of the material to a higher quality class could lead to thinner tower shell thicknesses and with this to reduced self weight of the tower. The reduction of the self weight of the tower leads to lower material, fabrication, welding and transportation costs. These factors have an important influence on the total costs of a wind turbine. A reduction of the material thickness of the tower shell influences the stability of the tower and causes needs to review the stability of the structure.

This report investigates the lower tower section which includes the door opening which is used for service and maintenance inside the tower. The loading of the tower generates a stress distribution around the door opening, and these stresses were analysed using the FEM software Abaqus 6.7-1. To investigate the influence on the stress level and the ultimate load of the tower, the tower shell thickness and the thickness of the stiffener around the door opening varied in the simulation. Another criterion of thin walled structures is the resistance against buckling. The tower structure in all variations was also investigated concerning the possibility of buckling. The risk of buckling in a structure varies with its imperfection and therefore was the simulation performed with varied imperfection values.

The state of the art tower uses steel S355 with yield strength of 355MPa but a change of the material to steel with higher strength is desired. The steel chosen for furthermore simulations is S690 with yield strength of 690MPa. The influence of this high strength steel as material compared with reduced shell thickness of the tower was investigated in further simulations.

Concerning Eurocode 3, an analytical calculation of the buckling resistance of thin walled shells is provided. The results of the analytical calculation were compared to the results of the numerical analysis. To do this, the structure was simplified.

Notations

Capital Italic letters

A	Area
C_x, C_τ	Coefficient in buckling strength assessment, x and τ indicates the orientation in the coordinate system
E	Youngs modulus
L	Length
P_n, P_x	Force, n and x indicates the orientation in the coordinate system
P_{ref} –	Reference load, load entered by the user
P_{total}	Load applied into the simulation model
P_0 –	Dead load, load applied in a previous calculation step
Q	Fabrication quality parameter
U_{n}	Initial dimple imperfection amplitude parameter for numerical calculations

Minor Italic letters

k_x, k_τ	Parameter in interaction expressions for buckling under multiple stress components, x and τ indicates the orientation in the coordinate system
r	Radius
t	Material thickness
f_{yk}	Yield strength

Minor Greek letters

α_x	Elastic imperfection reduction factor in buckling strength assessment
β	Plastic range factor in buckling interaction
γ_{M1}	Partial factor
δ	Imperfection amplitude introduced in FE models
ε	Strain
λ	Relative slenderness of shell in analytical calculation or load proportionality factor in a simulation
λ_{p}	Plastic limit relative slenderness (value of λ below which plasticity affects the stability)
λ_0	Squash limit relative slenderness (value of λ above which resistance reductions due to instability or change of geometry occur)
η	Interaction exponent for buckling
σ_x	Result of the buckling strength verification
σ_x	Compression stress, x direction
$\sigma_{x\text{Ed}}$	Stress value arising from design action, x direction
$\sigma_{x\text{Rcr}}$	Critical buckling stress resistance, x direction
$\sigma_{x\text{Rd}}$	Design resistance stress, x direction
χ_x, χ_τ	Buckling resistance reduction factor for elastic-plastic effects in buckling strength, x and τ indicates the orientation in the coordinate system
ω	Relative length parameter for a shell

Capital Greek letters

Δw	tolerance normal to the shell surface

Table of content

1 INTRODUCTION 1

1.1 Background 1

1.2 Aims and scope 2

1.3 Structure of the thesis 2

2 GENERAL PROPERTIES OF THE MODELS 3

2.1 Material 3
2.1.1 Material model for the steel S355 3
2.1.2 Material model of the high strength steel S690 4

2.2 The geometric properties of the lower tower section 5
2.2.1 The geometry of the lower tower section 5
2.2.2 The introduction of imperfection into the model geometry 7

2.3 The mesh of the sections 8

2.4 Constrains used in the model 9
2.4.1 The coupling constrain between reference point and surface 9
2.4.2 The tie constraint between door frame and lower tower section 9

2.5 The boundary condition 11

2.6 The coordinate system 11

2.7 The colour code used for the result analysis 11

2.8 The loading of the model 12

2.9 The Step module in Abaqus 14
2.9.1 The static, Riks procedure 14
2.9.2 The buckling procedure 15

2.10 The data extraction 17

2.11 Model naming convention 18

3 NONLINEAR ANALYSIS OF THE LOWER TOWER SECTION 19

3.1 Parametric study of different shell or stiffener thicknesses 19
3.1.1 Influence of varied shell or stiffener thickness on the ultimate load 19
3.1.2 Stress around the door opening depending on shell or stiffener thickness 22
3.1.3 Stress around the door opening for fatigue load 25
3.1.4 Deformation of the door opening 26

3.2 Investigation of non linear effects at the lower tower section 29
3.2.1 The buckling phenomena and properties of the model used for the buckling analysis 29
3.2.1.1 Snap-through buckling: 30
3.2.1.2 Bifurcation buckling: 31
3.2.1.3 Imperfection values introduced to the model 33
3.2.2 Results of the buckling analysis with varied imperfection 35
3.2.2.1 Ultimate load of the buckling analysis with varied imperfection 35

3.2.2.2 Stress distribution around the door opening in the buckling analysis with varied imperfection 37
3.2.3 Buckling analysis of the model with varied stiffener thickness 39
3.2.4 Analysis of models with material changed to high strength steel and varied imperfections 42
3.2.4.1 Comparison of the models with an imperfection amplitude of 20% respective the shell thickness and material S355 and S690 43
3.2.4.2 Comparison of the models with varied imperfection amplitude and material S690 46
3.2.4.3 Comparison between the state-of-the-art-tower segment and the segment with high strength steel and higher imperfection value 49

3.3 Comparison of a simplified tower model with an analytical calculation 51
3.3.1 The simplified FE model 51
3.3.2 The analytical calculation 52
3.3.3 Comparison between perfect structure with and without door opening 53
3.3.4 Comparison of the simplified FE model with added imperfection and steel S355 to the analytical calculation 55
3.3.5 Comparison of the simplified model with added imperfection and steel S690 to the analytical calculation 59

4 SUMMARY 62

4.1 Future work 63

REFERENCES 64

APPENDIX A - DESIGN EXAMPLE FOR A CYLINDRICAL SHELL UNDER AXIAL COMPRESSION 65

APPENDIX B – PROCEDURE FOR THE DESIGN CHECK OF CYLINDRICAL SHELLS SUBJECTED TO AXIAL COMPRESSION 69

APPENDIX D – RESULT OF THE LOAD CASE SIMULATION 71

APPENDIX E – CONTOUR PLOTS OF THE PARAMETRIC STUDY 72

APPENDIX F – CONTOUR PLOTS OF THE STRESS DISTRIBUTION AROUND THE DOOR IN MODEL 1 76

APPENDIX G – CONTOUR PLOTS OF THE BUCKLING ANALYSIS 78

APPENDIX H – CONTOUR PLOTS OF MODELS 7, 15, 16 81

APPENDIX I – CONTOUR PLOTS OF THE MODELS USING S690 AND HIGH IMPERFECTION VALUES 84

APPENDIX J – SIMULATION MODELS USED FOR THE REPORT, PROPERTIES AND ODB FILE NAMES 86

APPENDIX K – TUTORIAL FOR ABAQUS 6.7, MODELLING OF A STRUCTURE IN SHELL ELEMENTS 88

List of Figures

Figure 1.1: Door opening at the bottom of a steel tower for a wind turbine [4]..... 1
Figure 2.1: Schematic material model of steel S355 3
Figure 2.2: Schematic material model of the high strength steel S690..... 4
Figure 2.3: Sketch of the door geometry 6
Figure 2.4: Assembled lower tower section showing the different sections and the stiffener used in the door opening 6
Figure 2.5: Lower tower section with mesh..... 8
Figure 2.6: Position tolerance of a tie constrain..... 10
Figure 2.7: Tie and coupling constrain in the model 10
Figure 2.8: Coordinate system defined by Germanischer Lloyd on the left and Abaqus coordinate system on the right [1]..... 11
Figure 2.9: Colour code for stress used in the contour plots..... 11
Figure 2.10: Orientation of the moment M_r and the forces in the x-z-plane 13
Figure 2.11: Load displacement graph for an unstable loading response 15
Figure 2.12: Start position and direction of the path used for the data extraction..... 17
Figure 2.13: Position of node 2 in the model 18
Figure 3.1: Load-displacement response depending on shell or stiffener thickness variation at node 2 20
Figure 3.2: Model 1, 99,5 % Load..... 21
Figure 3.3: Model 1, 188 % Load..... 21
Figure 3.4: Model 1, 199,9 % Load..... 21
Figure 3.5: Model 1, 209,6 % Load..... 21
Figure 3.6: Model 1, 217,3 % Load..... 21
Figure 3.7: Model 1, 223,1 % Load..... 21
Figure 3.8: Model 1, 227,2 % Load..... 21
Figure 3.9: Model 1, 229,9 % Load..... 21
Figure 3.10: Stress distribution around the door opening depending on the shell thickness at design load 22
Figure 3.11: Stress distribution around the door opening depending on the stiffener thickness at design load 23
Figure 3.12: Model 1, Stress distribution at 99,5 % Load 24
Figure 3.13: Model 1, Stress distribution at 188,0 % Load 24
Figure 3.14: Model 1, Stress distribution at 199,9 % Load 24
Figure 3.15: Model 1, Stress distribution at 209,6 % Load 24
Figure 3.16: Stress distribution around the door opening with varied stiffener thickness and damage equivalent load..... 25
Figure 3.17: Edges used for the data extraction at tower shell and the stiffener 26
Figure 3.18: Deformation of the door in radial direction at design load..... 26
Figure 3.19: Rotational deformation of the door opening at design load 27
Figure 3.20: Deformation of the door opening in longitudinal direction at design load 27
Figure 3.21: Example for a snap-through buckling case [3]..... 30
Figure 3.22: Load displacement response for snap-through buckling [3] 31
Figure 3.23: Column under axial compression [3] 32
Figure 3.24: Bifurcation buckling on a column [3]..... 32
Figure 3.25: First Eigenmode shape of the lower tower section 33
Figure 3.26: Load displacement response at node 2 depending on the imperfection value..... 35
Figure 3.27: Influence of the imperfection amplitude on the ultimate load..... 36

Figure 3.28: Stress distribution around the door opening at design load for models with varied imperfection amplitude 37
Figure 3.29: Model 11, 98,6 % load 38
Figure 3.30: Model 11, 179,6 % load 38
Figure 3.31: Model 11, 193,2 % load 38
Figure 3.32: Model 11, 203,9 % load 38
Figure 3.33: Model 11, 212,3 % load 38
Figure 3.34: Model 11, 218,4 % load 38
Figure 3.35: Load displacement response of node 2 at models with varied stiffener thickness and 20% imperfection regarding the shell thickness 39
Figure 3.36: Stress distribution around the door opening of the tower shell of models with varied imperfection amplitude at design load 40
Figure 3.37: Stress distribution around the stiffener on the inside of the tower of models with varied imperfection at design load 41
Figure 3.38: Normalised stress distribution around the door opening of models with varied shell thickness and proportional imperfection amplitudes at design load 43
Figure 3.39: Load displacement response of the models with an imperfection value of 20% respective the shell thickness and varied shell thickness 44
Figure 3.40: Model 7 at ultimate load 45
Figure 3.41: Model 7 at 197% load in the descending path 45
Figure 3.42: Model 15 at ultimate load 45
Figure 3.43: Model 15 at 175% load in the descending path 45
Figure 3.44: Model 16 at ultimate load 45
Figure 3.45: Model 16 at 103% load in the descending path 45
Figure 3.46: Load displacement response of the original tower and the tower with high strength steel using the original geometry and higher imperfections 46
Figure 3.47: Normalised stress distribution around the door opening of the original tower and the tower with high strength steel using the original geometry at design load with higher imperfections 47
Figure 3.48: Model 14 at ultimate load 48
Figure 3.49: Model 14 in the descending path 48
Figure 3.50: Model 17 at ultimate load 48
Figure 3.51: Model 17 in the descending path 48
Figure 3.52: Comparison between the load displacement response of the model using high strength steel S690 and reduced shell and stiffener thickness to the state of the art tower at higher imperfection values 49
Figure 3.53: Stress distribution around the door opening at design load of the model using high strength steel S690 and reduced shell and stiffener thickness and the state of the art tower at higher imperfection values 50
Figure 3.54: Simplified simulation model without door opening used to compare analytical results to a FE model 51
Figure 3.55: Simplified simulation model with door opening 52
Figure 3.56: Load displacement response of the simplified FE models with and without door opening and the marked point when first yield occurred 53
Figure 3.57: Model 19-0, P = 95 MN 54
Figure 3.58: Model 19-0, P = 144 MN (first yield) 54
Figure 3.59: Model 19,-0 P = 145 MN (ultimate load) 54
Figure 3.60: Model 19-0, P = 125 MN (descending path) 54
Figure 3.61: Model 28-0, P = 26 MN 54
Figure 3.62: Model 28-0, P = 60 MN (first yield) 54
Figure 3.63: Model 28-0, P = 106 MN (ultimate load) 54

Figure 3.64: Model 28-0, P = 63 MN (descending path) 54
Figure 3.65: Load displacement response of three simplified FE models with different imperfections and the design resistance from the analytical calculation 55
Figure 3.66: Ultimate load depending on the imperfection amplitude introduced in the models using steel S355 compared to the design resistance from the analytical calculation 56
Figure 3.67: Load where the first yield occurred depending on the imperfection amplitude for steel S355 compared to the design resistance from the analytical calculation 57
Figure 3.68: Model 23-10, P=61MN 58
Figure 3.69: Model 23-10, P=90MN (first yield) 58
Figure 3.70: Model 23-10, P=103MN (ultimate load) 58
Figure 3.71: Model 23-10, P=83MN (descending path) 58
Figure 3.72: Ultimate load depending on the imperfection amplitude introduced in the model for steel S690 compared to the design resistance from the analytical calculation 59
Figure 3.73: Load when the first yield occurred depending on the imperfection amplitude for steel S690 compared to the design resistance from the analytical calculation 60
Figure 3.74: Load displacement response of the simplified FE model using steel S690 depending on the imperfection amplitude and compared to the design resistance from the analytical calculation 61
Figure 4.1: Model 7 at ultimate load 81
Figure 4.2: Model 7 at 197% load in the descending path 81
Figure 4.3: Model 15 at ultimate load 82
Figure 4.4: Model 15 at 175% load in the descending path 82
Figure 4.5: Model 16 at ultimate load 83
Figure 4.6: Model 16 at 103% load in the descending path 83
Figure 4.7: Model 14 at ultimate load 84
Figure 4.8: Model 14 in the descending path 84
Figure 4.9: Model 17 at ultimate load 85
Figure 4.10: Model 17 in the descending path 85

List of Tables

Table 2.1: General material properties of S355 3
Table 2.2: Plasticity model used in the simulations for S355 3
Table 2.3: General material properties of the high strength steel S690 4
Table 2.4: Plasticity model used in the simulations for the high strength steel 4
Table 2.5: Geometric properties of the sections used in the simulations 5
Table 2.6: Design load applied in the model [2] 13
Table 2.7: Damage equivalent load applied in the model [3] 13
Table 3.1: Geometric variations in the models for the parametric study 19
Table 3.2: Maximum difference of the deformation values in the simulation 28
Table 3.3: Maximum difference between the stiffener edge inside and outside of the tower for model 1 28
Table 3.4: Dimple imperfection amplitude parameter U_n and amplitude of the geometric imperfection Δw depending on the fabrication quality class [3] 33
Table 3.5: Properties of the simulation models used for the investigation of the tower behaviour with steel S355 and varied imperfection amplitude 34
Table 3.6: Properties of the simulation models used for the investigation of the tower behaviour with steel S690 42
Table 3.7: Ultimate load and load at first yield of the simplified FE models with and without door opening 53
Table 3.8: Imperfection values and their value in percent of the shell thickness used in the simulation with steel S355 55
Table 3.9: Imperfection values and their value in percent of the shell thickness used in the simulation with high strength steel S690 59

1 Introduction

1.1 Background

Due to increasing energy prices and the growing consciousness of saving natural resources it is necessary to find new alternatives for nowadays energy need. The electric energy generated by wind became the last years more and more popular in many countries with regions of constant wind. To compete in the market it is an important factor to produce wind turbines in a competitive way.

Steel towers for multi megawatt turbines consist usually of several conical steel segments which are welded together to sections. These sections are connected by bolted flange connections.

A European research project called HISTWIN has the aim to improve the competitiveness of steel towers for wind turbines.

This report describes stress concentrations at the door opening on the bottom of steel towers for wind turbines. The influence of material thickness and the type of the steel was investigated. The commercially available FEM software Abaqus 6.7-1 was used to determine the stresses around the door opening. Abaqus provides the possibility to analyse linear and nonlinear problems which are of interest in this report. The user interface called Abaqus/CAE offers the alternative to import CAD data, create simulation models and analyse them on a graphic surface and also the possibility to add model information through keywords.

Figure 1.1: Door opening at the bottom of a steel tower for a wind turbine [4]

1.2 Aims and scope

The main objective of this report is to investigate the stresses around the door opening for the load case that creates the highest stresses. The influence of different material thicknesses at the tower shell and at the stiffener used around the door opening is determined.

The project name HISTWIN stands for “High Strength Steel Tower for Wind Turbine” and one topic is to analyse the possibility to use high strength steel for the tower construction. The state of the art tower uses steel with yield strength of 355MPa (S355) but an evaluation of the use of steel with yield strength of 690MPa (S690) is performed too.

A comparison between numerical and analytical results of a simplified structure is included into the report.

1.3 Structure of the thesis

Chapter 2 – General properties of the models

This chapter gives an overview of the geometric and material properties for the simulation model. Furthermore the chapter describes properties regarding the design of the model in Abaqus. The boundary conditions and the loading of the model are also included into this chapter.

Chapter 3 – Nonlinear analysis of the lower tower section

Here is the analysis of the model described. The first part includes a parametric study of the lower tower section to achieve possible material reduction on the state of the art tower. The fatigue stresses around the door opening were also obtained. The following part deals with the buckling phenomena. The influence of different imperfection amplitudes is investigated. A buckling analysis of different stiffener thicknesses is included. The influence of a change of the material to a high strength steel was investigated as part of the buckling analysis. The third part of the chapter compares an analytical calculation given by Eurocode 3 to a simplified numerical model. The numerical model as the analytical calculation uses the materials S355 and S690 to show the influence of the material in a simplified case.

Chapter 4 – Summary

This chapter summarises the investigation of the lower tower section and gives proposals for future work.

2 General properties of the models

The model represents the lower section of the wind turbine tower; this means that just the first seven meters of the tower were modelled. This procedure is connected to the “Background document, design approximation of wind loads”, it suggests that only parts of interest of the tower were modelled. The detail of interest should be around three to four meters away from the section were the force and moment is applied into the model. The top of the door opening is on a height of 3,65m and the next section available in the design load tables is the section in a height of 6,99m. This results in a distance between the top of the door and the top section of 3,34m. This is in the, by the background document, suggested range and therefore applicable.

2.1 Material

2.1.1 Material model for the steel S355

As material properties were standard steel values chosen, see Table 2.1.

Table 2.1: General material properties of S355

E-modulus	210 GPa
Poisson’s ratio	0,3
Yield stress	360 MPa
Density	7850 kg/m³

To introduce the hardening and the plasticity into the model, it was extended with further material properties. The values used are shown in Table 2.2 and in Figure 2.1 is the graph of the material behaviour printed.

Table 2.2: Plasticity model used in the simulations for S355

Stress [MPa]	Strain ε [%]
361	0,0
365	1,2
492	4,3
492	20

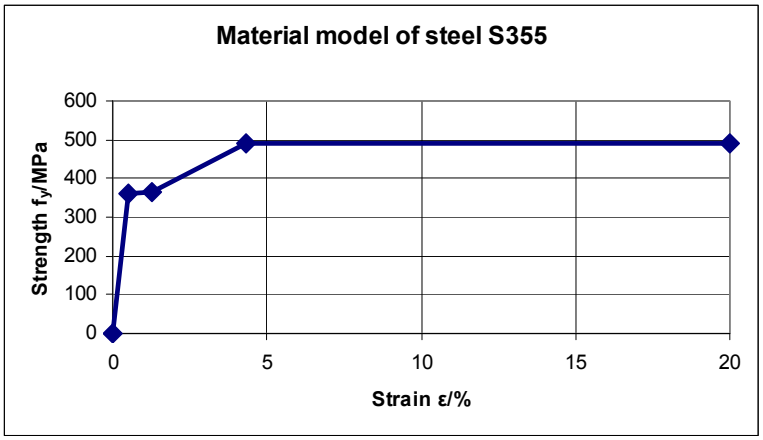

Figure 2.1: Schematic material model of steel S355

2.1.2 Material model of the high strength steel S690

As a possible improvement for the tower an investigation was performed which used high strength steel S690. High strength steel has higher yield strength than the steel used in the state of the art tower. High strength steel is dedicated for steel structure construction. It increases the possible load level and enables weight savings due to a reduction in plate thickness. The reduction of material reduces material and processing costs.
The properties of the high strength steel are printed in Table 2.3

Table 2.3: General material properties of the high strength steel S690

E-modulus	210 GPa
Poisson's ratio	0,3
Yield stress	690 MPa
Density	7850 kg/m³

Similar to the first steel material model, a plasticity model was created for the high strength steel. The values used in the simulation are printed in Table 2.4. In Figure 2.2 is the graph of the material behaviour printed.

Table 2.4: Plasticity model used in the simulations for the high strength steel S690

Stress [MPa]	Strain ε [%]
690	0,000
690	0,360
770	3,9
770	14

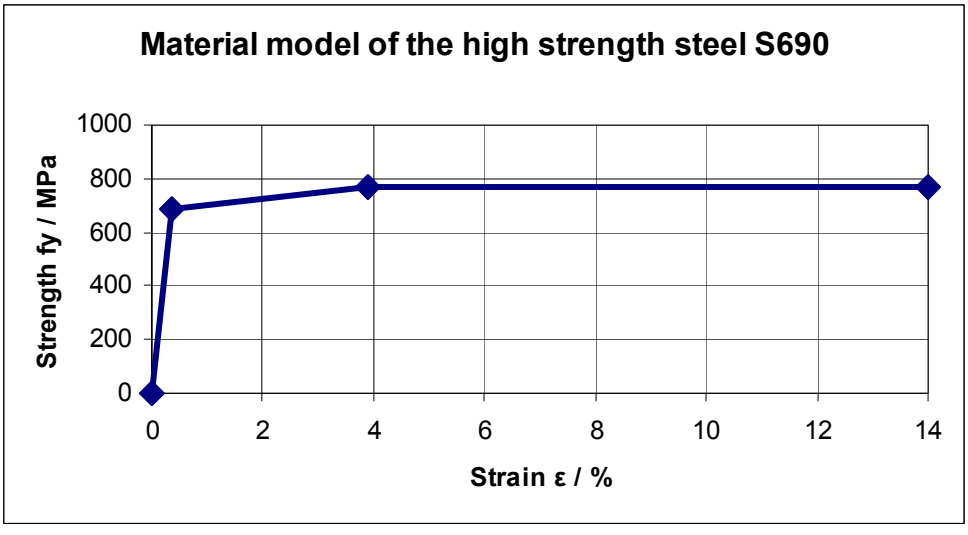

Figure 2.2: Schematic material model of the high strength steel S690

2.2 The geometric properties of the lower tower section

2.2.1 The geometry of the lower tower section

The shell of the tower is divided into four sections; they are representing the bottom flange and the three sections of the lower part of the tower. The door is represented as a second part and through a tie constraint added to the lower tower section. The geometric properties of the lower tower section used in the model are shown in Table 2.5. The geometry was created by a revolution around the middle axis of the tower. It was the outer surface of the tower drawn. This causes that an offset must be used to define the material on the inner side of the tower shell. The door stiffener is drawn on its outer surface and a shell offset value was set to place the material definition on the correct side. To choose the correct side it is necessary to check the shell normal vector in Abaqus.

Table 2.5: Geometric properties of the sections used in the simulations

Section name	Diameter at bottom [m]	Radius at bottom [m]	Section height [m]	Shell thickness [m]
Bottom Flange	4,3000	2,1500	0,15	0,030
Section 1	4,3000	2,1500	2,43	0,030
Section 2	4,2570	2,1285	2,33	0,030
Section 3	4,2150	2,1075	2,08	0,026

Section name (calculated values)	Diameter at top [m]	Radius at top [m]	Section height [m]	Shell thickness [m]
Section 3	4,1735	2,0868	2,08	0,026

In total has the lower tower section a height of 6,99m. This value was chosen because of the loads provided by the design load tables which offer load values for cross sections at different heights. Because the drawing of the tower provides no values for this tower height it was necessary to calculate the radius at the end of section 3. The drawing contains the dimensions of the real tower sections which are not similar to the calculation sections used in the design load tables.
The door is introduced as own section. The cross-section of the door frame is rectangular with the dimensions 160x70 mm. The door is in its shape not a standard ellipse. This fact made it necessary to extract the shape of the door from a three dimensional CAD model of the wind turbine tower. The extracted geometry was used for both, the door frame and the cut out in the lower tower section. This approach assure that the calculation can be done with a realistic door opening and the best fit between stiffener and cut out in the lower tower section. Figure 2.3 shows the used door geometry. Notice that the curvature cannot be measured because of its extraction through a native data format, which provides no data about curvature.

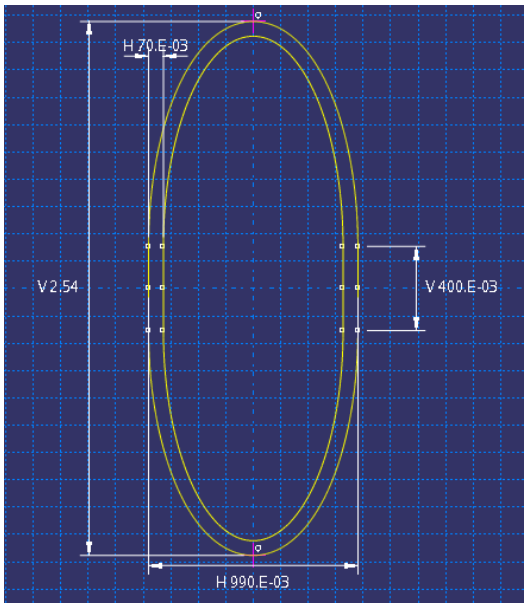

Figure 2.3: Sketch of the door geometry

Figure 2.4 shows the lower tower section with all tower sections and the door frame. Additionally are the two reference points visible and the coordinate system of the simulation. The plane with the broken line was used to create the door cut out in the lower tower section. The reference points will be mentioned in a following chapter.

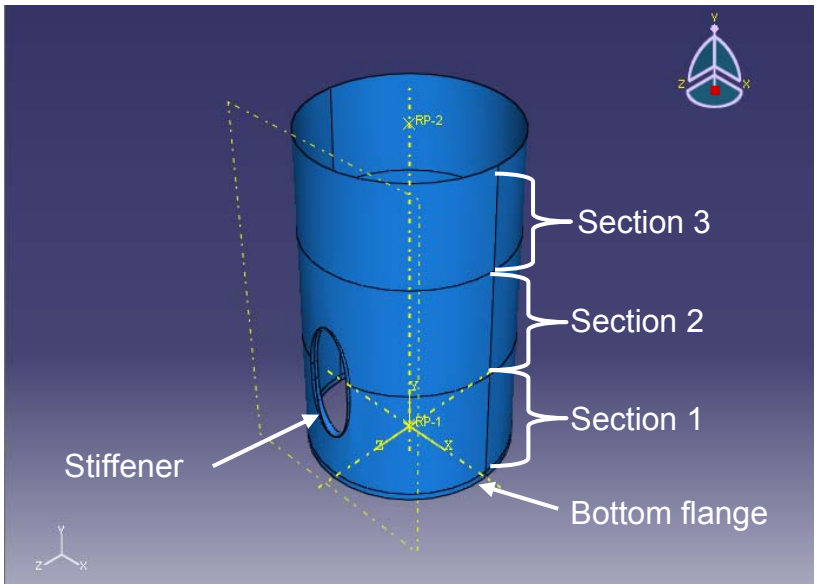

Figure 2.4: Assembled lower tower section showing the different sections and the stiffener used in the door opening

2.2.2 The introduction of imperfection into the model geometry

A geometric imperfection is usually introduced into a model for a postbuckling load-displacement analysis. The definition of it is created by a superposition of buckling eigenmodes, which were obtained from a previous buckling analysis or an eigenfrequency analysis. Other possible ways to create an imperfection pattern is to use the result of a previous static analysis or specify it directly based on data from a measurement.
Postbuckling problems cannot be analysed directly due to discontinuous response, so called bifurcation, at the point of buckling. This imperfections are introduced into a simulation model to turn the postbuckling problem into a problem with continuous respond. The imperfection is realised as a geometric imperfection pattern in the perfect model geometry. This allows a response in the buckling mode before the critical load is reached.

To create an imperfection based on a perturbation pattern in Abaqus, it is necessary as a first step to perform a buckling analysis, followed by a static Riks analysis to achieve results for stress, force and displacements. The connection between the two analysing steps is done by creating a result file which contains the values of the displacement in a normalised form.

To create a result file it is necessary to add a line into the input file. This can be done in Abaqus by using the Keyword editor or by writing an input file and adding the line with a text editor.

The command is: *nodefile
U

The input file of the following analysis step also needs a change. This change introduces the imperfection into the model geometry. The syntax is important, and the placement of commas and line changes is necessary.

The command is: *imperfection, file=*result_file_name (without .fil ending),*
Step=*step_number*
Eigenmode_number, *imperfection scaling factor*

The result file name is the name of the job under which it was created. The step number indicates from which step of the previous analysis the results were taken. If the buckling analysis contains more than one calculated eigenmodes, it is possible to choose which one shall be used to perform the perturbation pattern.
The perturbation pattern is the result of a buckling analysis and the only result of it are displacement values. This displacement values are normalised to the maximum value of the result.
The imperfection scaling factor is multiplied with the displacement values of the buckling analysis, the result of this is the imperfection amplitude. This means that the perturbation pattern is proportional to the imperfection scaling factor and the imperfection amplitude.

2.3 The mesh of the sections

The model consists of shell elements of the type S8R; this is an 8-node doubly curved thick shell with reduced integration. This is an element used for stress/displacement analyzes were moments are applied. The mesh consists of quad elements. The part was partitioned to use the option of structured mesh. Figure 2.5 shows the meshed lower tower section.

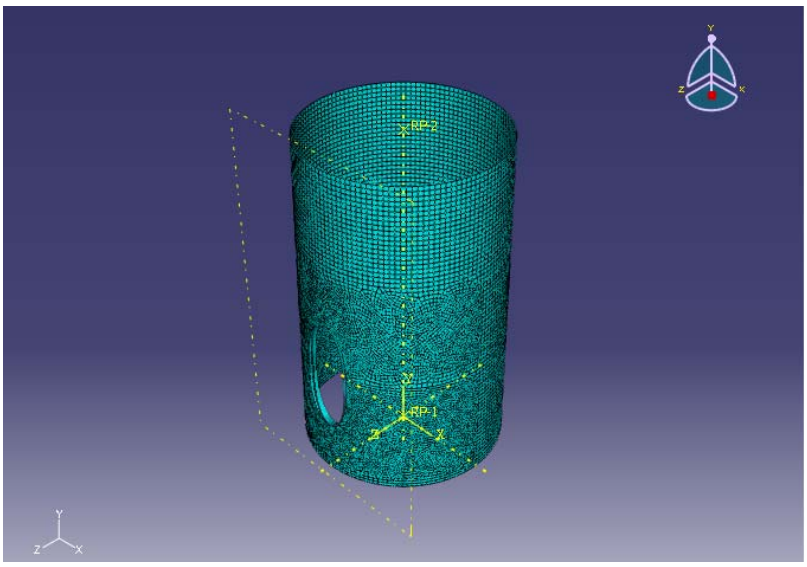

Figure 2.5: Lower tower section with mesh

2.4 Constrains used in the model

2.4.1 The coupling constrain between reference point and surface

To apply loads and boundary conditions onto the model it is very convenient to use reference points. It is necessary to refer to a reference point if a rigid body constraint from the interaction module is used. The reference points were added to the geometry by entering their coordinates, the reference points are positioned on the centre axis. Reference points can be created on the part or on the assembly of the model. The difference is that in the part module is only one reference point possible but in the assembly module several reference points are possible.
The proper way to connect a reference point to the surface of a model geometry is to use the “coupling” constrain. A coupling constrain allows it to constrain the motion of a surface to the motion of a single point. The coupling constrain is a rigid body constrain which means that the space between reference point and constraint surface is not deformed while loading. The constraint surface follows the displacement caused by loading in the reference point. The nodes within the surface are selected by picking a surface in the viewport. The coupling constraint can be used with two or three dimensional stress or displacement elements. The constraint is not influenced by changing between a geometrical linear or non linear analysis. The position of one coupling constraint is shown in Figure 2.7, the second coupling constraint uses similar properties and lies on the lower side of the tower shell.

2.4.2 The tie constraint between door frame and lower tower section

Between the door frame and the tower shell is a constraint necessary. Both parts consist of shell elements. The proper constraint for this interaction is the tie constraint which allows a connection between two regions even though the mesh created on them is not similar. The two surfaces which define the tie constraint are tied together for the duration of the simulation, and the thickness and the offset of a shell element is taken into account. The degrees of freedom of the nodes on the slave surface are constrained if it is not specified in another way. The tie constraint is in two different approaches available surface-to-surface and node-to-surface. This model uses the first one because it provides, regarding to the manual, an optimised stress accuracy.
To define a tie constraint it is necessary to choose a master- and a slave-surface. The master surface is the edge of the door cut-out in the tower shell; the slave surface is the outer surface of the door frame or stiffener. It is necessary to have a finer mesh on the slave surface than on the master surface; this is done in the model. Because the whole surface of the stiffener is used as slave surface are not all nodes tied to the tower shell. This is of course realistic because it represents the free surfaces of the real structure which are not welded to the tower shell. The nodes that are tied to the master surface have to lie in a position tolerance distance from the master surface. The position tolerance is calculated by Abaqus by default. The calculation of the position tolerance takes into account the shell thickness and the offset value of the shell. The nodes, which are not tied to the master surface in the beginning of the simulation, can penetrate the master surface if no further contact is defined. Figure 2.7 shows the lower tower section with the tie constrains at the door opening and the coupling constrain between the reference point and the top surface. It is also possible to define the position tolerance manually. In this approach the user

specifies a distance from the master surface within all nodes of the slave surface must lie to be tied. Figure 2.6 shows the principle of the position tolerance in a tie constraint with surface-to-surface definition.

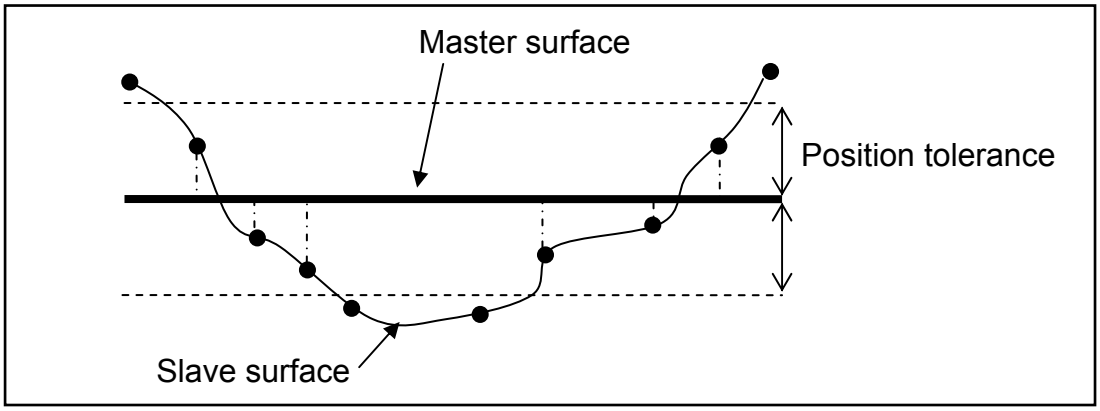

Figure 2.6: Position tolerance of a tie constrain

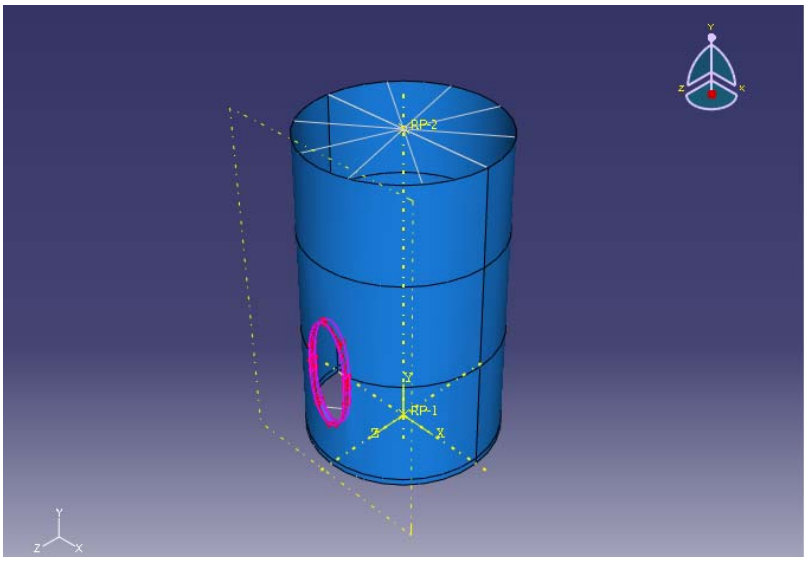

Figure 2.7: Tie and coupling constrain in the model

2.5 The boundary condition

The boundary condition is applied to the lower surface through a reference point. The real wind turbine tower is at this point connected to the foundation of the wind turbine tower. The connection is realised by two flanges that are bolted together. In the model it was assumed that the tower is fully constrained in the foundation. The stiffness of the foundation and the soil is not relevant for this type of analysis and therefore it is not considered here. This behaviour is in the model represented by a constraint with zero displacement in all three directions. The chosen boundary condition is in Abaqus named “ENCASTR”.

2.6 The coordinate system

The coordinate system used for the design of wind turbines is not harmonised. The load tables provided by RePower use the most common coordinate system defined by the guidelines of Germanischer Lloyd. The simulations in Abaqus were performed with the default coordinate system of the software; therefore, it was necessary to transform the loads into this coordinate system. See in Figure 2.8 the different coordinate systems. Another topic to mention in context with coordinate systems is the fact that in Abaqus the naming convention for axis is 1, 2 and 3 regarding to x, y and z.

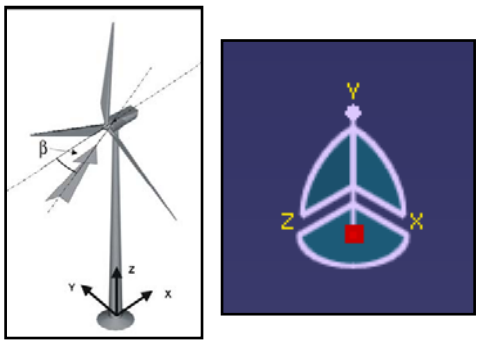

Figure 2.8: Coordinate system defined by Germanischer Lloyd on the left and Abaqus coordinate system on the right [1]

2.7 The colour code used for the result analysis

The colour code used in the result analysis follows the pattern to see in Figure 2.9. To make yielding easily visible, all stresses higher than the yield stress are plotted in grey. The colour code is valid for all figures containing stress values.

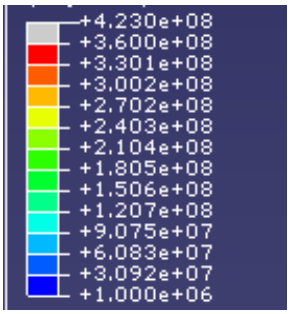

Figure 2.9: Colour code for stress used in the contour plots

2.8 The loading of the model

The forces and moments used in the model regard to the design load tables provided by RePower. The load tables include not all possible load cases but they contain the cases with the extreme loads. The load used for the simulation already contains a safety factor. The loading of a wind turbine is affected by the environment and by the electrical conditions while it is in use. The environmental conditions are first of all the wind, followed by other actions which possibly occur.
The full design load tables include a list of possible circumstances, which have to be checked to certify a wind turbine tower regarding to the guidelines of “Germanischer Lloyd”. Using the design load tables is a very convenient way because they include all relevant influences such as dead weight, wind load on the tower, dynamic reaction of the tower and the load safety factor. The wind load that is distributed along the tower height is also included and can be neglected in the simulations of the lower tower parts.
The load used for the following simulations is taken from the load case which created the highest stresses around the door opening. A comparison of the stresses around the door opening for three different load cases is to see in appendix G.
The circumstances for how the load is calculated is mentioned in source [1] “Guideline for the certification of Wind Turbines”.
The load case used for the simulations represents a wind turbine that is in electricity production and a one-year-gust in combination with the loss of the connection to the electrical grid occurs in the same time. The possibility of a gust and the loss of the connection to the electrical grid could happen any time.
The fatigue loads for the simulation are also provided by RePower. The load tables contain, as for the extreme loads, load values for different section heights and additional calculated load values for different Wöhler slopes. The damage equivalent loads given in the table can be handled like static loads; the only thing which has to be mentioned is the Wöhler slope and the reference number of cycles. The Wöhler slope m = 4 contains the for steel structures relevant values, the number of reference cycles is N = 2*10^8. Fatigue loads are calculated in a simulation which includes a time domain. The result of this simulation is a time series for different load cases and load components. The time series include information about the load range and the load level. The frequency of the occurrence of events, which means change of the load case, is also registered and used for the calculation of the damage equivalent load.

The moments in the cross-section of the tower were combined to a resulting moment and the forces acting in this section were recalculated to act in the same coordinate system as the resulting bending moment. The bending moment is oriented that the door opening is under compression. Figure 2.10 shows the approach that was used to recalculate the forces into the direction of the resulting bending moment.
Values of the extreme moments and forces used in the simulation are given in Table 2.6. The values for the fatigue analysis are presented in Table 2.7. The complete load tables are appended in appendix C.
Abaqus uses in the load module the naming convention 1, 2, 3 for the axis's which equals x, y, z in a usual coordinate system.
During the simulations, the load is applied in steps and a load proportionality factor is printed to the output database. This factor equals a normalised load and because of the load vector which consists of five components, this normalised load factor is used in all diagrams which contain the load on an axis.

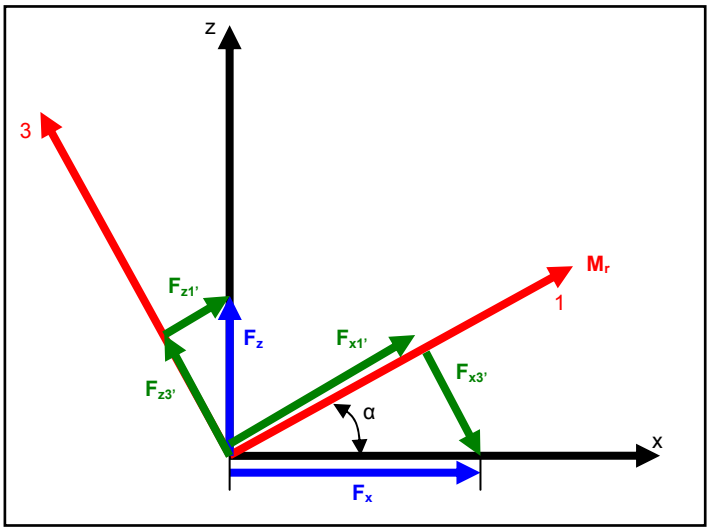

Figure 2.10: Orientation of the moment M_r and the forces in the x-z-plane

Table 2.6: Design load applied in the model [2]

	Force [kN]
1- axis	-40,5
2- axis	-3056,1
3- axis	901,9
	Moment [kNm]
1- axis	63786,0
2- axis	-1350,0

Table 2.7: Damage equivalent load applied in the model [3]

	Force [kN]
1- axis	-9,0
2- axis	-20,9
3- axis	102,3
	Moment [kNm]
1- axis	8025,3
2- axis	1328,7

2.9 The Step module in Abaqus

The step module is used to define the analysis which will be calculated. In the beginning Abaqus always creates an initial step where the boundary conditions and interactions are applied to the model. It is possible to use more than one analysing step in a model after the initial step. This is done in the buckling analysis. The first step is a buckling analysis and the second step is a static, Riks analysis. The step manager distinguishes between the two available types of steps, the general nonlinear steps and the linear perturbation steps. In a general nonlinear step the state of the model at the end of an analysis is the initial state for the start of the next general step. This is for example useful when forces or moments were applied separately from each other. A linear perturbation analysis step provides the linear response of the model at the state reached at the end of the last general nonlinear step. For each step it is also possible to define if a nonlinear effect from large displacement or deformation is taken into account. This decision is in the responsibility of the developer of the model, it is to decide if the displacement or deformation is relatively small or not. If displacements are big the effect off a nonlinear geometry can become important.

2.9.1 The static, Riks procedure

The Riks procedure is used in geometrically nonlinear static problems which often involve buckling or collapsing behaviour. In this case the load-displacement response shows a negative stiffness. To remain in equilibrium, strain energy must be released. The Riks method is able to find static equilibrium during unstable phases of the model response. The static, general step ends with full applied load or displacement, the Riks step is not acting like this. A given load is applied onto the structure and will be increased automatically because the loading magnitude is a part of the solution. The load applied can be calculated afterwards because a load proportional factor is added to the output database. With Eqt. 2-1 is it possible to calculate the loading of the model. To end a Riks analysis it is necessary to specify a maximum load proportionality factor, a maximum displacement of a node region with the degree of freedom in which it occurs or a number of increments which will be calculated. Figure 2.11 shows a typical graph for a model with an unstable loading response. The load reached in the first peak is the ultimate load that the structure is able to resist.

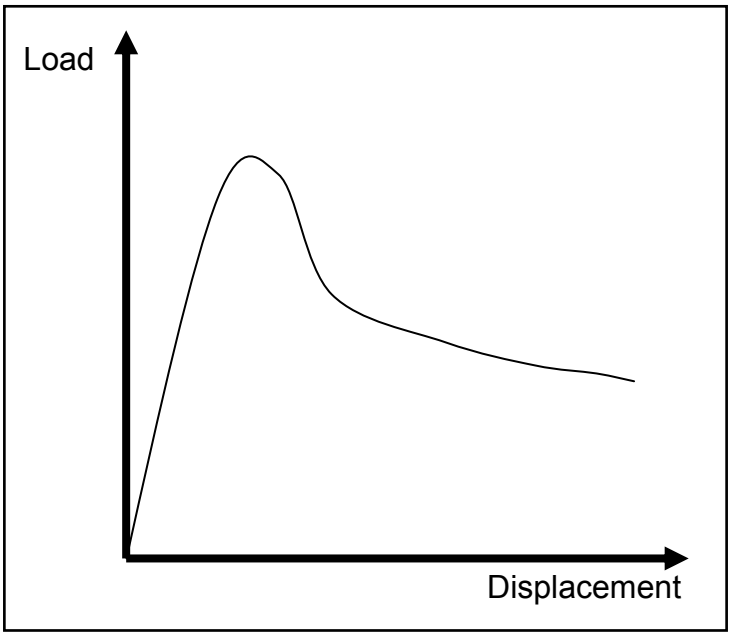

Figure 2.11: Load displacement graph for an unstable loading response

Eqt. 2-1: $P_{total} = P_0 + \lambda * (P_{ref} - P_0)$

To use the Riks procedure for solving a post buckling problem, it is necessary to introduce an initial imperfection into the perfect geometry of the model. This leads to response in the buckling mode before the critical load of the perfect structure is reached.
Imperfections are usually introduced by perturbations in the geometry which are achieved through buckling modes of a previous buckling analysis. Another possibility is to measure imperfections on an existing structure and introduce them to the model. The method used in the simulations for this report is to introduce perturbation onto the model which was achieved through a previous buckling analysis.

2.9.2 The buckling procedure

An eigenvalue buckling analysis is generally used to estimate the critical buckling loads of stiff structures. This type of analysis is a linear perturbation procedure and buckling loads are calculated relative to the base state of the structure. This means that if the structure is preloaded in a previous step this state will be used to perform the buckling analysis. It is also possible to perform a buckling analysis as a first step and then continue with a static analysis of the structure while an imperfection is introduced into it. The result of a buckling analysis are the buckling mode shapes, this are normalised vectors and do not represent magnitudes of deformation at a critical load. The maximum displacement component has a magnitude of 1,0 and in a following static analysis it is possible to set this value to a specific imperfection value were all vectors follow in a proportional way.
During an eigenvalue buckling analysis, the response of the model is defined by its linear elastic stiffness in the base state where all nonlinear material properties are ignored.

To extract the eigenvalue from a model it is possible to choose between two different solving methods. The first method solver is the Lanczos method, the second one the subspace iteration method. Abaqus uses by default the subspace iteration method but a change to the Lanczos method is possible and in some cases useful. If many eigenmodes are required the Lanczos method is the better choice, but for a smaller number of eigenvalues, the subspace iteration method is faster. The suggested value for a change is at about twenty requested eigenvalues. For both method solvers it is necessary to specify the desired number of eigenvalues. Abaqus will choose a number of vectors for the subspace iteration method or a block size for the Lanczos method. The amount of vectors or the block size can be changed by the user if necessary. An overestimation of the number of eigenvalues can create very large files and because of that, it should be avoided. An underestimation of eigenvalues is also to be avoided but in this case, Abaqus is printing a warning message.
The Lanczos solver cannot be used for buckling analyses in which the stiffness matrix is indefinite.

This case happens if a model,

- contains hybrid elements
- contains contact elements
- has been preloaded above the bifurcation load
- has rigid body modes
- contains distributing coupling constraints, this includes coupling constraints and shell-to-solid couplings

All simulations performed have no limitation in the use of a solver so that both solvers can be used.
In some cases it is possible that Abaqus prints a warning message containing the information that the matrix contains negative eigenvalues. Usually this means that a structure would buckle if the load is applied in the opposite direction. Negative eigenvalues are also possible if a preload is applied on the model which causes significant geometric nonlinearity.

The load module of a buckling analysis is limited to concentrated forces, to distributed pressure forces or body forces. Abaqus takes the preload into account when solving the eigenvalue buckling, therefore it is important that the structure is not preloaded above the critical buckling load. As preloads are applied in a previous step, loads are applied during the buckling analysis used to define the load pattern for which the buckling sensitivity is being investigated. The magnitude of this load is not important. Forces which follow the nodal rotation during the analysis may not yield to correct results because Abaqus can extract eigenvalues only from symmetric matrices and following forces lead to asymmetric matrices.
Another possibility is to apply displacements on the model to load the structure.
The values of the eigenvalues are listed in the output file. If the output of stress, strain or reaction forces is requested, this information will be printed for each eigenvalue. These quantities are perturbation values and represent mode shapes and not absolute values. The buckling mode shapes can be visualised in Abaqus.

2.10 The data extraction

Abaqus offers the possibility to extract data from the models in two different ways. One way is the specify output variables in the keywords of the model, the results of this variables are printed into different output files depending on the variable or the added keyword. This approach can decrease the evaluation time because the results are delivered in a tabular form and can be added in second party programs. The only necessity is that the user needs to know which variable at which point or region needs to be extracted.
Another way is to extract data from the output database. The output database includes all available data of the simulation. The graphical surface of Abaqus offers the possibility to selected single points or regions and extracts the requested data from there. This approach is easy to handle and delivers a clear picture of requested data, the variables and located points. Due to this, mistakes are easier avoided.
If more simulations are performed with the same model, it is useful to define regions and variables graphically and add them to the keywords in the following simulations. This is only possible if the mesh of the model is not changed, otherwise the points are changing their number.
Data values were extracted and added into second party programs after all simulations. The stresses around the door opening were extracted using a path around the door opening. The path contains all points around the door opening on the edge of the tower shell. The start and the direction of the path are shown in Figure 2.12.

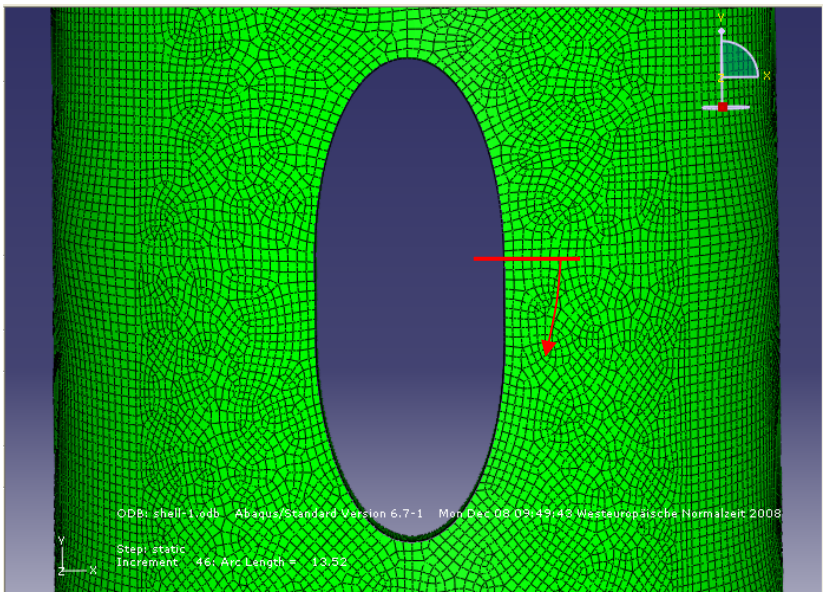
ODB: shell-1.odb Abaqus/Standard Version 6.7-1 Mon Dec 08 03:49:48 Westeuropäische Normalzeit 2008
Step: static
Increment 46: Arc Length = 13.52

Figure 2.12: Start position and direction of the path used for the data extraction

The diagrams measured displacement was taken in node 2. Node 2 is the reference point where the load is applied into the model. This point was chosen because of its similar behaviour in all simulations. Nodes in the tower structure can behave different depending on the properties of the model. Another advantage is that node 2 also exists in the models without door opening so that it is possible to compare models with and without door opening with each other. In Figure 2.13 is node 2 marked as a red point.

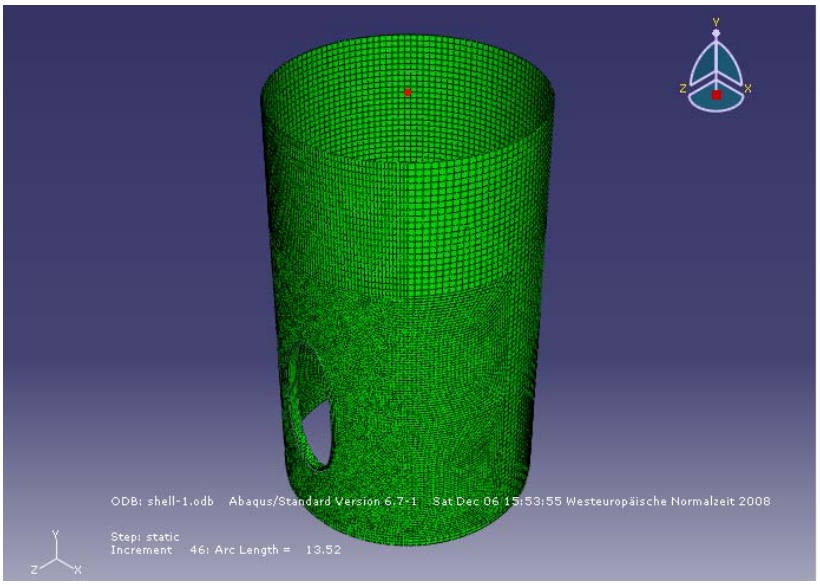
ODB: shell-1.odb Abaqus/Standard Version 6.7-1 Sat Dec 06 15:53:55 Westeuropäische Normalzeit 2008
Step: static
Increment 46: Arc Length = 13.52

Figure 2.13: Position of node 2 in the model

2.11 Model naming convention

Due to the amount of models with different properties, a naming convention for the models was used. The naming of the models includes a consecutive number, the geometry of the structure and also the material and a possible imperfection. Additionally, a colour code was used for the different models. Every model has its own colour used in the graphs so that an easy separation is possible. The colour code for the models and an overview of all models and their properties is added to the report in appendix J.

Naming convention:
Model -- material -- shell thickness -- stiffener thickness -- imperfection

Model + number:	Consecutive number for every model
Material:	Value of the yield strength in MPa
Shell thickness:	Written in percent of the original shell thickness described in the tower geometry
Stiffener thickness:	Written in percent of the original stiffener thickness described in the tower geometry
Imperfection:	Imperfection amplitude introduced to the model in mm

For chapter 3.3 Comparison of a simplified tower model with an analytical calculation is the nomenclature changed. The model name consists only of the simulation number and the imperfection amplitude. The geometry is not changed in the chapter. The material change is mentioned in the beginning of the chapter.

3 Nonlinear analysis of the lower tower section

3.1 Parametric study of different shell or stiffener thicknesses

3.1.1 Influence of varied shell or stiffener thickness on the ultimate load

Part of the analysis of the lower tower section was a parametric study. Shell thickness and stiffener thickness were the variation parameters. Due to the fact that the shell thickness of the lower tower section is not constant over the height, the wall thickness of section three was proportionally reduced. The simulations with change in stiffener thickness were performed with the original geometry of the tower. Table 3.1 shows the geometric properties of the simulation model. All other simulation properties regard to chapter 2 General properties of the models.

Table 3.1: Geometric variations in the models for the parametric study

Simulation model name	Yield strength [MPa]	Shell thickness Section 1 and 2 [m]	Shell thickness Section 3 [m]	Stiffener thickness [m]	Imperfection amplitude δ [m]
Model 1	360	0,030	0,026	0,070	0
Model 2	360	0,020	0,017	0,070	0
Model 3	360	0,015	0,013	0,070	0
Model 4	360	0,030	0,026	0,050	0
Model 5	360	0,030	0,026	0,030	0

The first result of the simulations is the load-displacement response of the five different models. The load-displacement graphs give information about how much load the structure can carry until failure occurs. Figure 3.1 shows the load-displacement graphs depending on shell or stiffener thickness.

The models with reduced stiffener thickness show a slightly lower stiffness than the original geometry. The influence on the ultimate load and the deformation is not very high so that a reduction of the stiffener thickness is possible. The influence on the buckling behaviour with reduced stiffener thickness needs to be studied.

The models with reduced shell thickness have an obvious lower stiffness and also a lower ultimate load. The simulations with reduced shell thickness do not show the same failure graph than the one from the original structure. A reason for these load-displacement graphs is the use of node two to extract the displacement values. Section three has a lower shell thickness and because of this a lower resistance. The section shows a different deformation because of the different shell thickness. This deformation behaviour leads to different graphs.

Regarding to these results, a reduction of the stiffener thickness would be possible because the structure is in both cases able to bear the load. The ultimate load is in all cases at around the same displacement values of node two. This shows that the global deformation of the tower structure is similar for all different stiffener thicknesses. The influence of the stiffener on the ultimate load is rather small. A reduction of the shell thickness seems not to be possible. The design load is reached

only in one case. Failure of the structure occurs before reaching the design load in the other case. Model 2 which reach the design load shows local yielding already at design load.

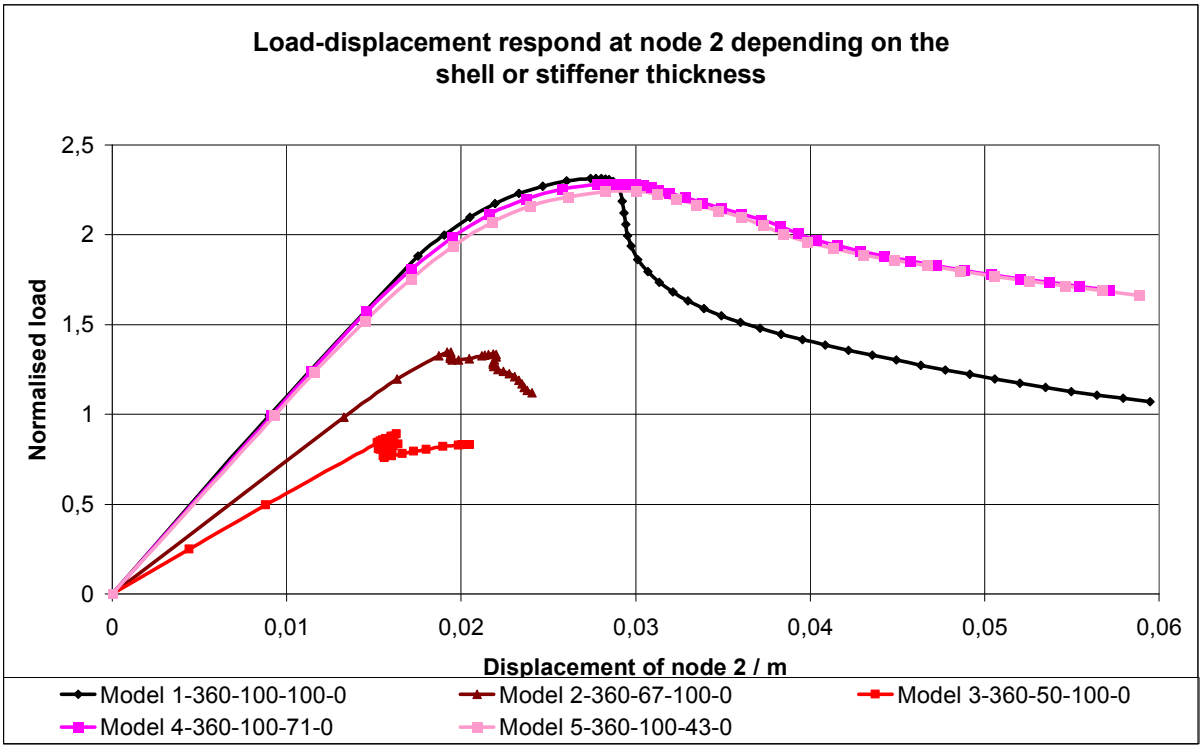

Figure 3.1: Load-displacement response depending on shell or stiffener thickness variation at node 2

The stresses around the door opening with varied shell and stiffener thickness are analysed in the following chapter. The stress level varies locally around the door opening and peaks where the distribution can reach the yield strength of the material.

The influence of the stiffener on the ultimate load and the deformation is small in these simulations. The influence of imperfections in the model and the occurring of local buckling is another topic which has to be investigated. This is done in one of the following chapters

Another question regarding the possibility of reducing the stiffener thickness, is the value of the stresses around the door opening in a fatigue analysis. Fatigue stresses are used to design welds. For this reason, a simulation was performed with the two different stiffeners. The extreme load was replaced with a damage equivalent fatigue load. The results are discussed later in the chapter.

The behaviour of the model 1 during loading is shown in the following contour plots, Figure 3.2 till Figure 3.9. The contour plots include the loading steps from beginning of loading until the ultimate load is reached. The following figures are just an overview; larger plots are printed in appendix D.

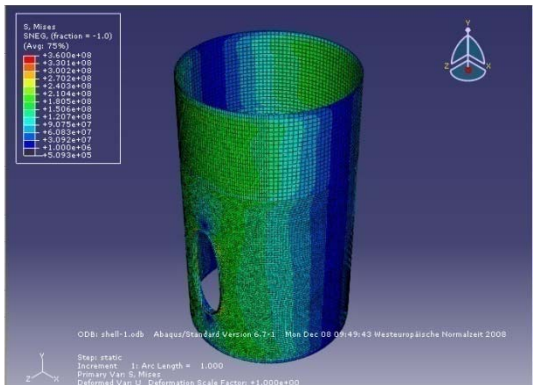

Figure 3.2: Model 1, 99,5 % Load

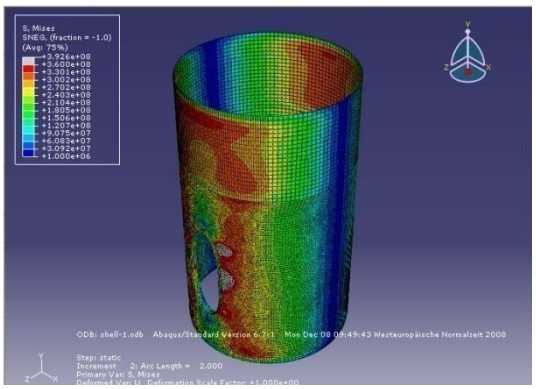

Figure 3.3: Model 1, 188 % Load

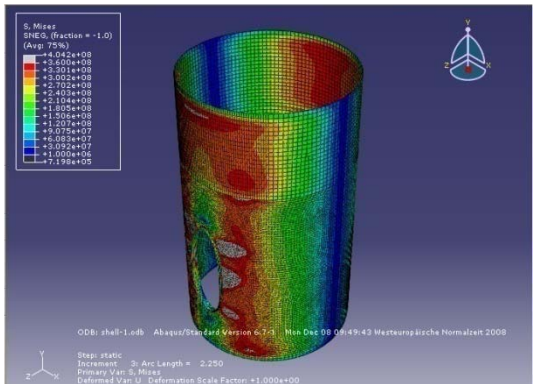

Figure 3.4: Model 1, 199,9 % Load

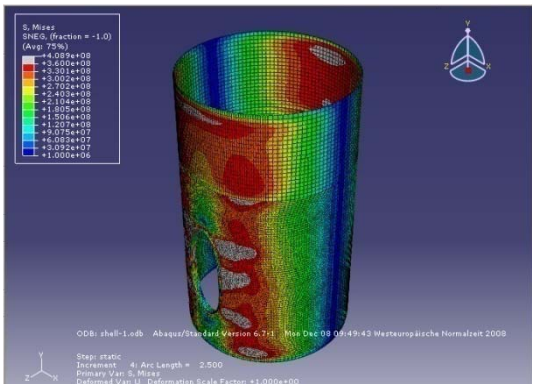

Figure 3.5: Model 1, 209,6 % Load

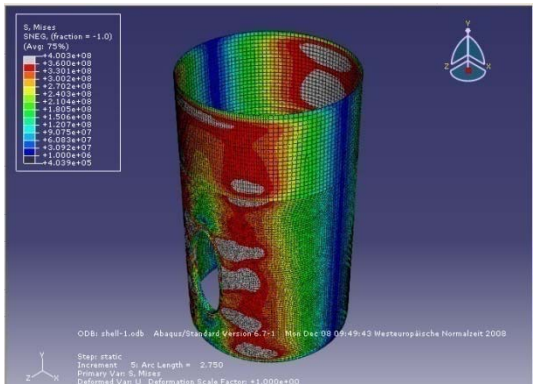

Figure 3.6: Model 1, 217,3 % Load

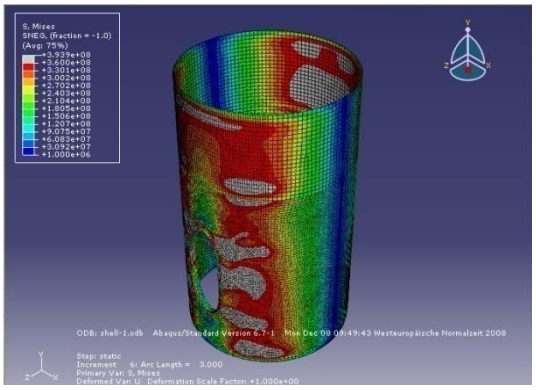

Figure 3.7: Model 1, 223,1 % Load

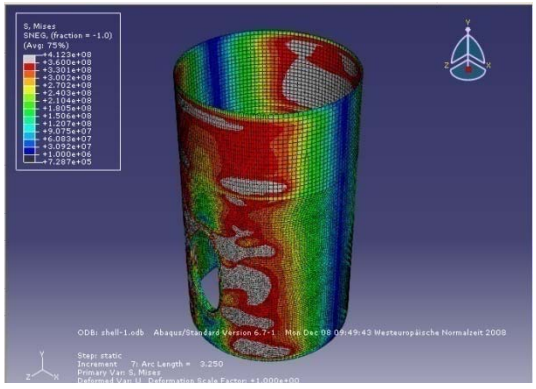

Figure 3.8: Model 1, 227,2 % Load

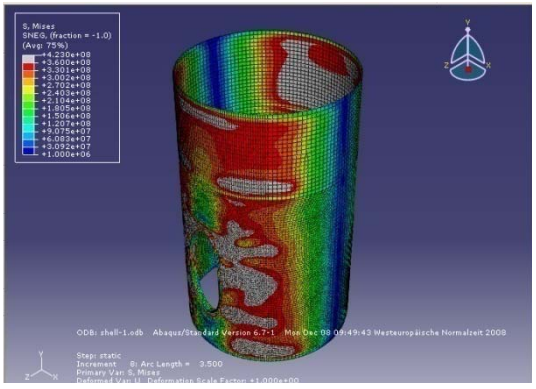

Figure 3.9: Model 1, 229,9 % Load

3.1.2 Stress around the door opening depending on shell or stiffener thickness

Another criterion which was checked during the analysis is the stress distribution around the door opening. The consideration of stress concentration around the opening of tubular steel towers is standard for the certification of wind turbine towers. In Figure 3.10 the stress distribution at varied shell thickness is to seen, and in Figure 3.11 are the stresses depending on the stiffener thickness presented. The values for the stress were taken from the first analysis frame which regards approximately to the design load from the design load table. An exception is model 3 which never reached the load value of the design load table, the highest reached load was here used to plot the stress distribution.

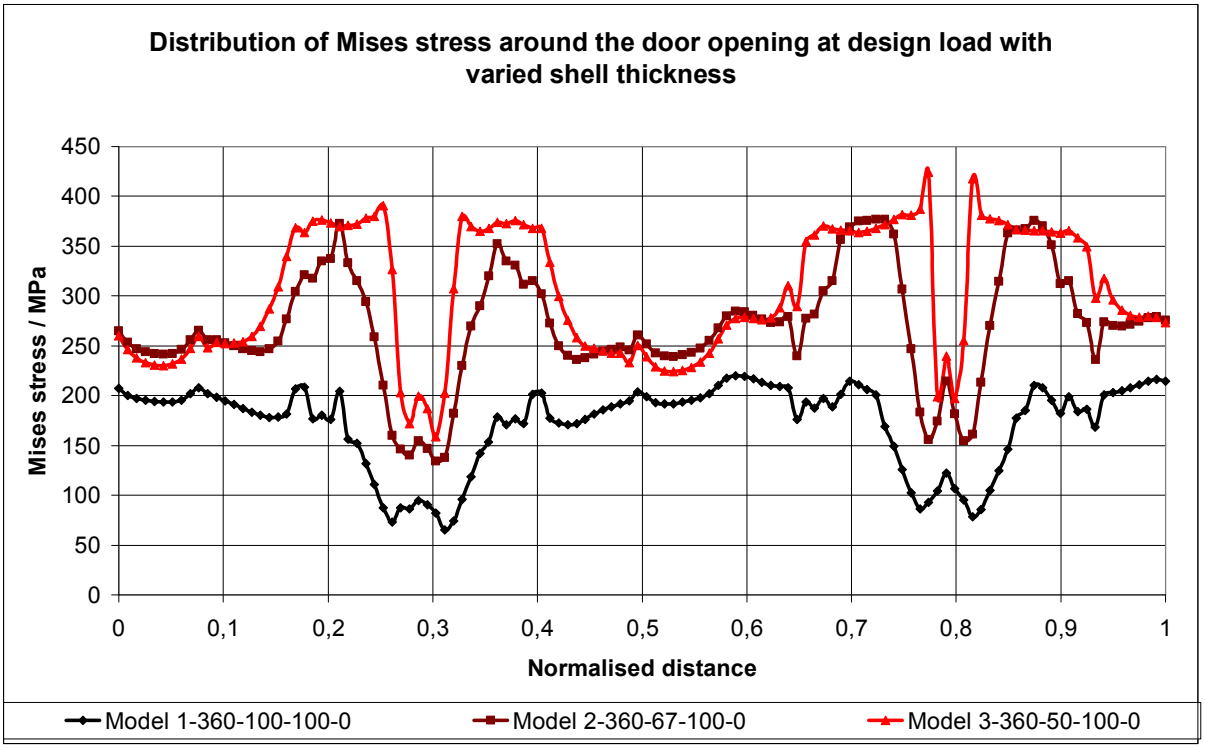

Figure 3.10: Stress distribution around the door opening depending on the shell thickness at design load

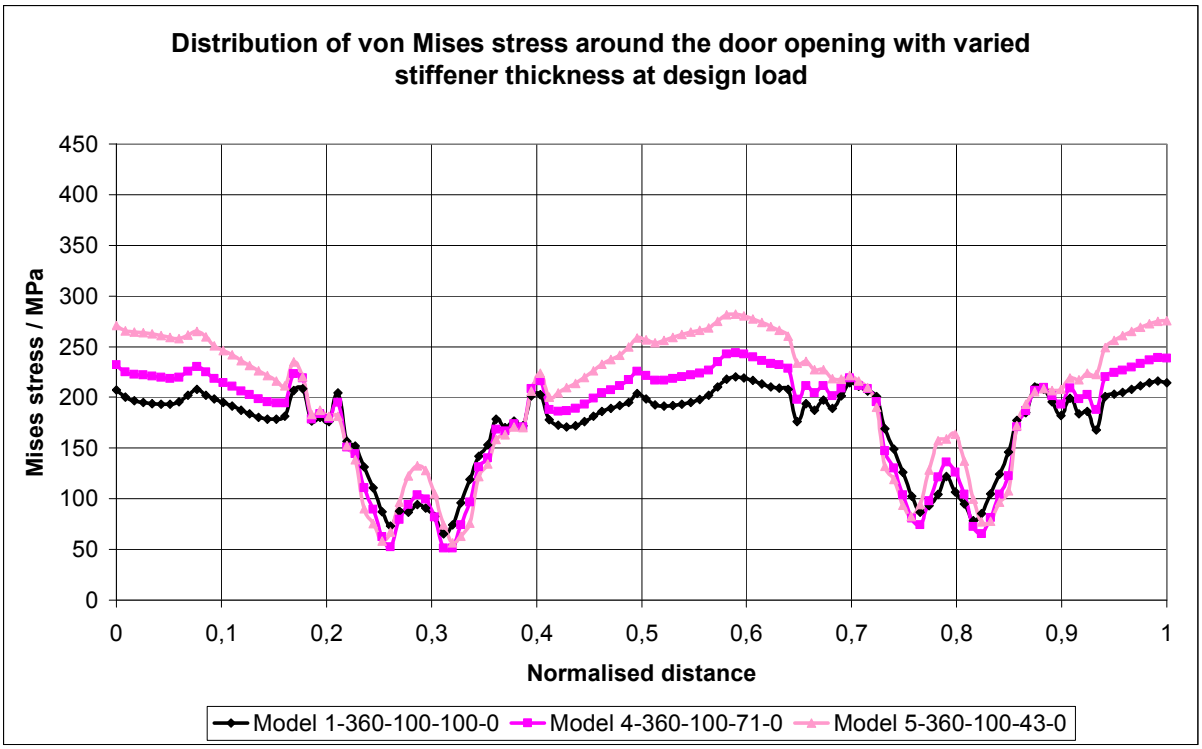

Figure 3.11: Stress distribution around the door opening depending on the stiffener thickness at design load

The graphs for the models with reduced shell thickness show yielding already at the design load, whereas the models with changed stiffener thickness show increased stress values but do not reach the 300MPa line. The range between minimum and maximum stress is increasing with reduction of the shell thickness as well as with stiffener thickness. The structure becomes softer in both cases, and the peaks of the stress values become wider.

The consequence of the stress levels is similar to the one of the ultimate load. A reduction of the shell thickness is not possible because the material will fail locally around the door opening because it is reaching the yield strength. A reduction of the stiffener thickness is still feasible. In the case of a reduction of the stiffener thickness, the stress level increases but it does not exceed the level of 300MPa.

From Figure 3.12 till Figure 3.15, the increasing plasticisation of the door surrounding is presented. The plasticisation spreads from the regions with high stress concentrations and becomes with increasing load larger. The door surrounding is not the only spot in the model which shows plasticity or stress concentrations. The intersection between section 2 and section 3 where the material thickness changes shows also stress concentrations and regions with plasticisation. This two spots are, regarding to this part model, the regions for a collapse of the structure. The following figures are just an overview and are printed in full size in appendix E.

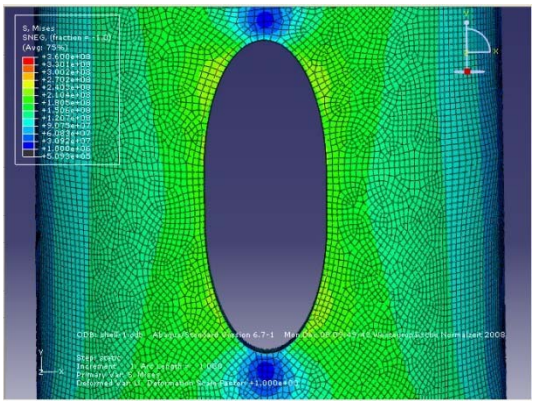

Figure 3.12: Model 1, Stress distribution at 99,5 % Load

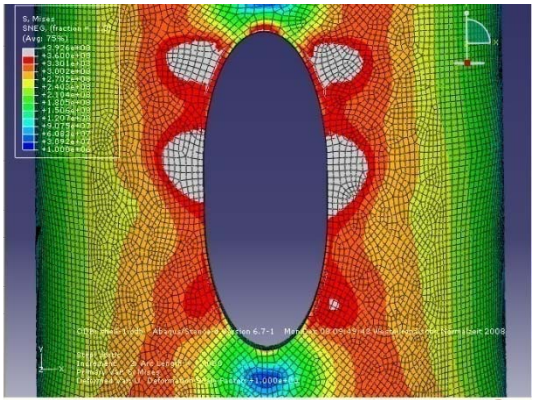

Figure 3.13: Model 1, Stress distribution at 188,0 % Load

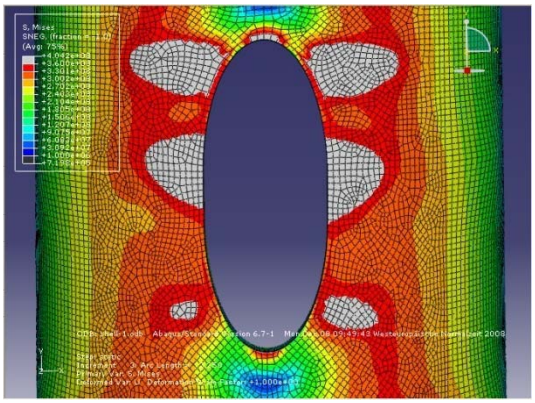

Figure 3.14: Model 1, Stress distribution at 199,9 % Load

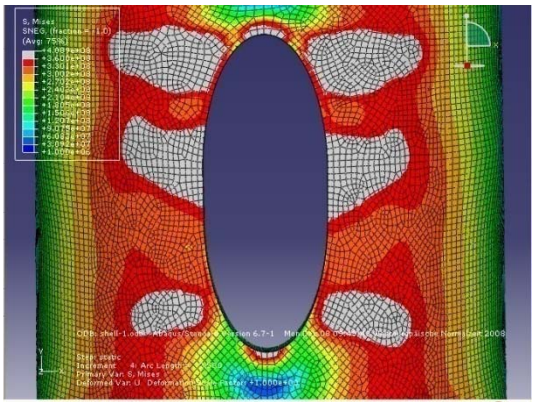

Figure 3.15: Model 1, Stress distribution at 209,6 % Load

3.1.3 Stress around the door opening for fatigue load

The stress distribution around the door opening was also checked for fatigue loads. Figure 3.16 shows the stress distribution around the door opening depending on the stiffener thickness and applied fatigue load.

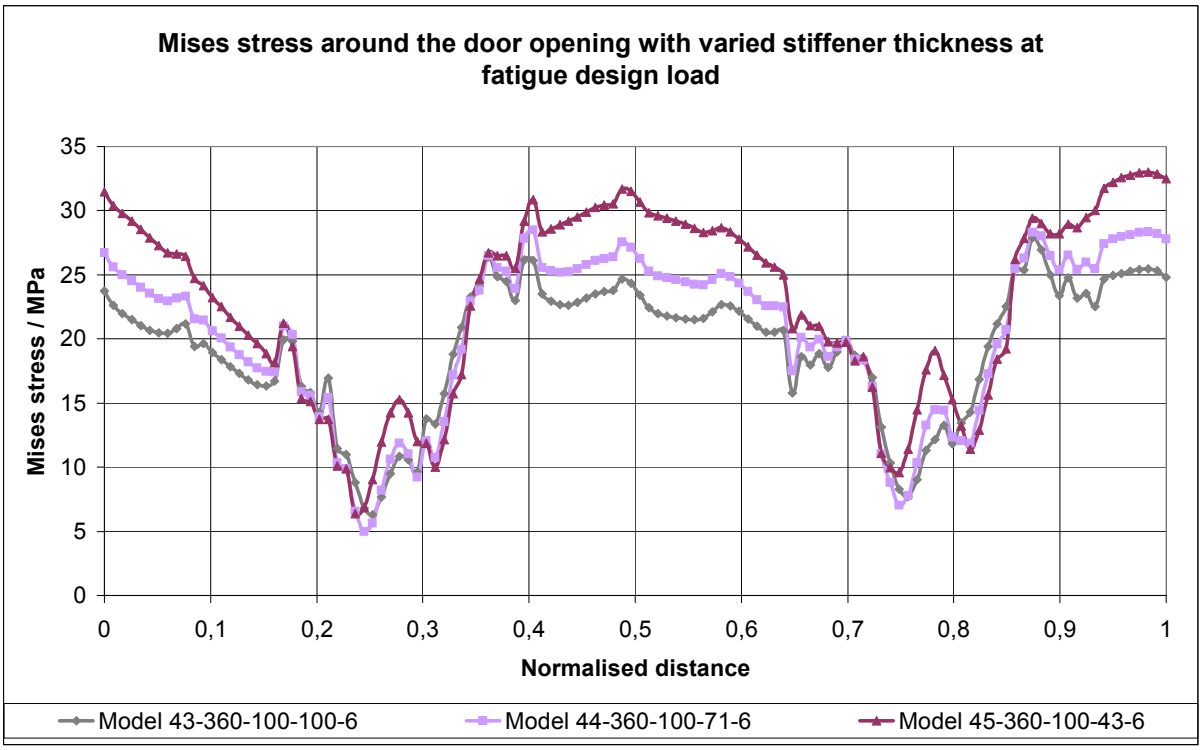

Figure 3.16: Stress distribution around the door opening with varied stiffener thickness and damage equivalent load

The stress achieved by applying fatigue loads is about ten times lower than with design loads. This is reasonable because of the damage equivalent loads which were applied to the model. These loads are lower than the ultimate loads. A prediction if the structure can resist the loading with reduced stiffener thickness for the time duration, depends not on the yield or tensile strength of the material. Instead it depends on the material specific value of the fatigue strength.
The fatigue strength of steel is usually at about 30-50% of the tensile strength. The tensile strength used for the simulations is 492 MPa which leads to a fatigue strength of 148-246 MPa. If these estimated values are used for the comparison, the structure would last over the required time period.
Fatigue stresses are also used for the calculation of the durability of weld seams, this calculation is not part of the report.

3.1.4 Deformation of the door opening

Another question regarding the door opening is if it is possible to open the door during the occurrence of a failure mode, which take the design loads into account. Because of the fact that the drawings only include the dimensions of the door frame and not of the door, this question cannot be answered.
The deformation of the door is plotted from Figure 3.18 until Figure 3.20. The graphs show the deformation of the door on three different edges, on the stiffener outside of the tower, on the inner side of the tower and on the shell of the tower. The measured edges which include the nodes are marked in Figure 3.17.

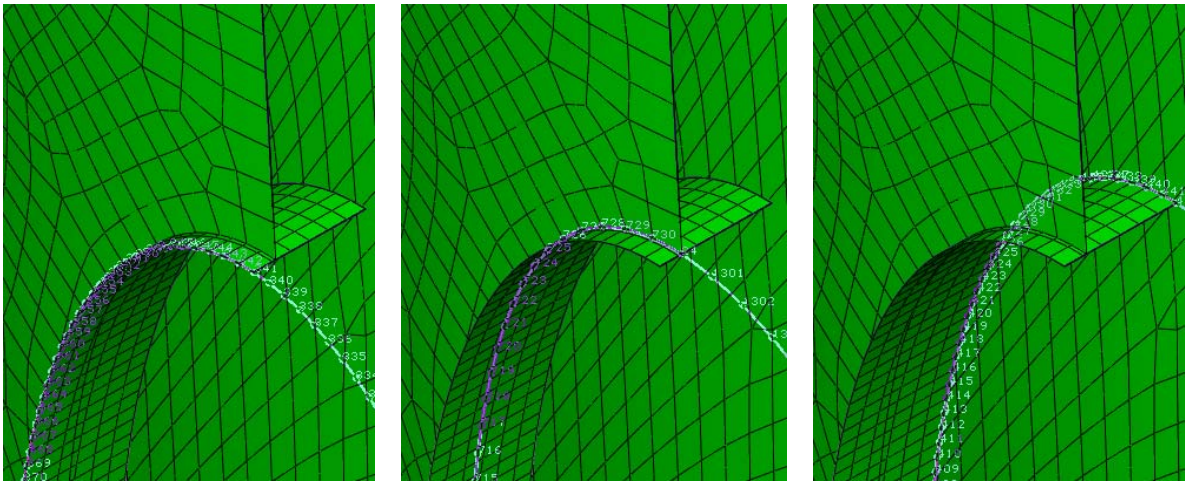

Figure 3.17: Edges used for the data extraction at tower shell and the stiffener

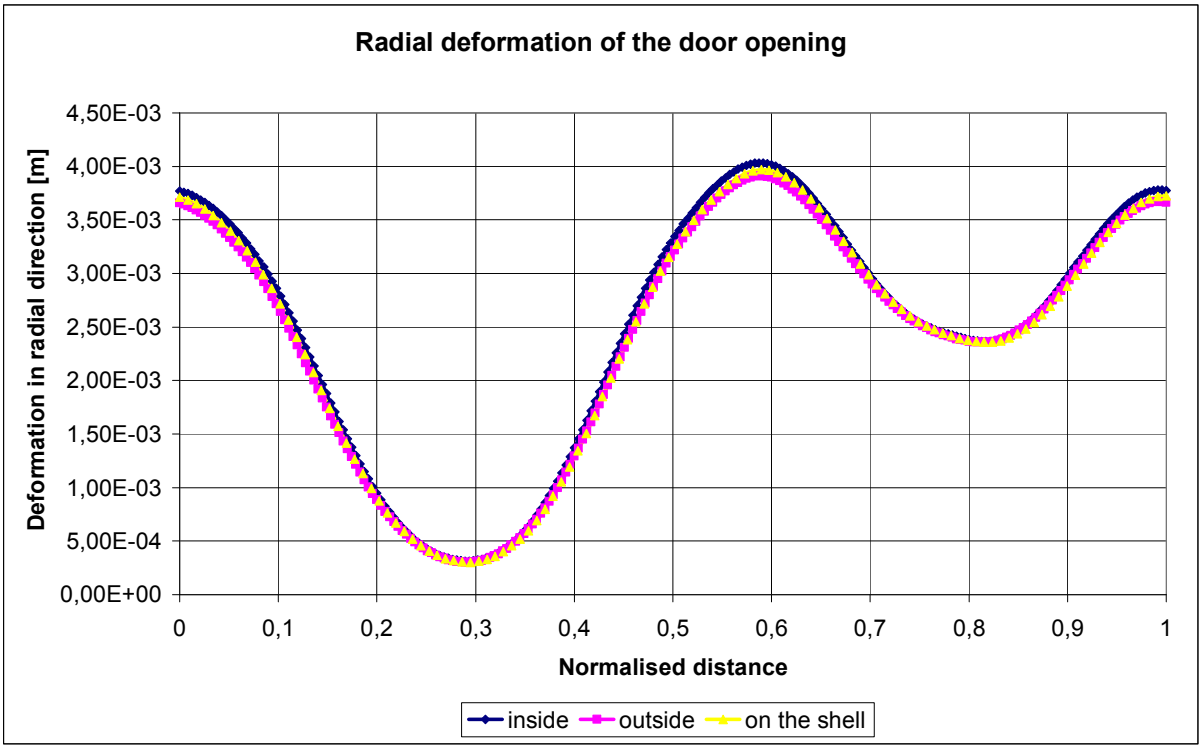

Figure 3.18: Deformation of the door in radial direction at design load

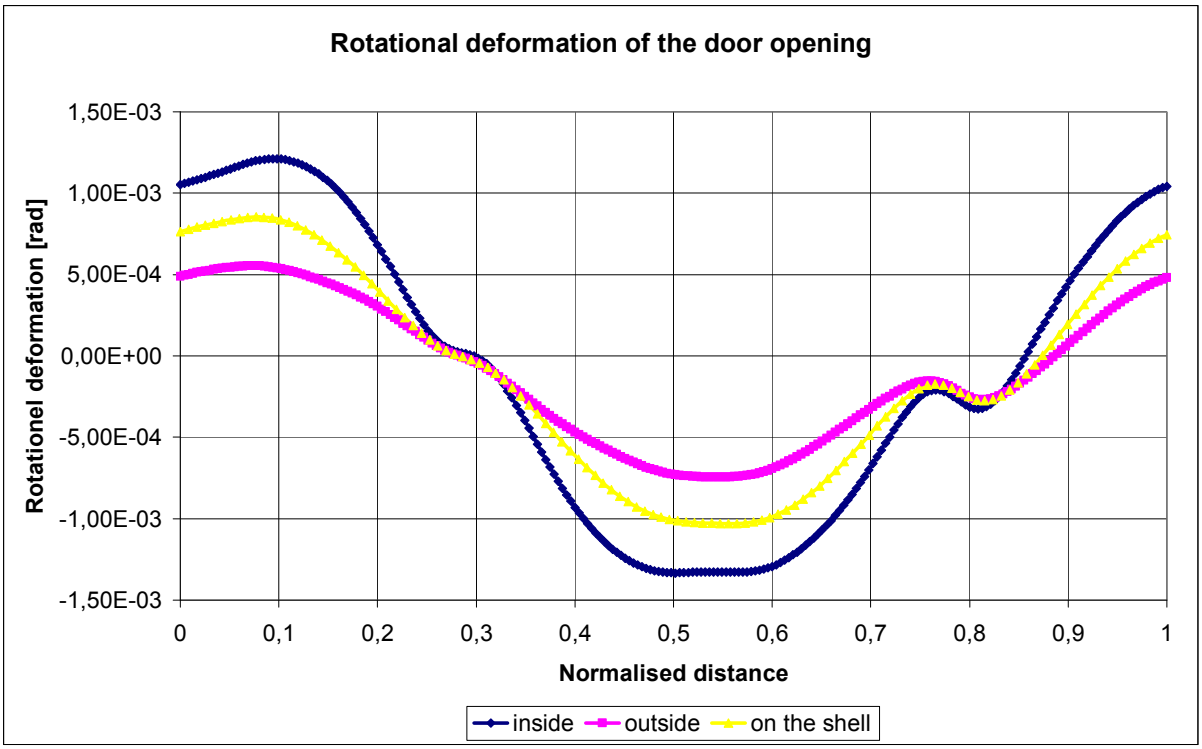

Figure 3.19: Rotational deformation of the door opening at design load

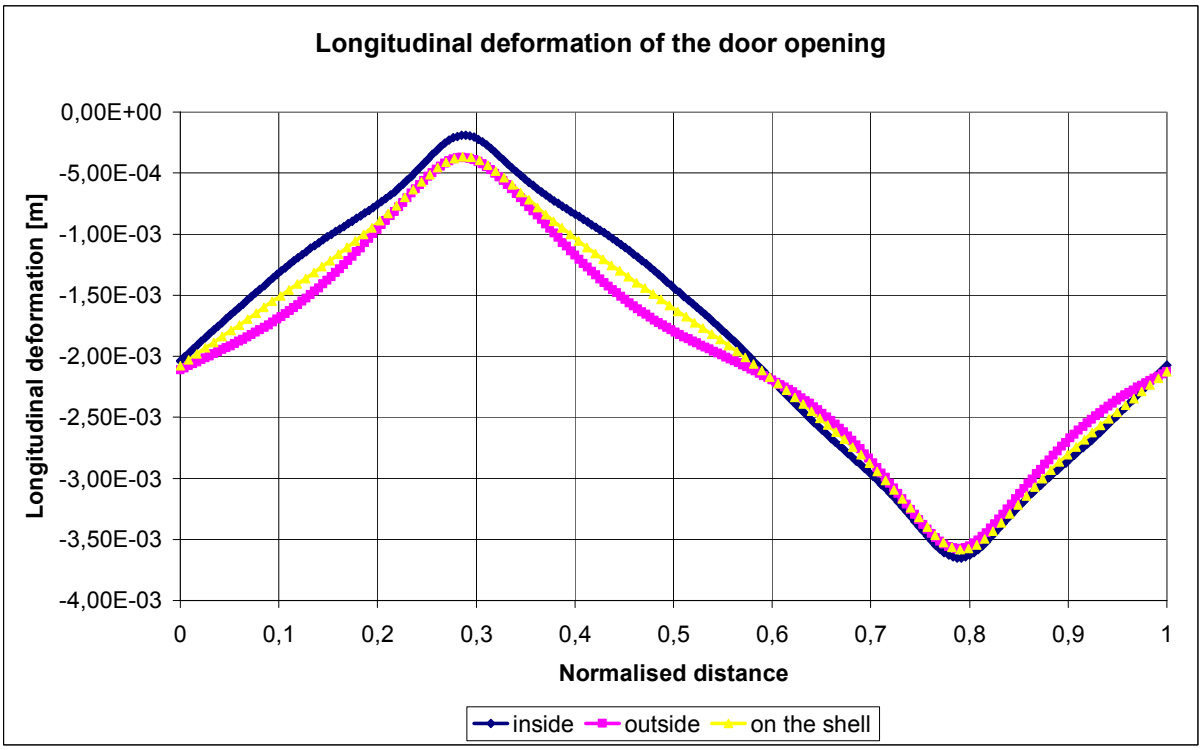

Figure 3.20: Deformation of the door opening in longitudinal direction at design load

The biggest difference between the maximum and the minimum value of the displacement values around the door opening at the edge of the shell were calculated to give an impression of the occurred deformation. Table 3.2 show the results of this calculation and a comparison can be made of the different models with original shell thickness and varied stiffener thickness. The values are taken from the path around the door opening on the tower shell.

Table 3.2: Maximum difference of the deformation values in the simulation models with varied stiffener thickness

	Model 1	Model 4	Model 5
Displacement in	[mm]	[mm]	[mm]
radial direction	3,67	3,68	3,97
longitudinal direction	3,22	3,43	3,71
	[rad]	[rad]	[rad]
rotation	1,88E-03	2,04E-03	2,29E-03

The deformation values show slight differences but this should not influence the function of the door. The shell structure seems to resist the occurring deformation and the stiffener has only a slight influence.

The measured deformation on the different edges of the stiffener also show differences. The result is printed in Table 3.3: Maximum difference between the stiffener edge inside and outside of the tower. The stiffener deforms different on both sides but the difference is rather small and an influence into the function of the door is probably not possible to find.

Table 3.3: Maximum difference between the stiffener edge inside and outside of the tower for model 1

	Model 1
Displacement in	[m]
Radial direction	1,22E-04
Longitudinal direction	1,84E-04
	[rad]
rotation	6,58E-04

The function of the door or the influence of the structure which is built into the door opening cannot be analysed because of a lack of available information. Figure 1.1 shows the door opening of the tower. It is visible that the door is not built directly into the stiffener. Instead a cover and a door are added into the stiffener. The influence of this structure is neglected in this report.

3.2 Investigation of non linear effects at the lower tower section

3.2.1 The buckling phenomena and properties of the model used for the buckling analysis

The safe design of shell structures against failure by buckling requires the designer to understand many complicated phenomena. The behaviour of a shell before, during and after buckling is very sensitive to the geometry, geometric imperfections and to the boundary conditions. All these factors make this part of structural mechanics challenging to understand.
Shells differ radically from other structural forms, most experiments show that the strength is often far below the calculated buckling load, which is calculated using simple stability theory. The stability of a shell is controlled by the membrane stresses in the shell wall.
In general, two ways are known in which an elastic structure may become unstable. These are usually named snap-through buckling and bifurcation buckling. These two cases are mentioned and explained in the following chapters. [3]

The imperfections used in the model were chosen in percent of the shell thickness. The model used here works with a perturbation pattern of the structure provided by a previous buckling analysis. The perturbation pattern is the shape of the first eigenmodes. The Eurocode 3 provides three geometrical relevant tolerances for buckling which are known to have a large impact on the structure.

These three tolerances are:

- Out-of-roundness
- Unintended eccentricity
- Dimple tolerance

These imperfections are provided in a form to measure the geometry on an existing structure to tolerances given in Eurocode 3.
More possible forms of imperfection exist but these are not further mentioned in detail.

The simulation does not directly include one of this tolerances but the dimple tolerance was used to achieve an imperfection value which was introduced in the model. The recommendations for the tolerances give an impression of in which quality structures are built and should be built.

3.2.1.1 Snap-through buckling:

The geometry of the structure changes as the load increases. The changed geometry has a lower stiffness than the undeformed shape and is due to this unstable. The deformed structure stays in its deformed shape until a local maximum load is reached; this load is called snap-through load or limit load P_{lim}. The structure buckles rapidly at this point. The material which was deformed in one direction experiences a jump in the opposite direction and comes to rest there. The shape is now stable. After this has happened the structure undergo large deformations and the shape at the region where the snap-through occurred has usually the inverted shape of the original structure.

The behaviour of a snap-through buckling case is to be seen in Figure 3.21, where an arch carries an eccentric load. Figure 3.22 shows the load-displacement response of the arch. Note that the displacement printed on the abscissa is not measured at a point that snaps through. The structure is loaded from point 1 to 2 and at point 2 the limit load is reached. Between point 2 and 3 the geometry of the structure snaps through. Beginning from point 3, the structure deforms further because its changed geometry.

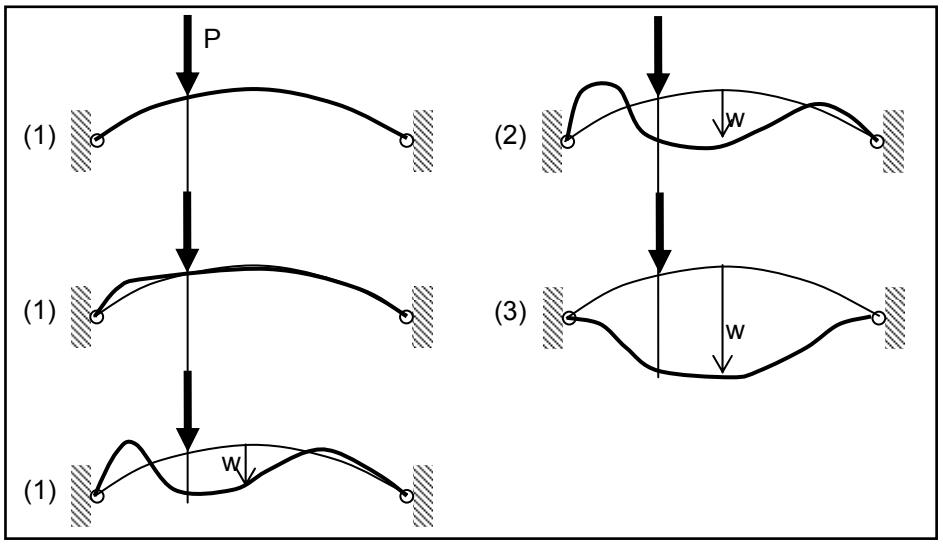

Figure 3.21: Example for a snap-through buckling case [3]

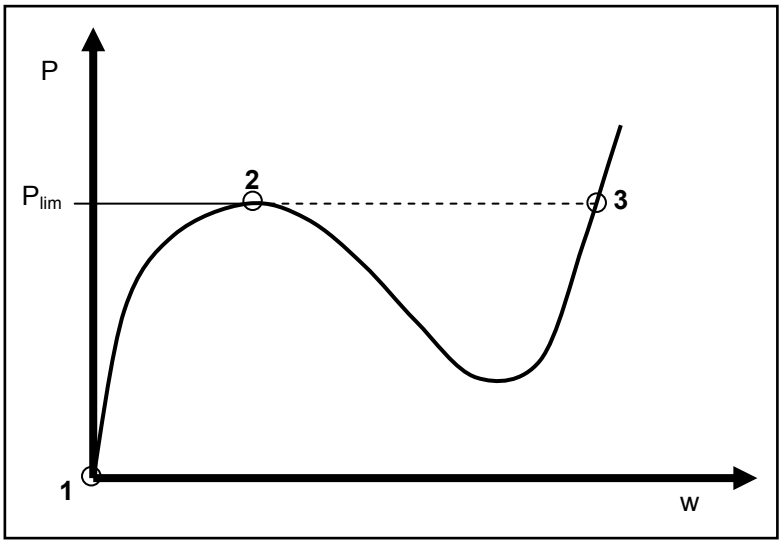

Figure 3.22: Load displacement response for snap-through buckling [3]

3.2.1.2 Bifurcation buckling:

The beam shown in Figure 3.23 is an example for bifurcation instability. Bifurcation instability occurs when two paths passes through the same point. The two possible, different geometries of the structure are also shown in Figure 3.23. A typical bifurcation in a load-deflection diagram is shown in Figure 3.24. The pre-buckling equilibrium path, starting from the origin, is intersected by the post-buckling path at the bifurcation point. The pre-buckling path is a stable condition for the structure until the bifurcation point is reached, thereafter it becomes unstable and a sudden departure from the pre-buckling path to the post-buckling path may occur. After the bifurcation of the beam, the deformation begins to grow in a new pattern. This is referred to as the buckling mode and it is usually different from the pre-buckling deformation pattern.

The buckling simulation contains the introduction of imperfections into the model geometry. The reference model is without imperfection so that the influence of increased imperfection values is visible.
All real structures are imperfect; imperfections can take the form of geometric imperfections, loading asymmetries, imperfectly realised boundary conditions, residual stresses or local thickness variations. The most important and most studied effects are those related to geometric imperfections of the shape. The load-deflection path of an imperfect structure is usually close to that of the corresponding structure but diverges from it.

Figure 3.24 shows the graph of the bifurcation buckling of a column under axial compression. Figure 3.23 shows the column, its loading and its shape of the primary and secondary deformation.

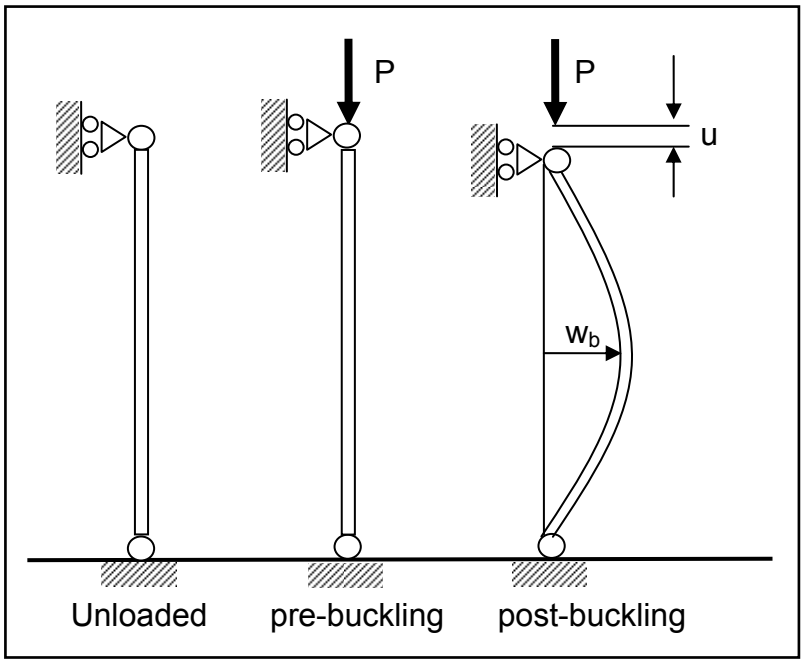

Figure 3.23: Column under axial compression [3]

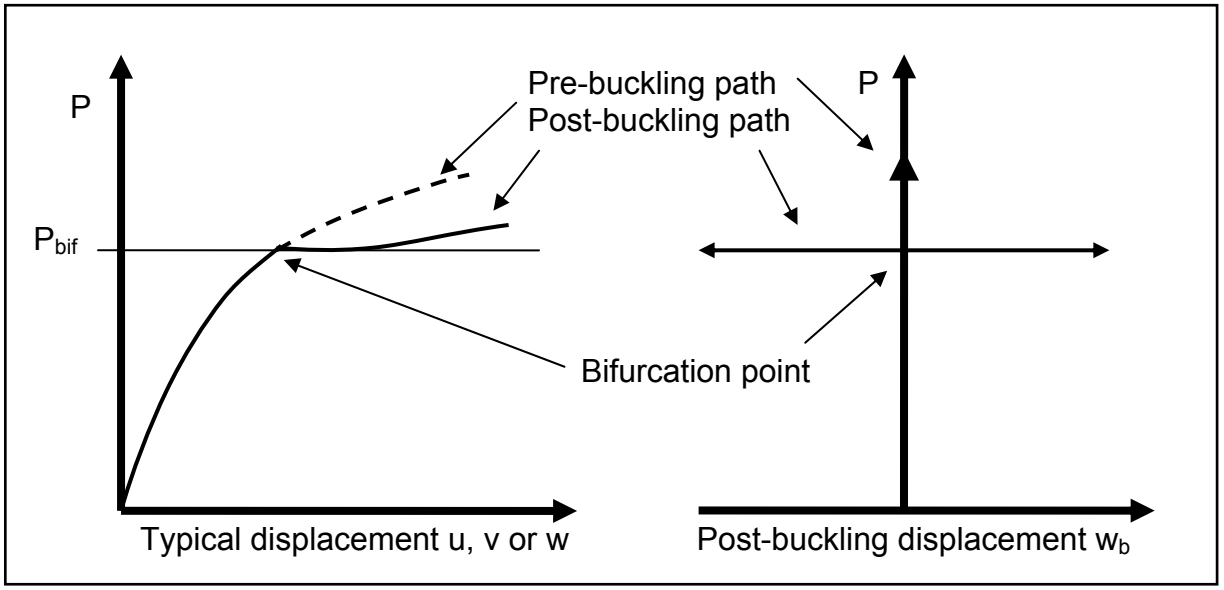

Figure 3.24: Bifurcation buckling on a column [3]

3.2.1.3 Imperfection values introduced to the model

After the buckling simulation was carried through, normalised displacements imperfection was introduced into the model. An imperfection pattern was the first used Eigenmode shape of the structure. Figure 3.25 shows the first Eigenmode shape of the lower tower section. The highest normalised displacement of the Eigenmode shape is proportional to the imperfection scaling factor which is introduced into the input file of the following static analysis. The normalised displacement of the Eigenmode shape and the imperfection scaling factor are multiplied and result in the imperfection amplitude. The imperfection amplitude changes the perfect structure to geometry with a deformation before load is applied on the model.

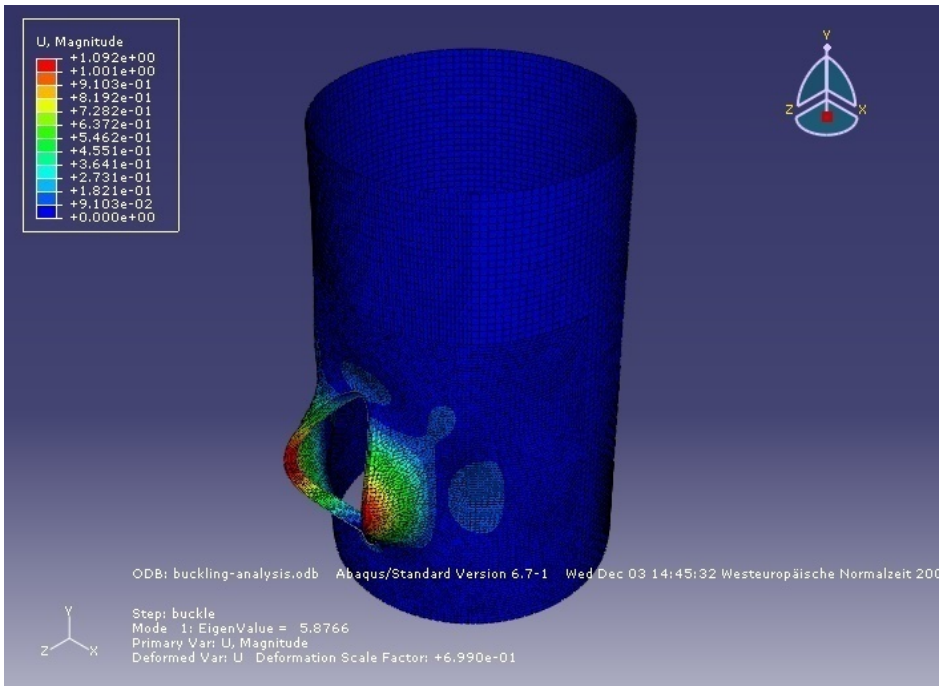

Figure 3.25: First Eigenmode shape of the lower tower section

Eurocode 3 provides values for dimple imperfection amplitude parameters and a calculation method for the amplitude of geometric imperfection. In Table 3.4 are the values for the dimple imperfection amplitude parameter and the resulting initial depth visible. The dimple parameter and Eqt. 3-1 were used to calculate the amplitude of geometric imperfection. The properties of the used simulation models for the investigation of the influence of varied imperfections are printed in Table 3.5.

Table 3.4: Dimple imperfection amplitude parameter U_n and amplitude of the geometric imperfection Δw depending on the fabrication quality class [3]

Fabrication tolerance quality class	Description	Value of U_n	Geometric tolerance normal to the shell surface Δw [m]
Class A	Excellent	0,010	0,0102
Class B	High	0,016	0,0163
Class C	Normal	0,025	0,0254

Eqt. 3-1 $$\Delta w = U_n \cdot 4 \cdot \sqrt{r \cdot t}$$

The radius of the structure is r=2,15m and the material thickness is t=0,03m.
The imperfection amplitudes provided by Eurocode are relatively high. The reason for this is the attempt to account for those imperfections that are not measurable. For this reason, the imperfection amplitude introduced to the model is effectively an equivalent imperfection.

The imperfection amplitude of fabrication tolerance quality class A was neglected in the simulations and an additional lower imperfection was added.
Furthermore were two higher imperfection amplitudes analysed. These imperfections are, regarding to Eurocode, not realistic and included only as additional information.

Table 3.5: Properties of the simulation models used for the investigation of the tower behaviour with steel S355 and varied imperfection amplitude

Simulation model name	Yield strength	Shell thickness t_1 in Section 1 and 2	Shell thickness t_2 in Section 3	Stiffener thickness	Imperfection amplitude δ	δ/t_1
	[MPa]	[m]	[m]	[m]	[m]	
Model 6	360	0,030	0,026	0,070	0	0
Model 7	360	0,030	0,026	0,070	0,0060	0,20
Model 8	360	0,030	0,026	0,070	0,0163	0,54
Model 9	360	0,030	0,026	0,070	0,0254	0,85
Model 10	360	0,030	0,026	0,070	0,0330	1,10
Model 11	360	0,030	0,026	0,070	0,0900	3,00

As reference was a model without imperfection generated. The models with added imperfection were then compared to the perfect structure and with this the influence of the imperfection were visible. Some imperfection amplitudes introduced in the model are chosen very high, just to point out the influence of imperfections.

The provided imperfection amplitudes and values for the calculation from Eurocode are meant for shells without opening. The influence of the door opening on imperfection values is not mentioned in Eurocode.
The fabrication quality of the state of the art tower is also not know and therefore not further mentioned.

3.2.2 Results of the buckling analysis with varied imperfection

3.2.2.1 Ultimate load of the buckling analysis with varied imperfection

The buckling analysis provided results with similar tendency, compared to simulations with shell or stiffener thickness variation. Figure 3.26 shows the result for the load-displacement response depending on the imperfection value.

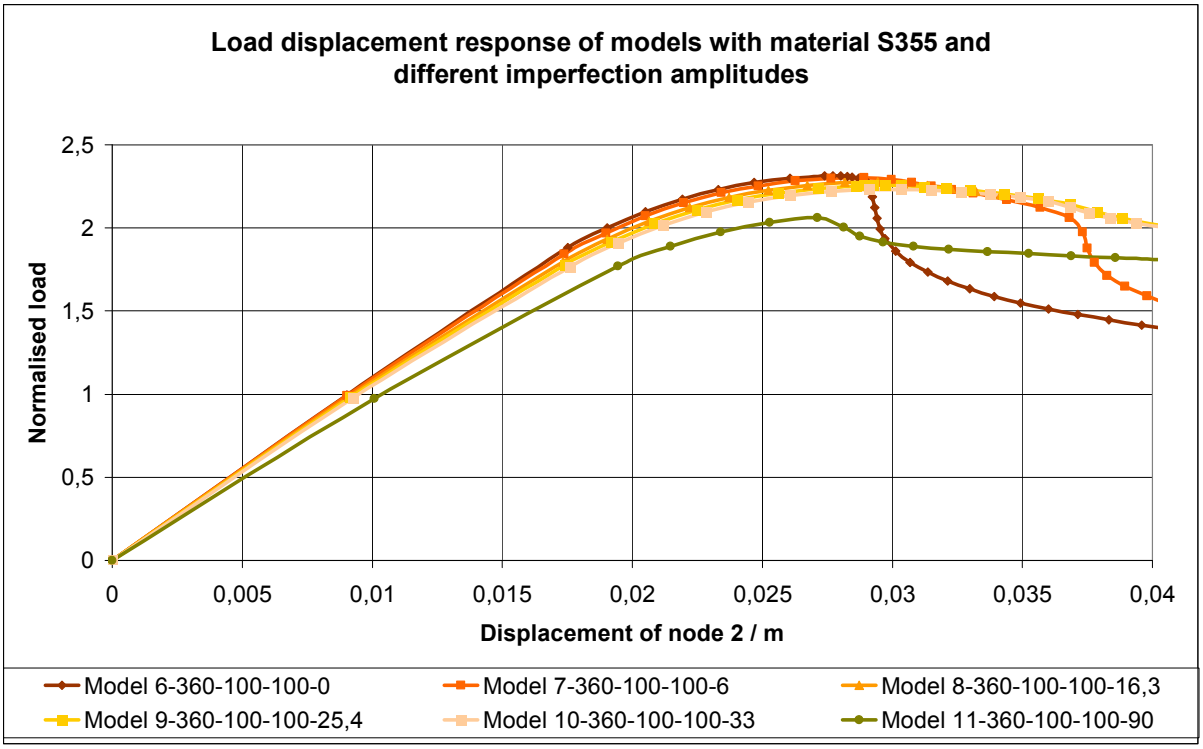

Figure 3.26: Load displacement response at node 2 depending on the imperfection value

The stiffness of the structure and the maximum load is decreasing with increasing imperfection values. This is logic because the structure weakens with introduced imperfections. Except of model 11 with 90mm imperfection amplitude, all models show similar stiffness until design load. The decrease of the ultimate load from model 6 to model 10 is only about 4%. The sensitivity of the structure regarding imperfections seems to be small.

Following the graph in Figure 3.27 it is visible that with increasing imperfection value the resistance of the structure drops rapidly. The maximum bearable loads of the buckling analysis have to be handled with care regarding to imperfection. The used imperfection pattern is mathematical generated and does not represent real imperfections which have many different forms. Local imperfections are not introduced into the model.
The lowest ultimate load reached in the simulations is still more than two times higher than the load value from the design load table. This high difference gives certain reliability that local imperfections in the real structure does not cause collapse at the lower part of the tower.

The structure does not seem to be very sensitive to imperfections around the door opening. The reduction of the ultimate load in the models with imperfections up to 100% of the shell thickness is marginal. The decrease of the ultimate load is less than 4%. The highest imperfection introduced into the model is unrealistically high for state of the art tower productions and can be neglected.

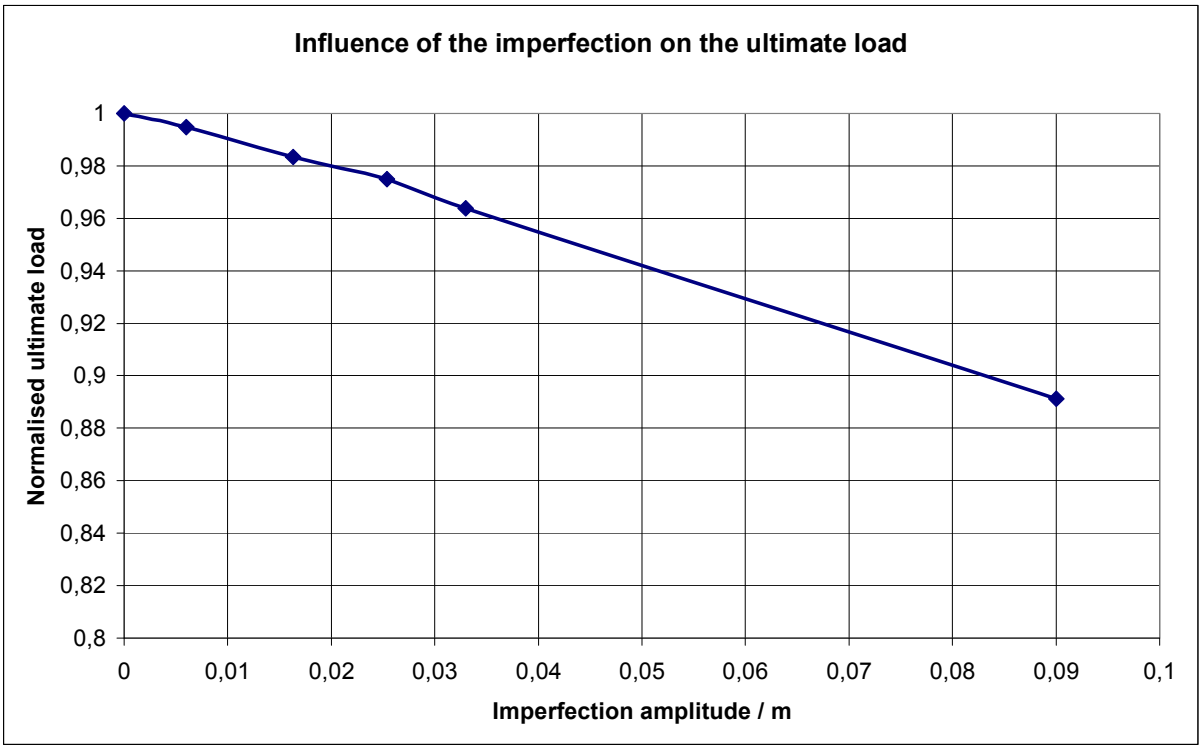

Figure 3.27: Influence of the imperfection amplitude on the ultimate load

3.2.2.2 Stress distribution around the door opening in the buckling analysis with varied imperfection

Similar as to in the parametric study, the stress distribution around the door opening was taken into account. The values of the Mises stress over the normalised distance of the door circumference for selected models are plotted in Figure 3.28. The models visualised in Figure 3.28 are model 6 without imperfection, model 7 with imperfection amplitude 6mm and model 9 with imperfection amplitude 25,4mm. Model 9 regards to the highest imperfection suggested by the design recommendations of Eurocode. The stresses achieved in the simulations do not reach the yield strength. Another conclusion is that with increasing imperfection value, the peak value of the stress that occurs above and below the door opening increases.

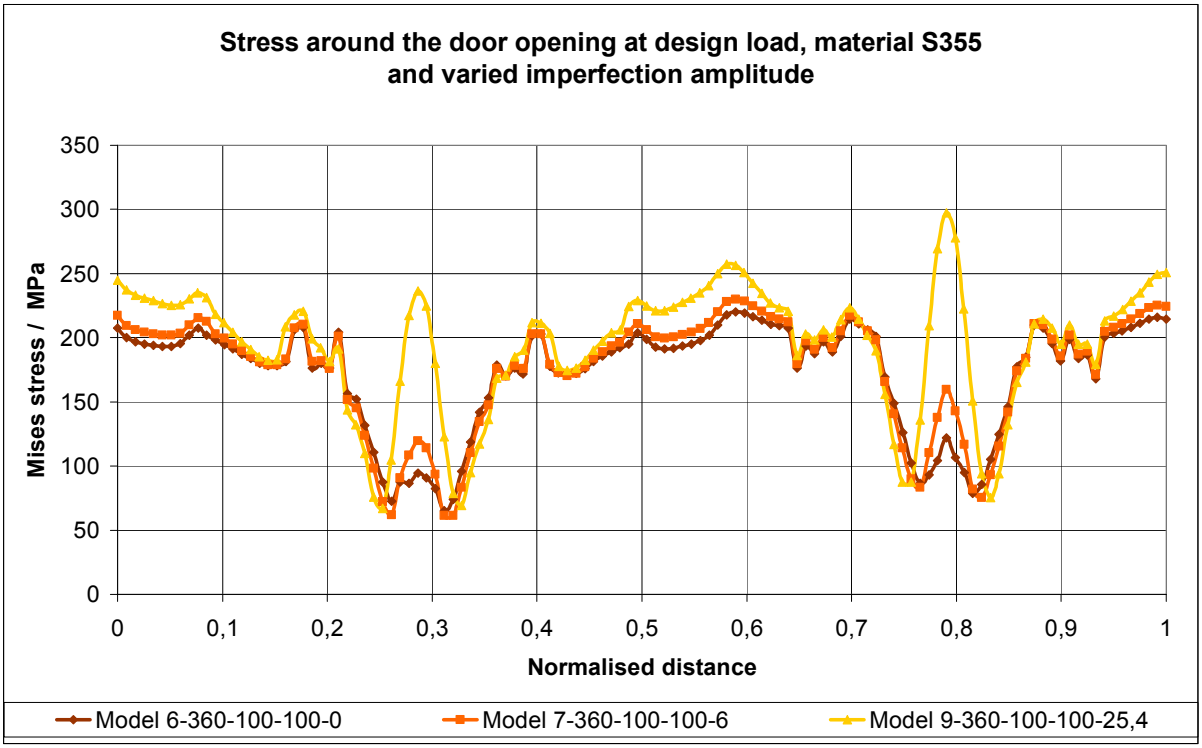

Figure 3.28: Stress distribution around the door opening at design load for models with varied imperfection amplitude

An important factor is to know when the structure starts to yield. From Figure 3.29 till Figure 3.34 is the development of the stress on the tower section presented, the pictures correspond to the simulation with the highest imperfection value. The simulations with lower imperfection amplitudes show similar failure modes and are therefore not plotted.
Load frame 1 regards approximately to the design load and load frame 2 to around 1,77 times the design load. Because Abaqus did not provide a frame in between this two calculation points, it is not possible to say at which point the structure begins to yield exactly. In Figure 3.29 it is visible that yielding started early at the first spot. This result has to be handled with care because the imperfection value applied into the model was already very high and probably unrealistic for the real structure.
In this simulation, it is good to see that the joint between section 2 and section 3 also is a weak point. The following figures are just an overview and they are printed in full size in appendix G.

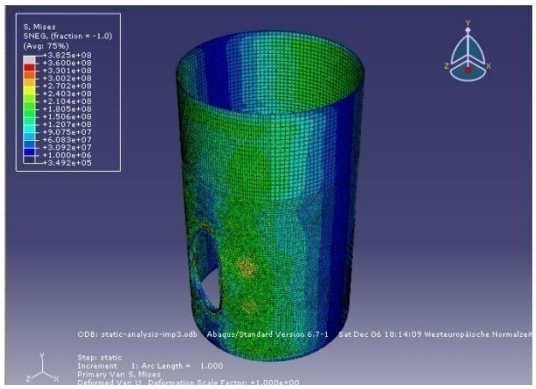

Figure 3.29: Model 11, 98,6 % load

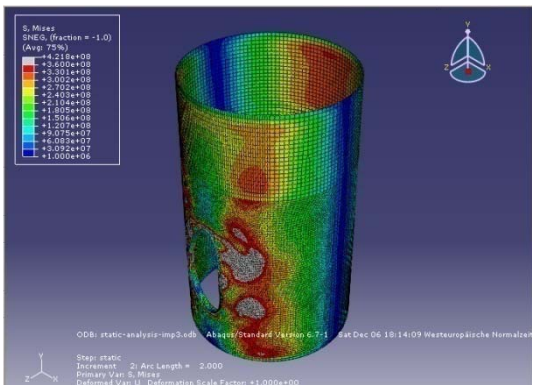

Figure 3.30: Model 11, 179,6 % load

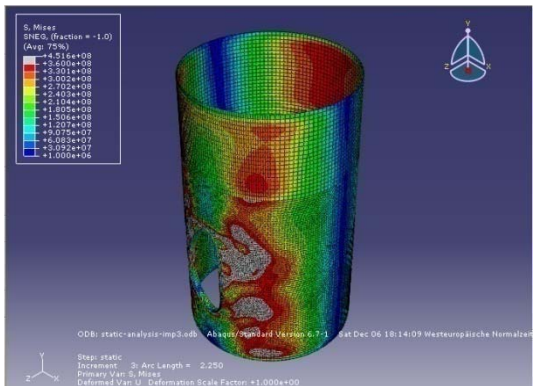

Figure 3.31: **Model 11, 193,2 % load**

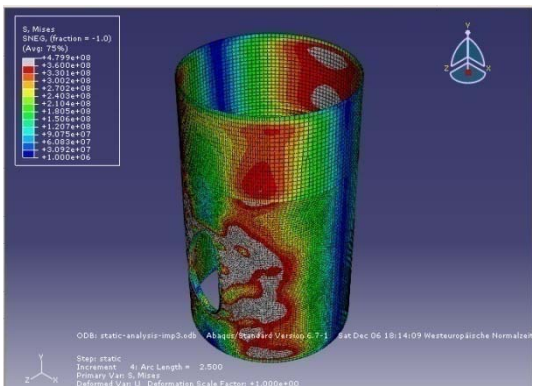

Figure 3.32: Model 11, 203,9 % load

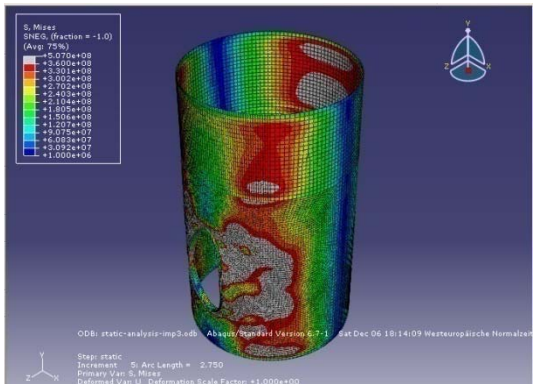

Figure 3.33: Model 11, 212,3 % load

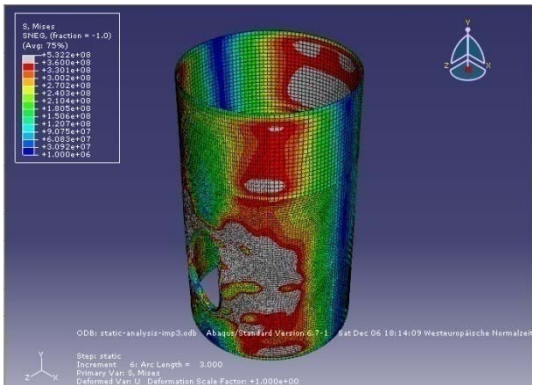

Figure 3.34: Model 11, 218,4 % load

3.2.3 Buckling analysis of the model with varied stiffener thickness

In the parametric study of the state of the art tower, it was concluded that a reduction of the shell thickness is not possible because of stress that exceed the yield strength. This fact was not valid for the models with varied stiffener thickness. A model without imperfections was used in the parametric study. The following buckling analysis introduces an imperfection of 20% of the shell thickness into the model.

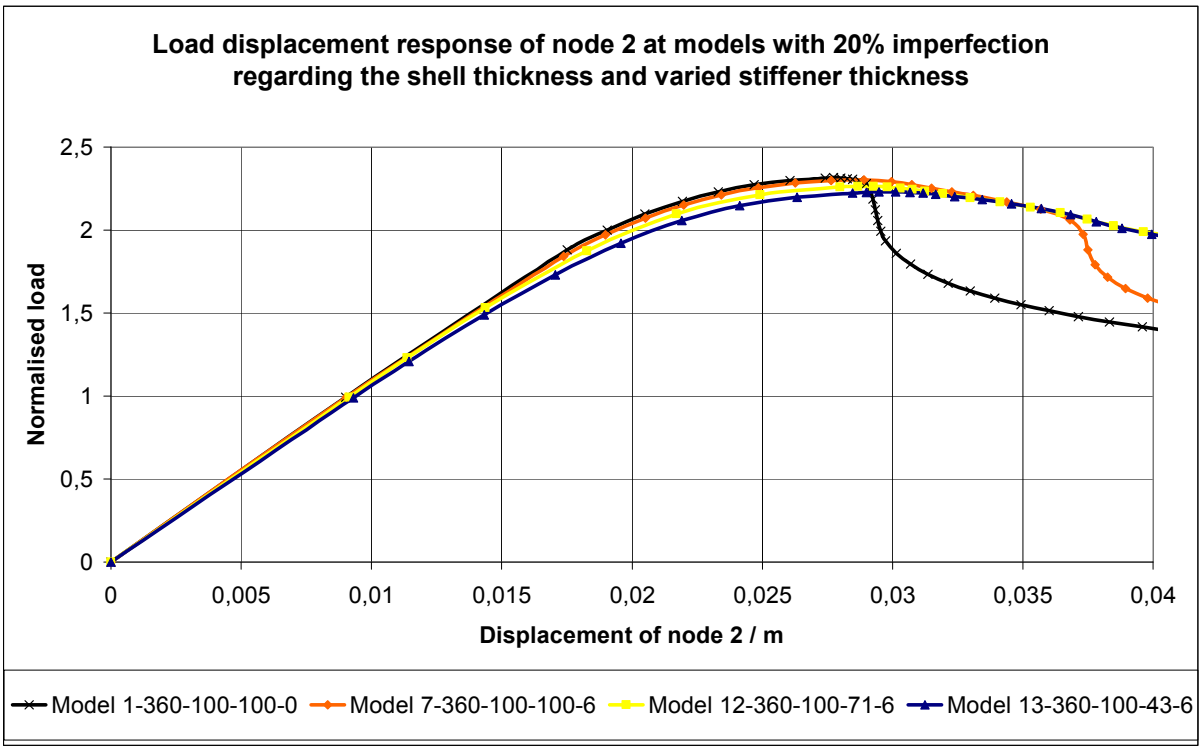

Figure 3.35: Load displacement response of node 2 at models with varied stiffener thickness and 20% imperfection regarding the shell thickness

The load displacement response of the models with different stiffener thickness is plotted in Figure 3.35. The influence of the reduced stiffener thickness is clearly visible but the difference in stiffness and ultimate load is not very high. The reduction of the ultimate load from the perfect structure to the model with the lowest stiffener thickness is at about 3,6%. The reduction of the stiffener thickness shows nearly no influence at the point of design load. The displacement of node 2 in radial direction is at design load approximately the same in all models and varies only about a tenth of a millimetre.

The stress on the tower shell at the door opening was the point of interest because the highest stresses occurred around the opening. With the introduced imperfection and at design load, the values of the stresses were plotted. Figure 3.36 shows the result of the analysis.

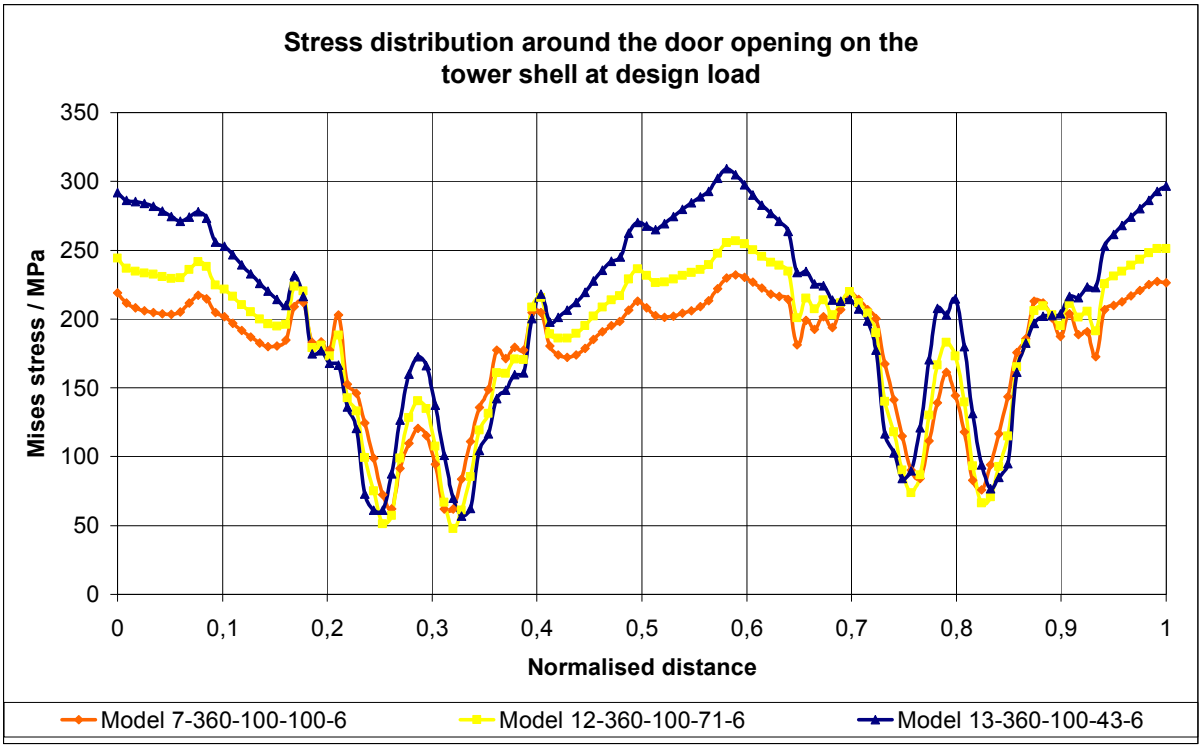

Figure 3.36: Stress distribution around the door opening of the tower shell of models with varied imperfection amplitude at design load

Compared to the result of the stress analysis of the parametric study, the values are higher. This difference is caused by the imperfection introduced into the model. The stress values do not reach the yield strength of the material and only the model with a stiffener thickness equal to the shell thickness shows stress values over 300MPa. From this point of the analysis, a reduction of the stiffener thickness is still possible. A side effect of the stiffener thickness reduction is that the highest stress values on the tower shell are no longer to be found. Instead, the stiffener itself shows higher stress values. In Figure 3.37 is the stress distribution around the stiffener inside of the tower printed. The position of the extraction path is presented in Figure 3.17 in the picture on the right.

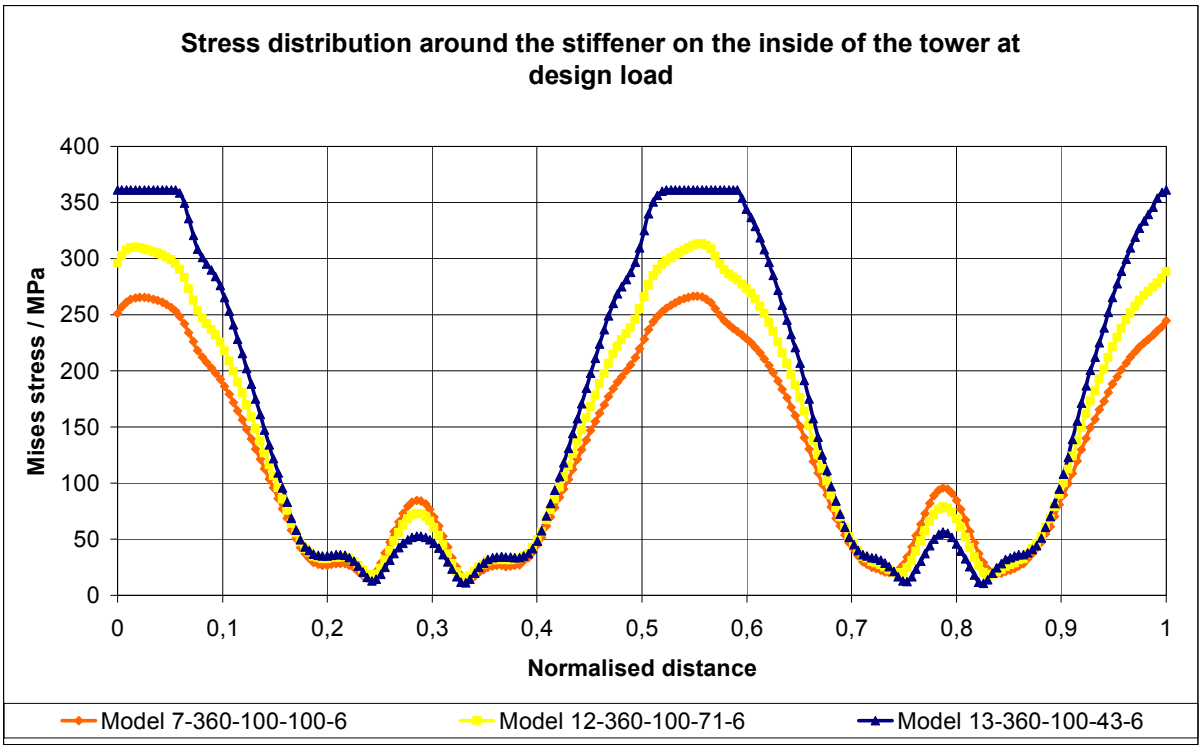

Figure 3.37: Stress distribution around the stiffener on the inside of the tower of models with varied imperfection at design load

The stress distribution shows that the reduction of the stiffener thickness to only 30mm thickness is too radical. The stress reaches the yield strength and consequently, a failure would occur. A reduction of the stiffener thickness to 50mm is a possible way of reducing the material. The increase of the maximum stress value is high but does not exceed the value of 315MPa.

In the fatigue analysis for model 2, described in Chapter 3.1.3, the stress on the tower shell as well as on the stiffener inside the tower reaches around the same values. The introduction of imperfection to the model would increase the stress value slightly but the safety against failure is high.
In the fatigue analysis, the maximum stress reached only 20% of the fatigue strength. Therefore, it is at this point of the report no fatigue analysis of the stiffener included.

3.2.4 Analysis of models with material changed to high strength steel and varied imperfections

The influence of a change of the material was further investigated in a buckling analysis. The used material for model 15 and model 16 is the high strength steel described in chapter 2.1.2. Model 7 describes the state of the art tower designed with the steel S355 described in chapter 2.1.1

The different shell thicknesses correspond with the changes from the parametric study, see chapter 3.1.

As imperfection value was 20% of the respective shell thickness of section one and two introduced into the model.

In another approach, the high strength steel material was used and the tower properties kept at its origin. The imperfection of the model was varied and which imperfection value that reduces the ultimate load to the level of the state of the art tower was investigated.

A third variation of the model is added in this chapter. The model uses high strength steel as material and the geometry has reduced shell and stiffener thickness. A higher imperfection was also introduced.

The properties of the simulation models are printed in Table 3.6.

Table 3.6: Properties of the simulation models used for the investigation of the tower behaviour with steel S690

Simulation model name	Yield strength	Shell thickness t_1 in Section 1 and 2	Shell thickness t_2 in Section 3	Stiffener thickness	Imperfection amplitude δ	δ/t_1
	[MPa]	[m]	[m]	[m]	[m]	
Model 7	360	0,030	0,026	0,070	0,006	0,2
Model 14	690	0,030	0,026	0,070	0,006	0,2
Model 15	690	0,020	0,017	0,070	0,004	0,2
Model 16	690	0,015	0,013	0,070	0,003	0,2
Model 17	690	0,030	0,026	0,070	0,030	1,0
Model 18	690	0,030	0,026	0,070	0,060	2,0
Model 39	690	0,020	0,017	0,050	0,021	0,7

3.2.4.1 Comparison of the models with an imperfection amplitude of 20% respective the shell thickness and material S355 and S690

The criterion that was of highest interest is the stress distribution around the door opening. A possible change to high strength steel offers the possibility to reduce the material thickness of the tower shell. On the other hand, a reduction of the material thickness leads to an increase of the stress in the material.
To compare the results between the models, the Mises stress around the door opening is normalised to the corresponding yield strength.

As it is visible in Figure 3.38 model 7 uses the material at design load, at its maximum stress, until a level of about 65% of the yield strength. Model 15 uses at maximum stress the material until around 60% of its yield strength. Because of this, a further reduction of the material would be possible. Model 15 is also generally lower in the normalised stress level. Model 16 is too radical in thickness reduction and the result is that the yield strength is exceeded at design load.

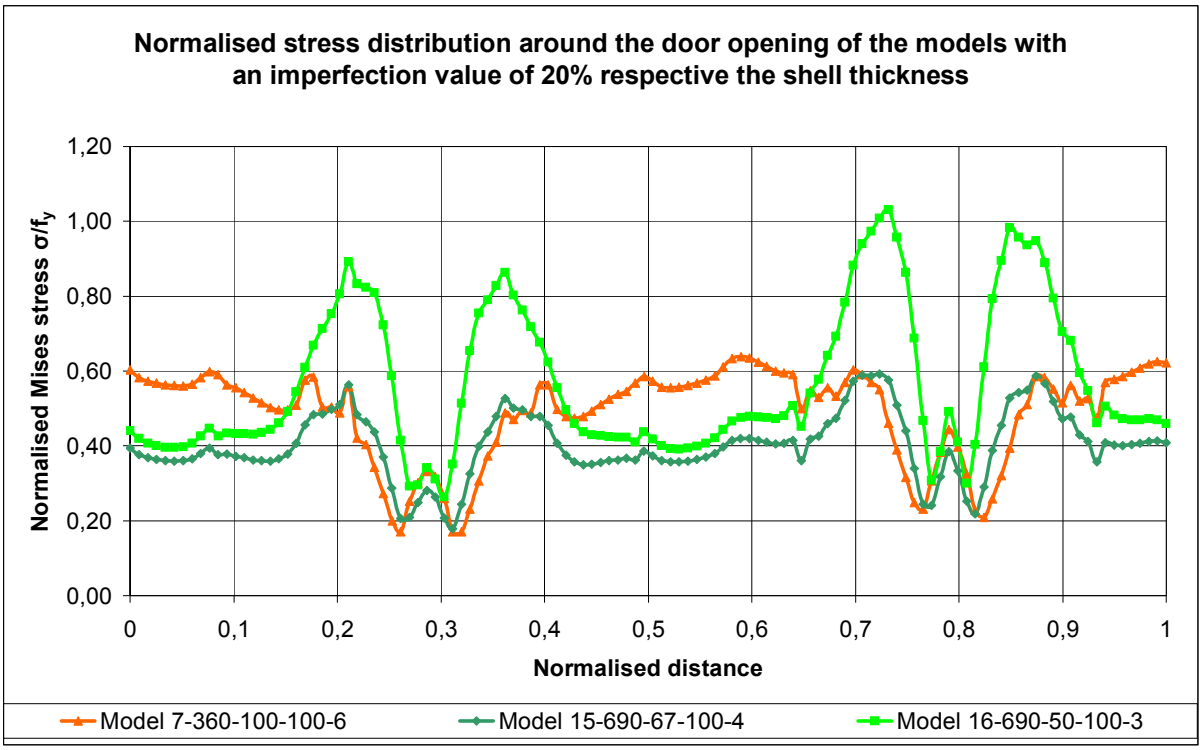

Figure 3.38: Normalised stress distribution around the door opening of models with varied shell thickness and proportional imperfection amplitudes at design load

A change of the material to high strength steel with reduced shell thickness is possible. The change of the material would need further investigation of the whole structure. A reduced shell thickness lead to a lower weight of the structure and the Eigenfrequency of the structure would change. An analysis of this is necessary because the rotor passes the tower and creates a pressure difference on the structure. The pressure difference occurs rhythmically every time one of the three rotor blades are passing the tower. If the Eigenfrequency and the excitation frequency of the rotor is too similar a failure of the structure would occur because of resonance.

Another result is the load displacement response of the three models. The response is presented in Figure 3.39. As a logical consequence of the material reduction, the stiffness of the reduced structure and the linear part of the graph shows a lower slope.
The reduction of the ultimate load from model 7 to model 15 is about 12% and from model 7 to model 16 about 43%.

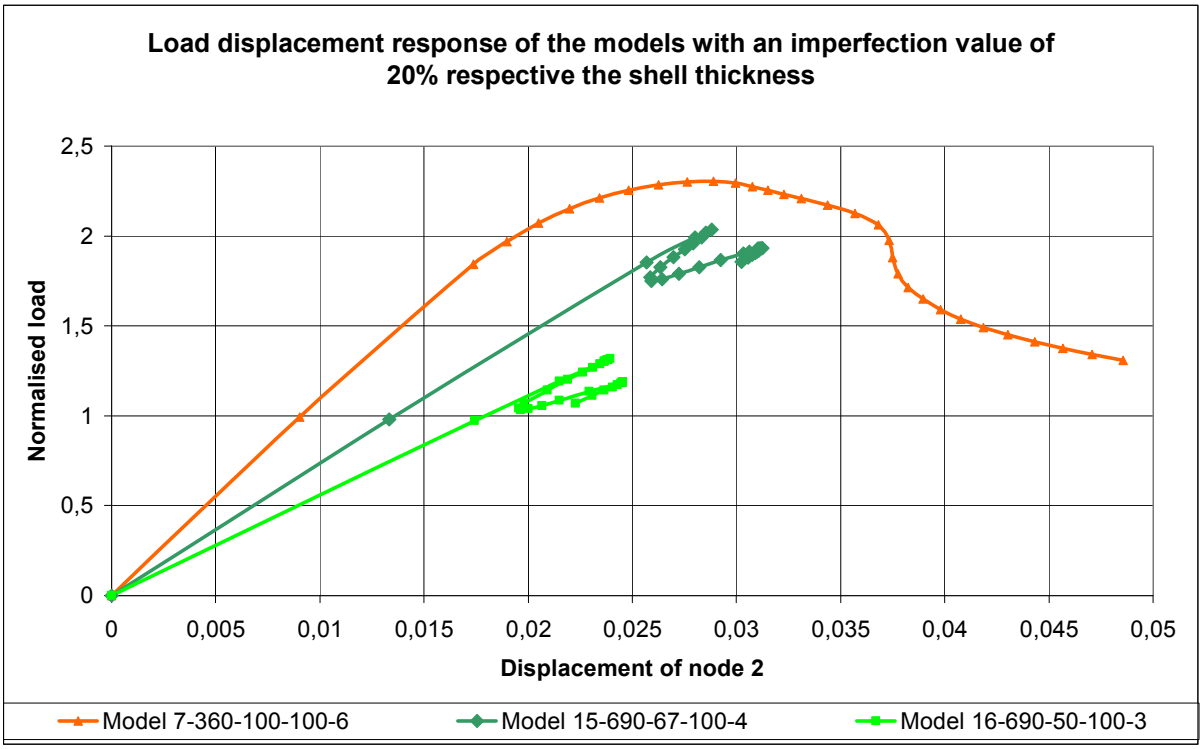

Figure 3.39: Load displacement response of the models with an imperfection value of 20% respective the shell thickness and varied shell thickness

Similar to the parametric study of different shell thicknesses with material fy=360MPa, are the graphs of the parametric study with the steel with fy=690MPa. Because of the higher strength of the material, the ultimate load reaches higher values.

The figures on the following page show the failure modes of the different models. The pictures show the structure at ultimate load and in the descending path. For the models 15 and 16, the lowest load after the ultimate load was chosen, and for model 7 the picture is taken at a load value of 1,97 in the descending path.
A scaling factor of ten was used to show the deformation clearly. The figures are only an overview and plotted in full size in appendix H.

As visible in the contour plots, the failure of the structure at ultimate load occurs around the door opening. The area of material that is yielding is smaller in the models with higher yield strength; the failure occurs more locally than in the model with lower yield strength. With higher material strength, the region between section two and three becomes less susceptible to failure. Model 7 also shows a region of yielding material between the sections. This does not occur in the other models.

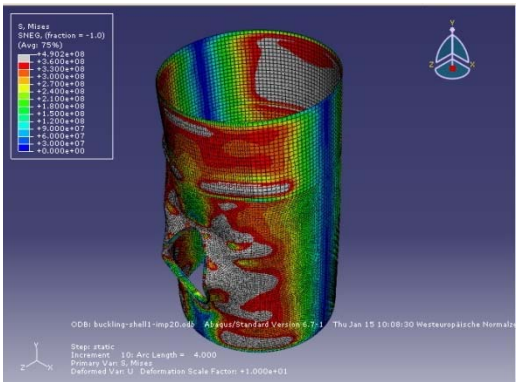

Figure 3.40: Model 7 at ultimate load

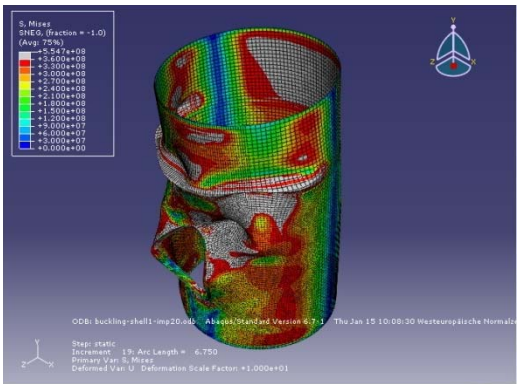

Figure 3.41: Model 7 at 197% load in the descending path

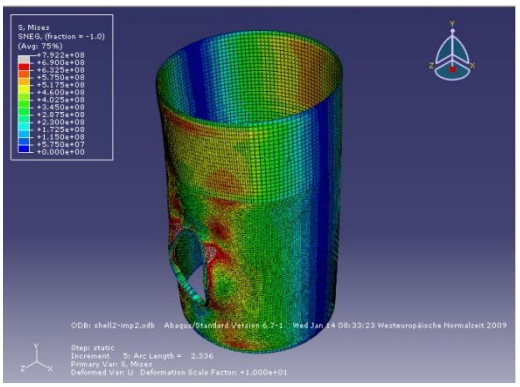

Figure 3.42: Model 15 at ultimate load

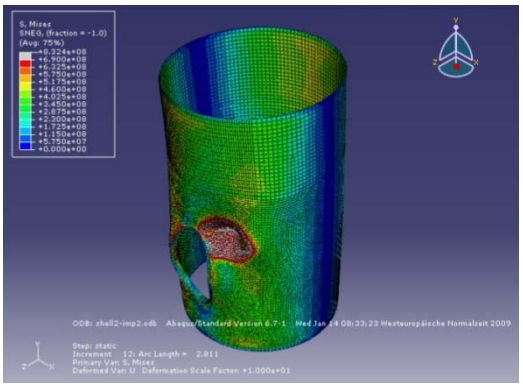

Figure 3.43: Model 15 at 175% load in the descending path

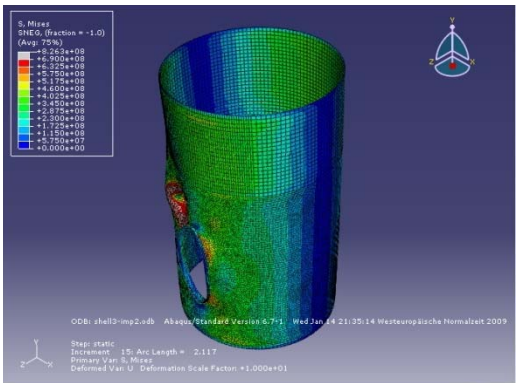

Figure 3.44: Model 16 at ultimate load

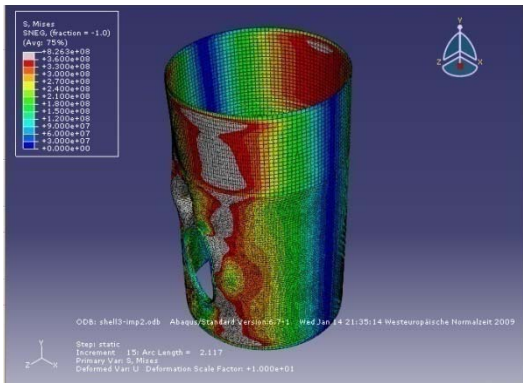

Figure 3.45: Model 16 at 103% load in the descending path

3.2.4.2 Comparison of the models with varied imperfection amplitude and material S690

In the following simulations was the influence of increased imperfection in the structure investigated. The reference is the state-of-the-art tower and it is compared to the tower with same geometry but with high strength steel as material. The only factor that was changed is the imperfection amplitude.

The simulations with the high strength steel material and the original tower geometry are presented in the following figures. In Figure 3.46 is the load displacement response of the original tower plotted and compared to the tower designed with high strength steel and varied imperfection. Model 14 equals model 7 with the exception that the material is changed from f_y=360MPa to f_y=690MPa. Model 17and 18 represent models with higher imperfection values.

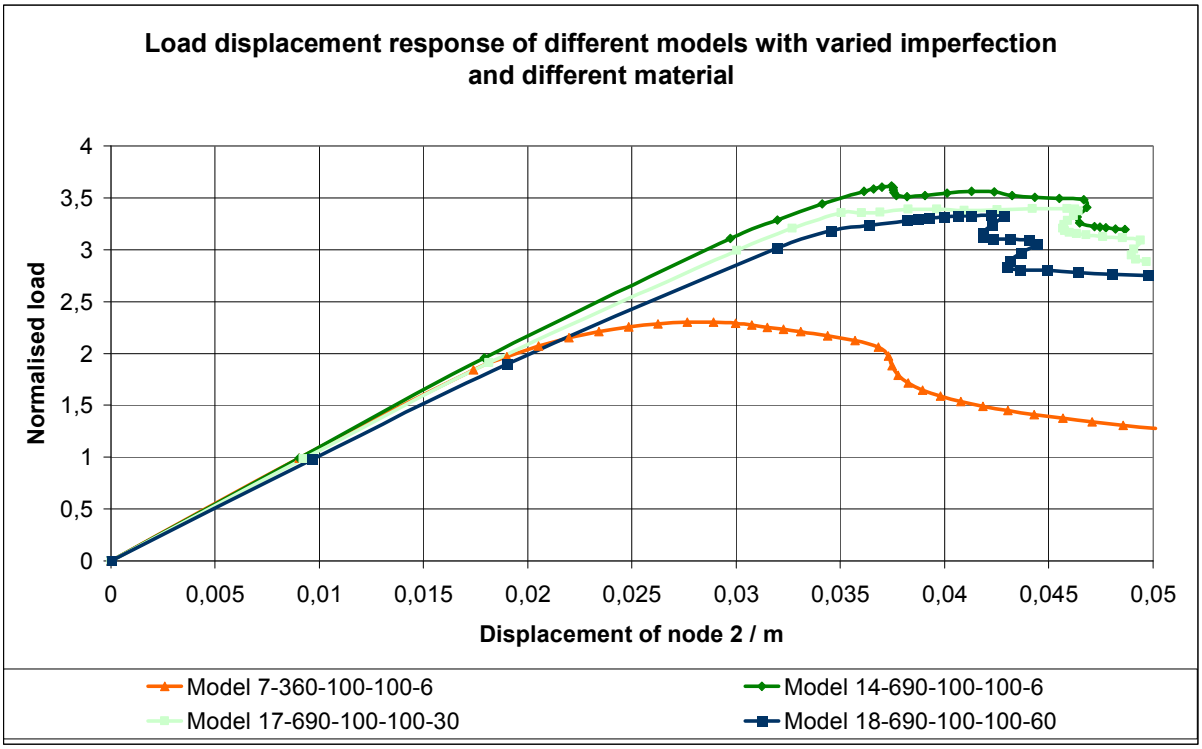

Figure 3.46: Load displacement response of the original tower and the tower with high strength steel using the original geometry and higher imperfections

The ultimate load reaches for both models with high strength steel values that are around 47% or 57% higher than the value of the original tower. The reduction of the ultimate load between the models with high strength steel is about 9% and shows the influence of an increase of the imperfection amplitude of the factor 5.
A reduction of the ultimate load to the same level as the original structure is only possible with extremely high imperfection values, which are unrealistic. Model 18 has already an imperfection of 200% of the shell thickness, which equals 60 mm imperfection amplitude. Such high imperfections are not expected in the real structure so that a further increase of the imperfection amplitude was not performed.

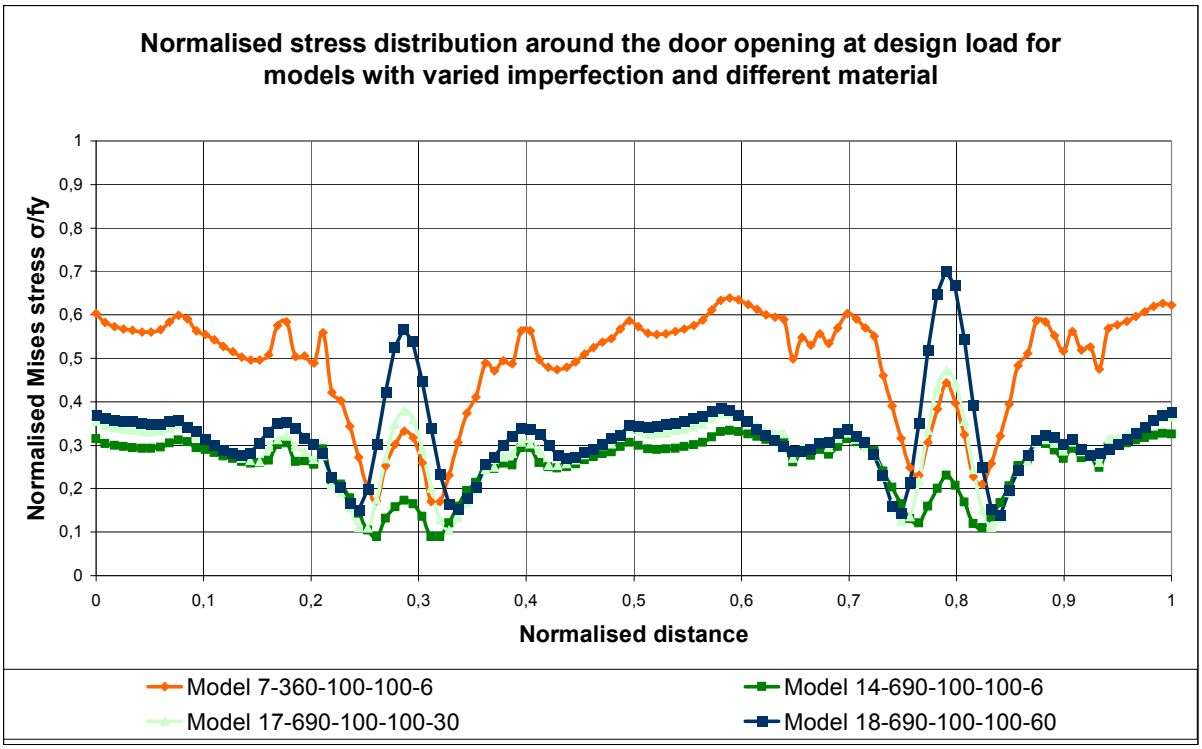

Figure 3.47: Normalised stress distribution around the door opening of the original tower and the tower with high strength steel using the original geometry at design load with higher imperfections

The stress distribution around the door opening is lower than in the original model. This is a logical consequence because of the higher yield strength of the material. The distribution around the door opening has a similar pattern as visible in previous stress distributions. Model 17 and 18 show the influence of increasing imperfection amplitude on the stress distribution around the door. The stress becomes higher on the top and on the bottom of the opening with increasing imperfection, which is visible at the normalised distance 0,28 and 0,78 in Figure 3.47. For model 17, the stress has at these points higher values than in the original structure.
Exceeding this stress value is without consequences because the stress value does not reach the 50% of the yield strength line. Model 18 has locally higher stress values than the original structure. The local stress concentration on top of the door opening has the highest stress value of all simulation but it is at design load still not higher than 70% of the yield strength.

Contour plots of model 14 and 17 are shown on the following page. Figure 3.48 and Figure 3.49 show model 14 at ultimate load and in the descending path. Figure 3.50 and Figure 3.51 show the same for model 17. The figures are only overviews and are printed in full size in appendix I.

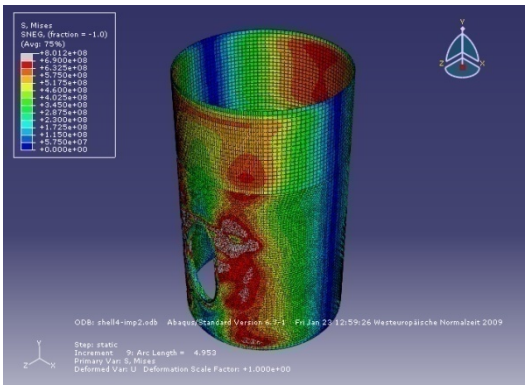
S, Mises
SNEG, (fraction = -1.0)
(Avg: 75%)
ODB: shell4-imp2.odb Abaqus/Standard Version 6.7-1 Fri Jan 23 12:59:26 Westeuropäische Normalzeit 2009
Step: static
Increment 9: Arc Length = 4.953
Primary Var: S, Mises
Deformed Var: U Deformation Scale Factor: +1.000e+00

Figure 3.48: Model 14 at ultimate load

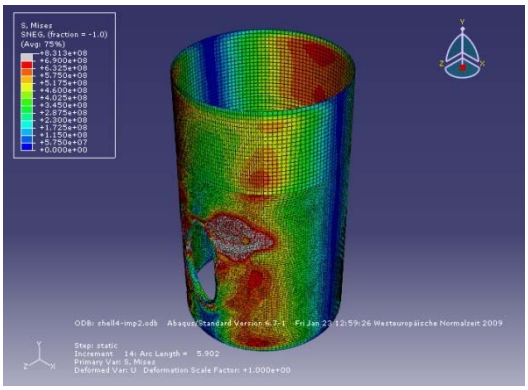
S, Mises
SNEG, (fraction = -1.0)
(Avg: 75%)
ODB: shell4-imp2.odb Abaqus/Standard Version 6.7-1 Fri Jan 23 12:59:26 Westeuropäische Normalzeit 2009
Step: static
Increment 14: Arc Length = 5.902
Primary Var: S, Mises
Deformed Var: U Deformation Scale Factor: +1.000e+00

Figure 3.49: Model 14 in the descending path

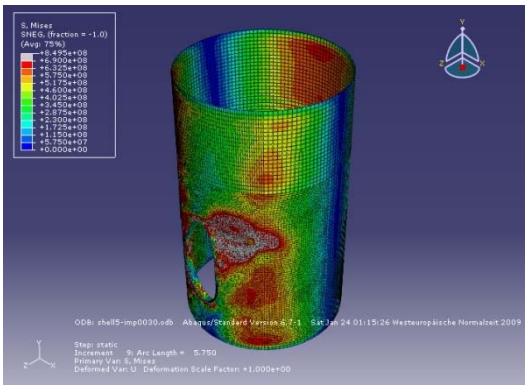
S, Mises
SNEG, (fraction = -1.0)
(Avg: 75%)
ODB: shell5-imp0030.odb Abaqus/Standard Version 6.7-1 Sat Jan 24 01:15:26 Westeuropäische Normalzeit 2009
Step: static
Increment 9: Arc Length = 5.750
Primary Var: S, Mises
Deformed Var: U Deformation Scale Factor: +1.000e+00

Figure 3.50: Model 17 at ultimate load

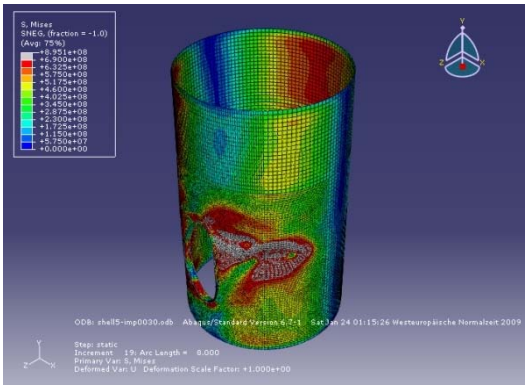
S, Mises
SNEG, (fraction = -1.0)
(Avg: 75%)
ODB: shell5-imp0030.odb Abaqus/Standard Version 6.7-1 Sat Jan 24 01:15:26 Westeuropäische Normalzeit 2009
Step: static
Increment 19: Arc Length = 8.000
Primary Var: S, Mises
Deformed Var: U Deformation Scale Factor: +1.000e+00

Figure 3.51: Model 17 in the descending path

3.2.4.3 Comparison between the state-of-the-art-tower segment and the segment with high strength steel and higher imperfection value

Previous chapters showed that a reduction of the tower shell and the stiffener thickness is possible. The reduction of the tower shell thickness is only possible with the use of high strength steel. A change of the stiffener is possible for the steel S355 and following the results of the analysis of the models using the high strength steel a reduction of the shell thickness is possible too. In chapter 3.2.4.1 was an imperfection of 20% used for the analysis of the shell thickness. The models with higher imperfections showed that their influence is not drastic for the stresses on the tower shell.

The following results compare the state of the art tower with perfect geometry and a higher imperfection to a model with reduced shell and stiffener thickness and the high strength steel as material for the tower.

Figure 3.52 shows the comparison between load displacement response of the model using high strength steel with reduced shell and stiffener thickness to the state of the art tower with higher imperfection values.

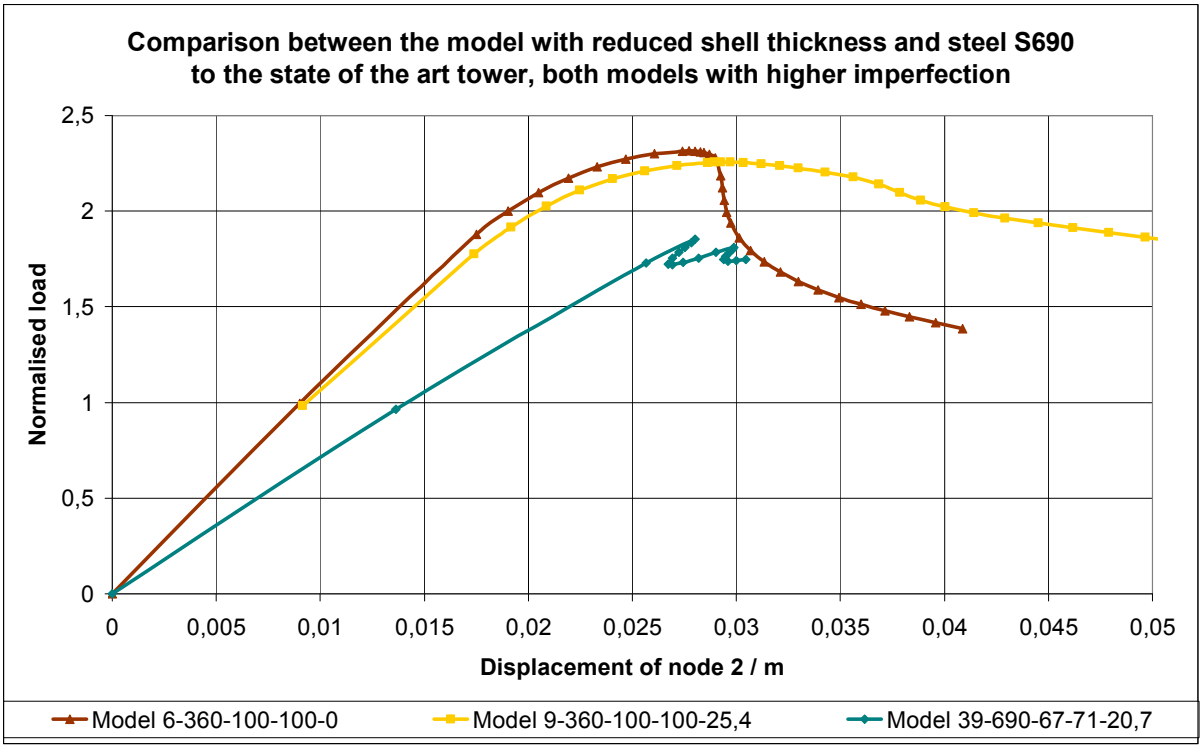

Figure 3.52: Comparison between the load displacement response of the model using high strength steel S690 and reduced shell and stiffener thickness to the state of the art tower at higher imperfection values

The influence of the higher imperfection between models that otherwise use the same material was already discussed in a previous chapter. The influence of a shell thickness reduction leads to a reduction of the stiffness of the structure. It is not possible to achieve the same ultimate load either. The influence of the reduced stiffener is negligible compared to the reduced shell thickness. Previous simulations showed that the stiffener is not influencing the ultimate load in any significant way.

Figure 3.53 shows the stress distribution for the models with higher imperfections and the influence of the change of material and shell thickness.

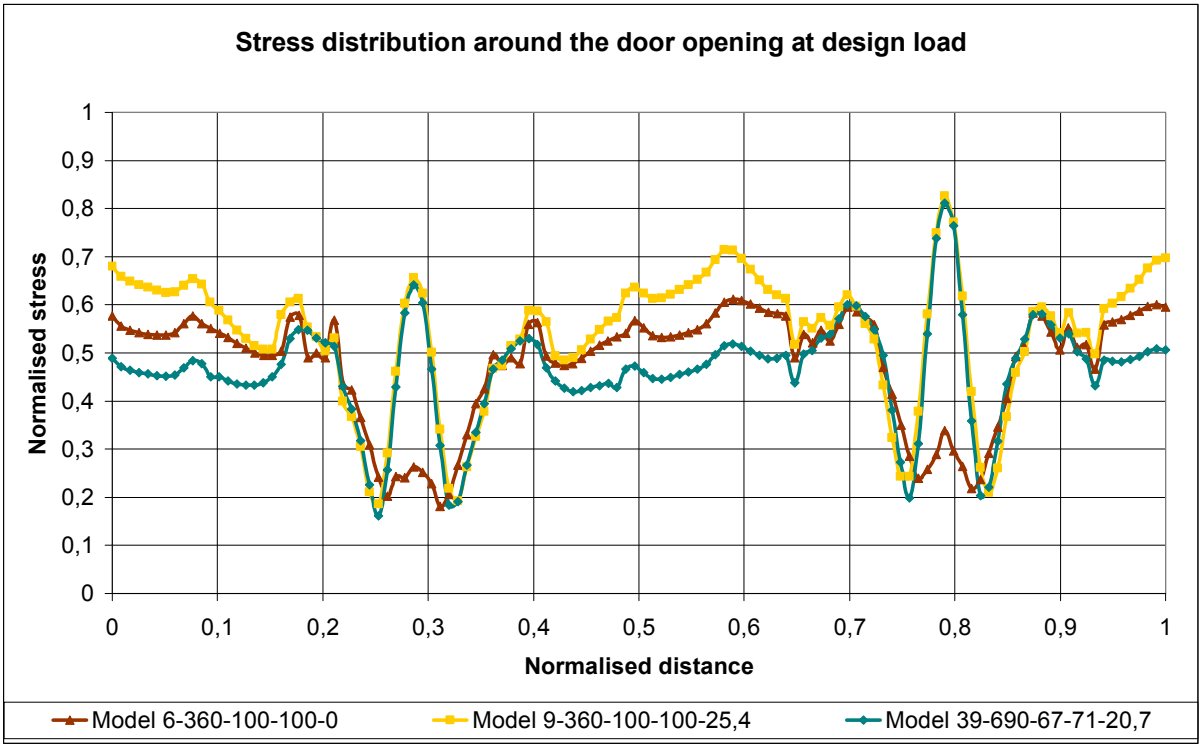

Figure 3.53: Stress distribution around the door opening at design load of the model using high strength steel S690 and reduced shell and stiffener thickness and the state of the art tower at higher imperfection values

The stress distribution around the door opening follows the same pattern as in the previous analysis. The influence of the higher imperfection is clearly visible and both models reach 80% of the yield strength. Model 39 with reduced shell thickness shows lower or comparable stress values around the door opening and exceeds the values of the original structure only above and below the opening. Model 9 with properties of the original structure shows similar stress values as model 39 with reduced shell thickness and high strength steel as material.

3.3 Comparison of a simplified tower model with an analytical calculation

3.3.1 The simplified FE model

The simulation model was also compared to an analytical calculation following the design check of Eurocode 3 for cylindrical shells under general loading.
To perform the analytical calculation, it was necessary to simplify the model.

The simplifications are:

- The load vector was changed from three forces and two moments to one axial force which is causing compression
- The shell thickness of section three was changed from its original value to the same value as section one and two
- The door opening with the stiffener was removed
- The shape of a truncated cone was changed to a cylinder

Due to the simplifications, the model was reduced to a cylinder. The reasons for these simplifications are that Eurocode 3 provides an analytical design check for cylindrical shells. The simulation model is shown in Figure 3.54. The model for the analytical calculation is exactly the same as the FE model. The result from the analytical and FE model of the simplified case are later on compared to a FE model with added door opening. The FE model with door opening follows the simplifications listed above except of the door opening, Figure 3.55 shows the simulation model with door opening.
The value of the vertical extreme load from the design load table was chosen as starting load for the simulation. That was only necessary to know how to calculate the loading of the model after the simulation and to compare it with the analytical calculation.
The value of the start load in the numerical analysis is P = 2873,3 kN.

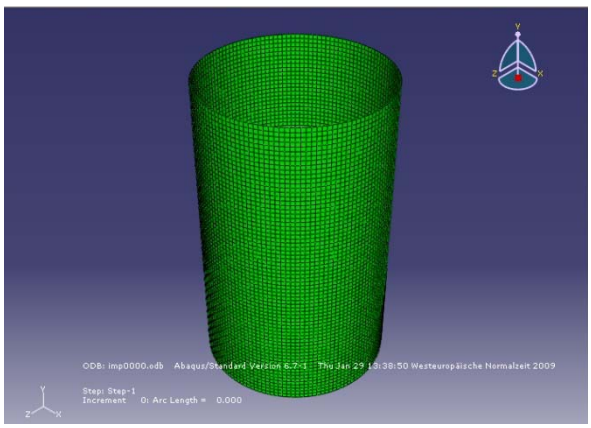
ODB: imp0000.odb Abaqus/Standard Version 6.7-1 Thu Jan 29 10:38:50 Westeuropäische Normalzeit 2009
Step: Step-1
Increment 0: Arc Length = 0.000

Figure 3.54: Simplified simulation model without door opening used to compare analytical results to a FE model

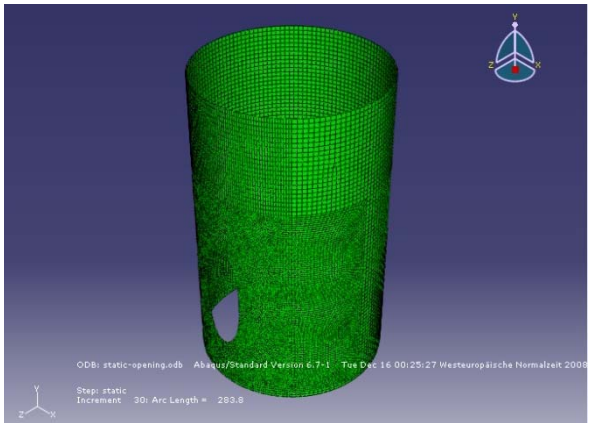
ODB: static-opening.odb Abaqus/Standard Version 6.7-1 Tue Dec 16 00:25:27 Westeuropäische Normalzeit 2008
Step: static
Increment 30: Arc Length = 283.8

Figure 3.55: Simplified simulation model with door opening

The simulation was performed in two steps, the first step is a buckling analysis and the second step a static, Riks analysis to achieve the ultimate load of the structure. The structure was kept in a perfect state, which means that no imperfection was added. In further analysis, it would be possible to add imperfections to figure out how to compare the elastic imperfection factor from the analytical calculation to the imperfection added in the simulation. In the evaluation of the analysis result, it was checked at which load the structure shows the first yielding.

3.3.2 The analytical calculation

The analytical calculation follows the European design recommendations from Eurocode 3. Most of the rules provided have substantial history and are common practice in the design of steel shells.
For cylindrical shells under axial compression, the buckling strength verification is simplified to equation 3-1. A complete design example of a cylindrical shell is found in appendix A.
The value σ_n needs to be equal or smaller than one to verify that a structure has enough resistance to avoid buckling. The resistance of a structure is defined with the design resistance stress σ_{xRd}, the value for it is calculated from the yield stress and influenced by two factors; the partial factor and the buckling resistance factor for elastic-plastic effects in buckling strength assessment. The value of σ_{xEd} is calculated from the force that is applied on the structure and the area of the material of the structure. The exponent k_x is a parameter for interaction expressions for buckling under multiple stress components. A value for k_x is calculated.

Eqt. 3-1

$$\sigma_n = \left(\frac{\sigma_{xEd}}{\sigma_{xRd}} \right)^{k_x}$$

The whole calculation of the buckling strength verification was written in Mathcad. This allows the values for the ultimate load of a structure to be calculated easily. The ultimate load of the structures for the following FE models was analytically calculated and compared to the FE results.

3.3.3 Comparison between perfect structure with and without door opening

The structure without door opening and the structure with door opening are compared in this chapter. Both models represent perfect structures without added imperfections. The load development over the displacement of node 2 and the load at the first yield are shown in Figure 3.56. The ultimate load that was reached in the simulations and the point where the first yield was observed are plotted in Table 3.7.

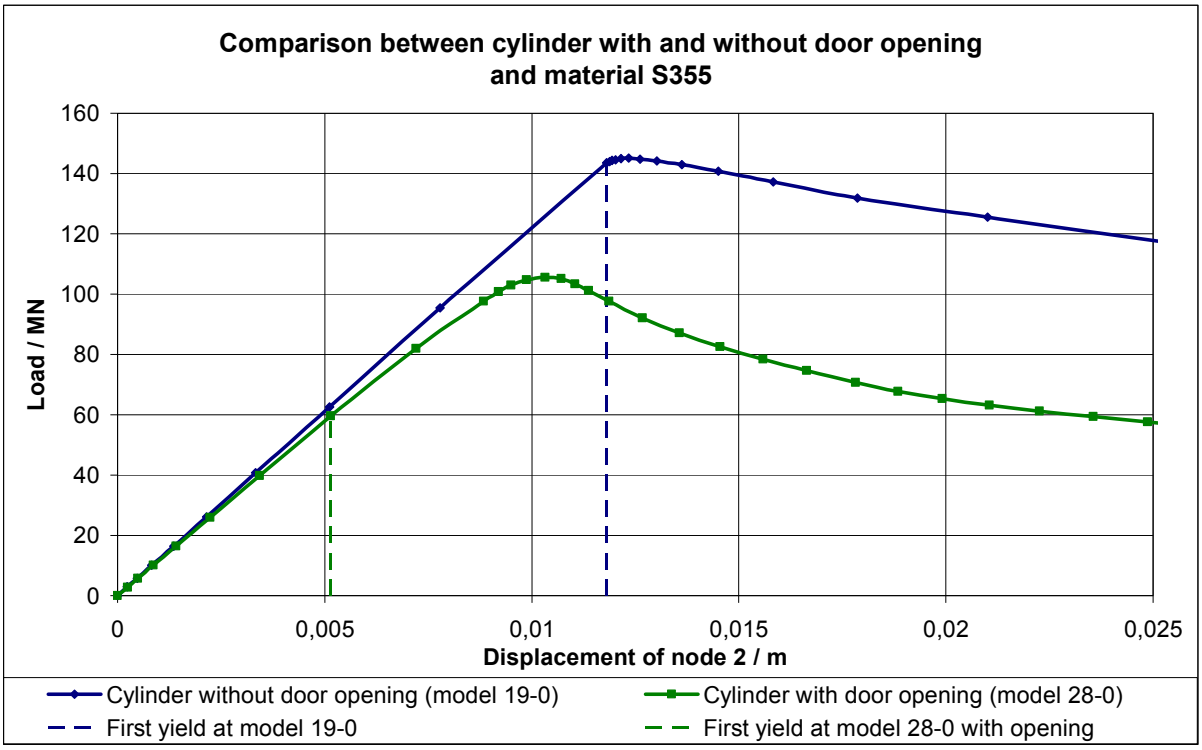

Figure 3.56: Load displacement response of the simplified FE models with and without door opening and the marked point when first yield occurred

Table 3.7: Ultimate load and load at first yield of the simplified FE models with and without door opening

Model name	Description	Load at first yield [N]	Maximum load [N]
Model 19-0	Model without opening	143589720	145050793
Model 28-0	Model with opening	59547131	105613026

The results of the simulation with door opening compared to the results from the simulation without opening show that the ultimate load decreases to about 72,8% and the load at the first yield decreases to about 41,5% from the applied load of the unweakened structure. The yielding in the unweakened structure, without door, is symmetric. In contrast, the model with opening shows the first yield very locally at the door opening. The failure mode of both simulations is rather different. Both models fail in the shape of their first Eigenmode but because of the door opening the Eigenmode shapes are different. From Figure 3.57 till Figure 3.60 is the stress development in the structure without opening printed, from Figure 3.61 till Figure 3.64 the behaviour of the structure with opening.

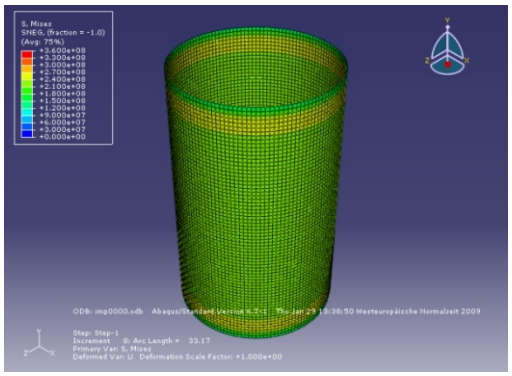

Figure 3.57: Model 19-0, P = 95 MN

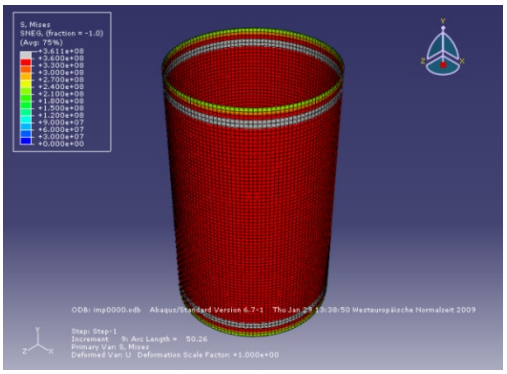

Figure 3.58: Model 19-0, P = 144 MN (first yield)

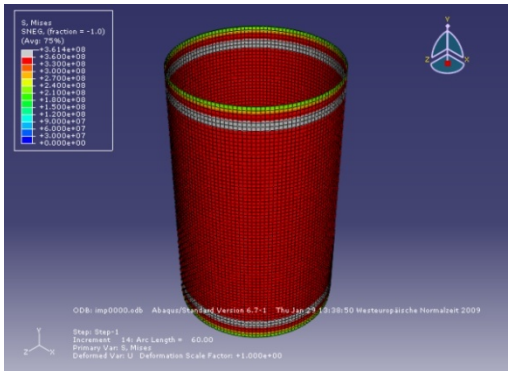

Figure 3.59: Model 19,-0 P = 145 MN (ultimate load)

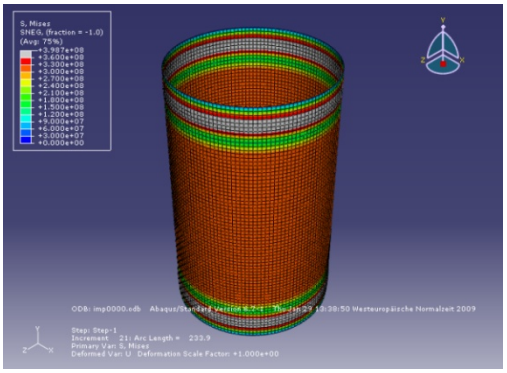

Figure 3.60: Model 19-0, P = 125 MN (descending path)

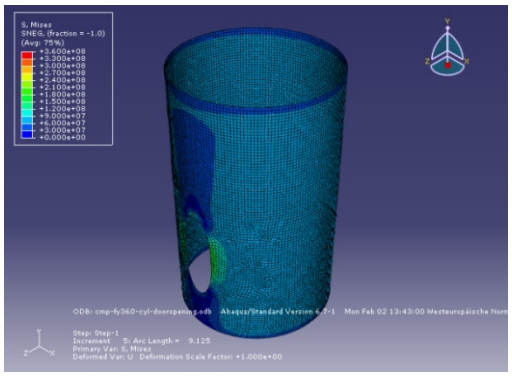

Figure 3.61: Model 28-0, P = 26 MN

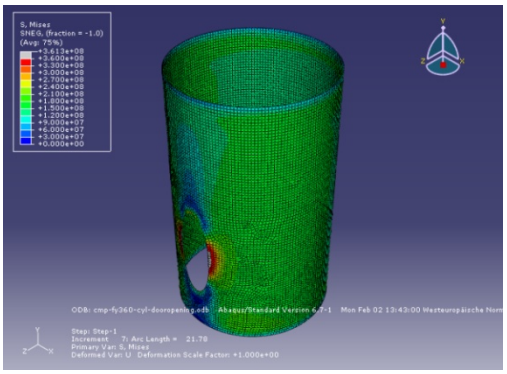

Figure 3.62: Model 28-0, P = 60 MN (first yield)

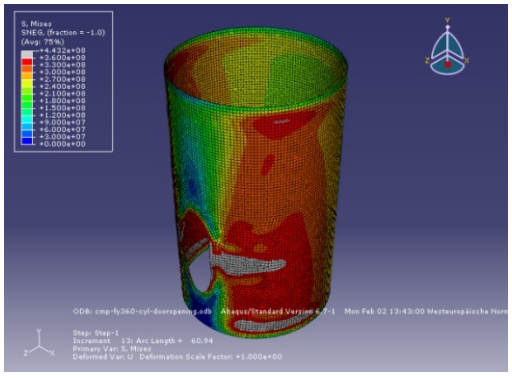

Figure 3.63: Model 28-0, P = 106 MN (ultimate load)

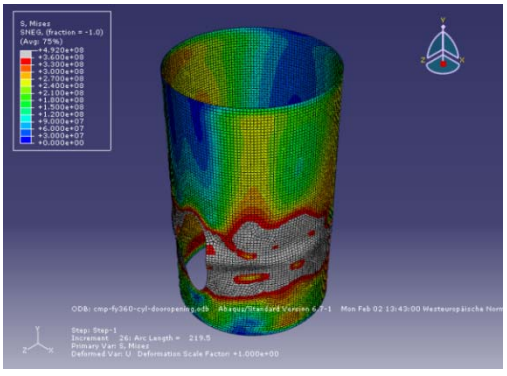

Figure 3.64: Model 28-0, P = 63 MN (descending path)

3.3.4 Comparison of the simplified FE model with added imperfection and steel S355 to the analytical calculation

As mentioned before it is possible to add imperfection into the FE model to investigate the influence of the imperfection scaling factor in the model. The imperfection scaling factor was varied and its influence on the ultimate load was investigated. Table 3.8 shows the values for imperfection scaling factor used in the simulation and its value in percent of the shell thickness. The load displacement response of some selected models is printed in Figure 3.65. The ultimate load over the imperfection scaling factor is later on printed in Figure 3.66.

Table 3.8: Imperfection values and their value in percent of the shell thickness used in the simulation with steel S355

Name of the simulation model	Imperfection amplitude δ [m]	Imperfection in percent of the shell thickness [%]
Model 19-0	0	0,0
Model 20-3	0,003	10,0
Model 21-5	0,005	16,7
Model 22-6	0,006	20,0
Model 23-10	0,01	33,3
Model 24-15	0,015	50,0
Model 25-20	0,02	66,7
Model 26-25	0,025	83,3
Model 27-30	0,03	100,0

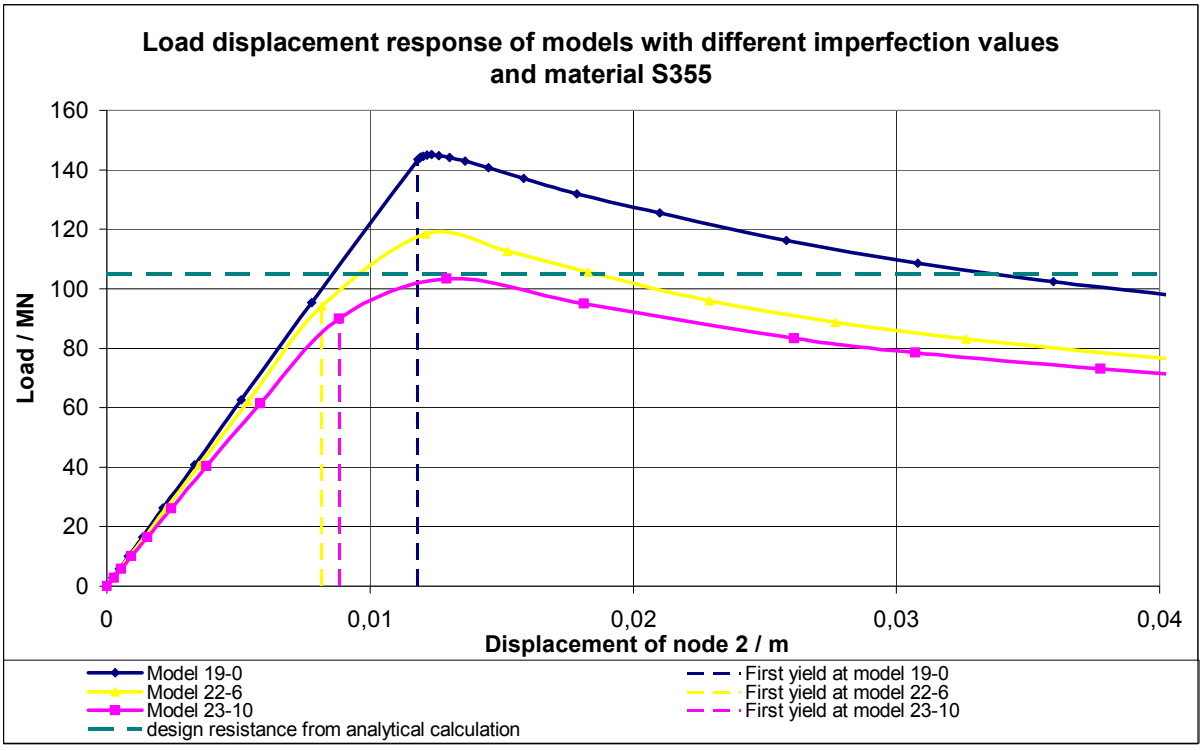

Figure 3.65: Load displacement response of three simplified FE models with different imperfections and the design resistance from the analytical calculation

The structure shows a reduced stiffness with increasing imperfection and the ultimate load that the structure can bear decreases. In Figure 3.65 are the points marked when the first time yielding occurs. The load when first yield occurs reduces with increasing imperfection amplitude. This behaviour is logic because of local occurring yielding caused by imperfections.

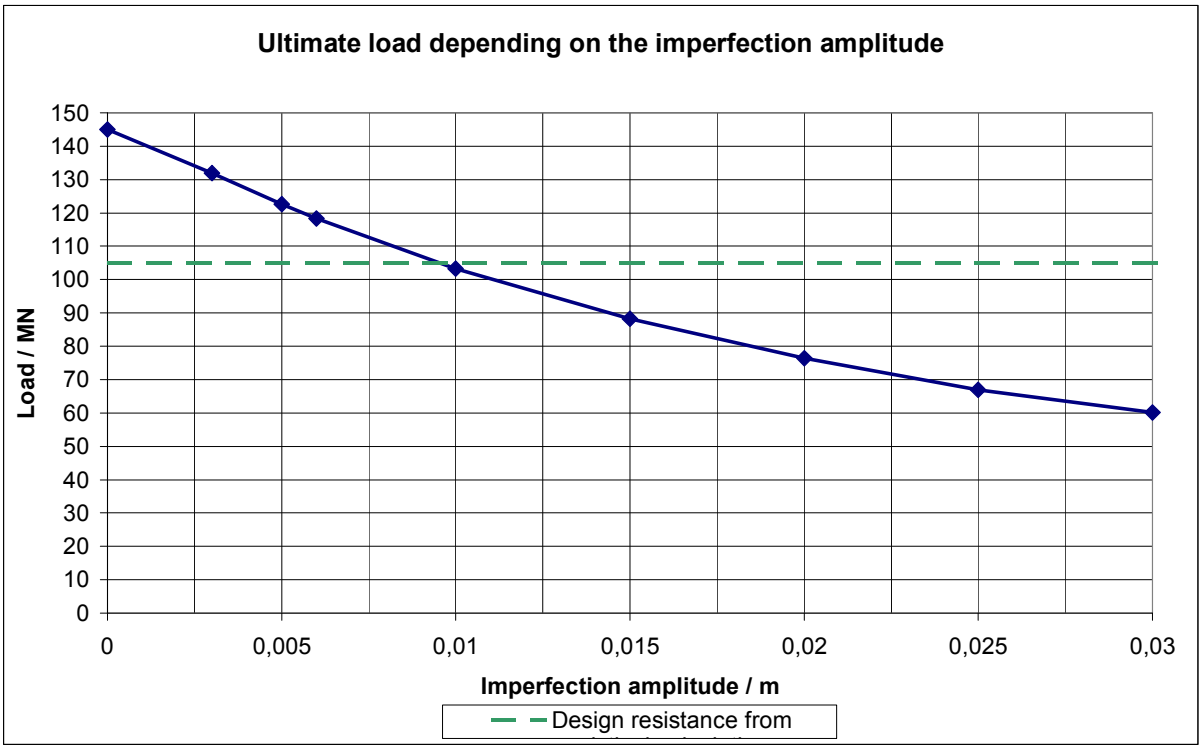

Figure 3.66: Ultimate load depending on the imperfection amplitude introduced in the models using steel S355 compared to the design resistance from the analytical calculation

The influence of the imperfection amplitude on the ultimate load is plotted in Figure 3.66. The ultimate load decreases to about 72% from the perfect structure until imperfection amplitude of one third of the shell thickness is reached.
Whereas the perfect structure yields symmetrically, the structure with increasing imperfection tends to more and more local yielding, All simulations created a data point at a stress level of around 361,1MPa. This fact offers the possibility to extract the load at the beginning of the yielding. In Figure 3.67 is the load at first yield depending on the imperfection scaling factor plotted.
Until an imperfection of 0,005m is reached is the load at first yield similar to the ultimate load. The difference becomes bigger with higher imperfection values and steps are clearly visible in Figure 3.67. The structure tends to yield at local spots on the shell att higher imperfection. Local buckling of the structure is now cause of failure, no longer is it because of the ultimate load and the reaching of the yield stress due to compression.
From the analytical calculation was a load value of P_1=105,5 MN estimated to guarantee safety against buckling. This load value would be reached for the case of ultimate load at an imperfection of around 33% of the shell thickness. The estimated load value is around 19% of the shell thickness when first yield occurs.

The analytical calculation varies the imperfection with the fabrication-tolerance-quality-class-factor. In the analytical calculation used for this comparison, is this factor set to “normal”, this value represents the lowest quality class. Higher quality classes in the analytical calculation would lead to higher buckling resistance. In the design guidelines is an elastic imperfection factor α_x used for the consideration of imperfections. In the analytical calculation influences the elastic imperfection factor the yield strength of the used material and leads to a design resistance stress. The design resistance stress σ_{xRd} has for the material with f_y=360MPa a value of σ_{xRd}=261MPa. The design resistance stress of the analytical calculation is at about 72% of the yield strength of the material. Because of the increments used by Abaqus were no loads at this stress level provided.

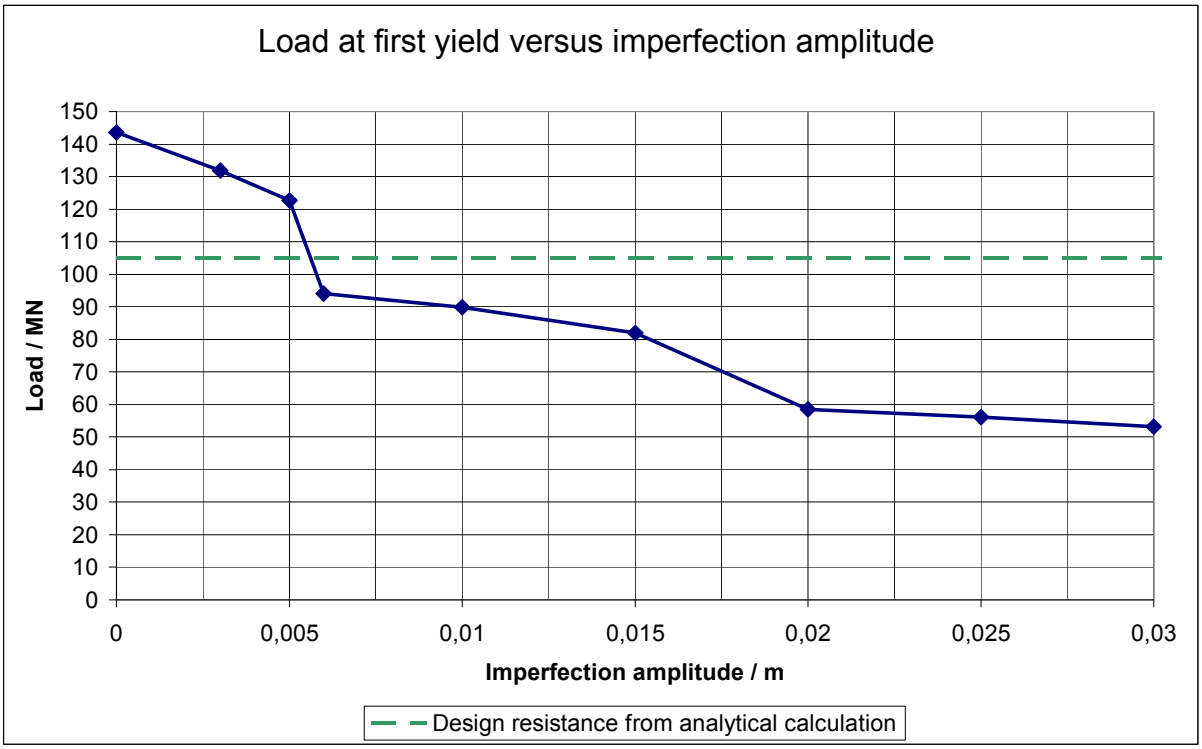

Figure 3.67: Load where the first yield occurred depending on the imperfection amplitude for steel S355 compared to the design resistance from the analytical calculation

A conclusion of the FE simulations is that imperfection values of around one third of the shell thickness already lead to ultimate load values around the analytical result. If the yield strength is seen as maximum limit for the structure, then the analytical maximum load is reached between imperfection amplitude of 17-20% of the shell thickness.

It is not possible to derive one imperfection value which is to be used in FE models. Every analysis of structures regarding buckling and imperfections needs several simulations to obtain the influence of different imperfection values in the model.
The imperfection amplitude for FE simulations suggested by Eurocode is in between 10-25mm depending on the production quality class. These values are conservative and lead to lower loads than the analytical calculation. A reason for this is that the imperfection introduced into the model needs to cover all kind of imperfection that can occur in a real structure. The imperfection amplitude in a FE model covers only a

theoretical imperfection pattern and not specific imperfections like asymmetric loading or imperfect boundary conditions. This fact leads to a higher suggested imperfection values.

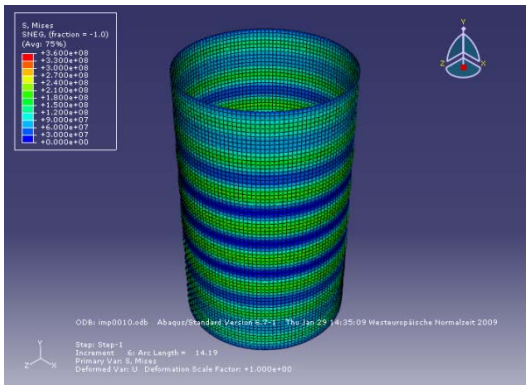

Figure 3.68: Model 23-10, P=61MN

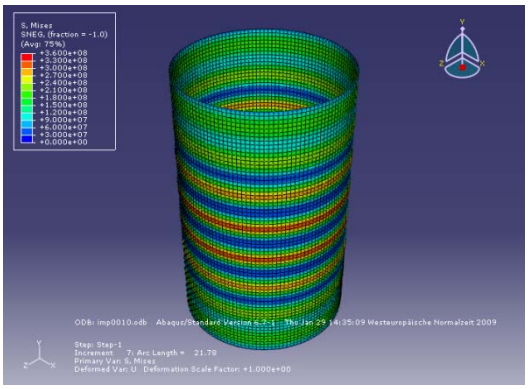

Figure 3.69: Model 23-10, P=90MN (first yield)

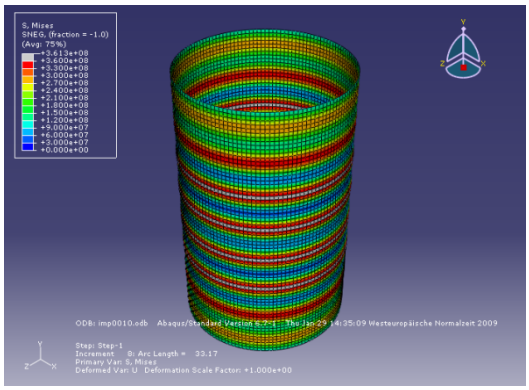

Figure 3.70: Model 23-10, P=103MN (ultimate load)

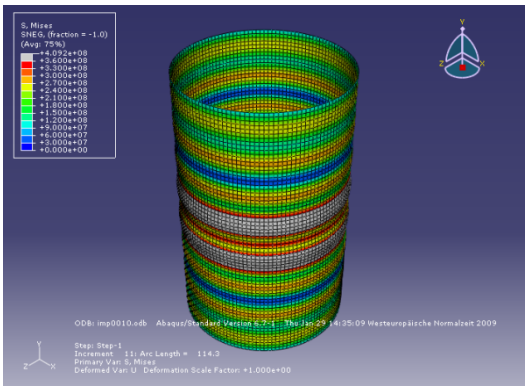

Figure 3.71: Model 23-10, P=83MN (descending path)

3.3.5 Comparison of the simplified model with added imperfection and steel S690 to the analytical calculation

The analysis for the high strength steel was performed similarly as in the previous chapter. The door opening was neglected in this chapter. The development of the ultimate load depending on the imperfection amplitude is plotted in Figure 3.72. In Figure 3.73 is the load plotted for when the first yield occurred. From the analytical calculation was a design resistance load value of P_1 = 162,8 MN estimated.
Table 3.9 shows the imperfection values used for the simulations with high strength steel.

Table 3.9: Imperfection values and their value in percent of the shell thickness used in the simulation with high strength steel S690

Name of the simulation model	Imperfection amplitude δ [m]	Imperfection in percent of the shell thickness [%]
Model 29-0	0	0,0
Model 30-3	0,003	10,0
Model 31-6	0,006	20,0
Model 32-10	0,01	33,3
Model 33-11,2	0,0112	37,3
Model 34-12,5	0,0125	41,7
Model 35-15	0,015	50,0
Model 36-20	0,02	66,7
Model 37-25	0,025	83,3
Model 38-30	0,03	100,0

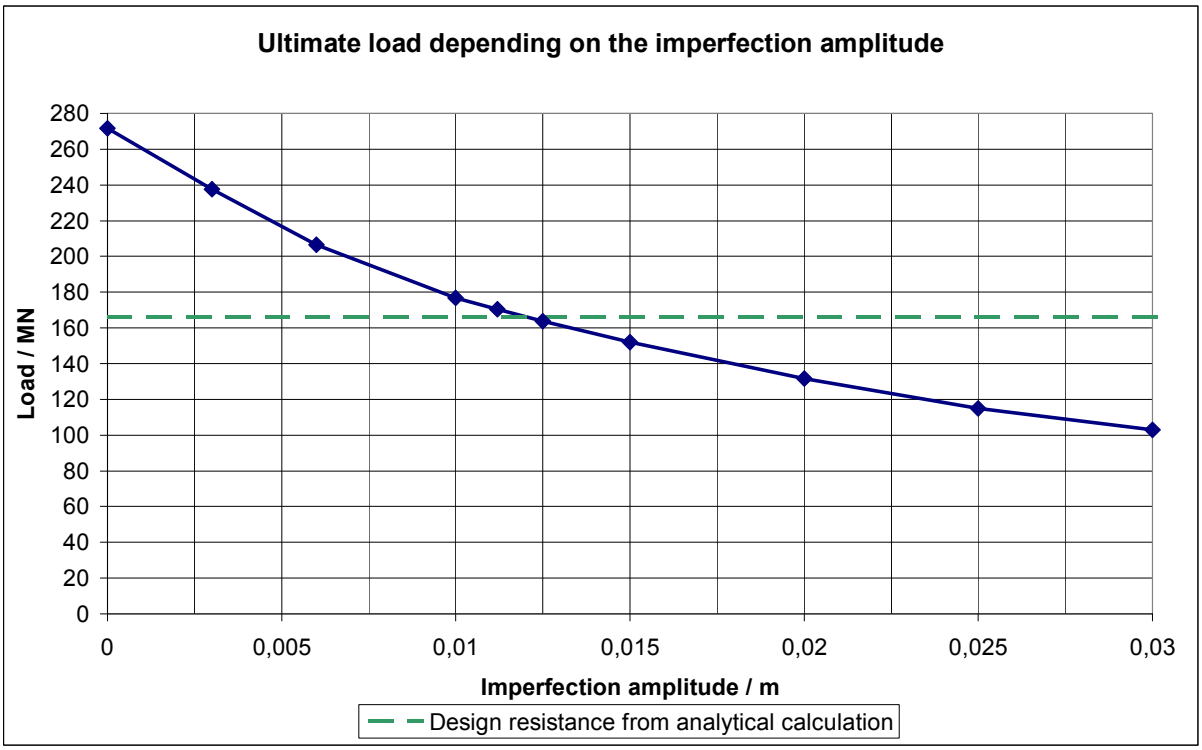

Figure 3.72: Ultimate load depending on the imperfection amplitude introduced in the model for steel S690 compared to the design resistance from the analytical calculation

The graph of the ultimate load is similar to the graph of the simulation with lower yield strength. The difference is that the load value where the maximum load against failure from the analytical calculation is reached at an imperfection value of around 42% of the shell thickness. The load at the first time yield is also reached at a higher imperfection value compared to the simulation with the lower quality steel. The stepwise decrease of the load at first yield is similar in both models and does not depend on the material; only the location differs from model to model.

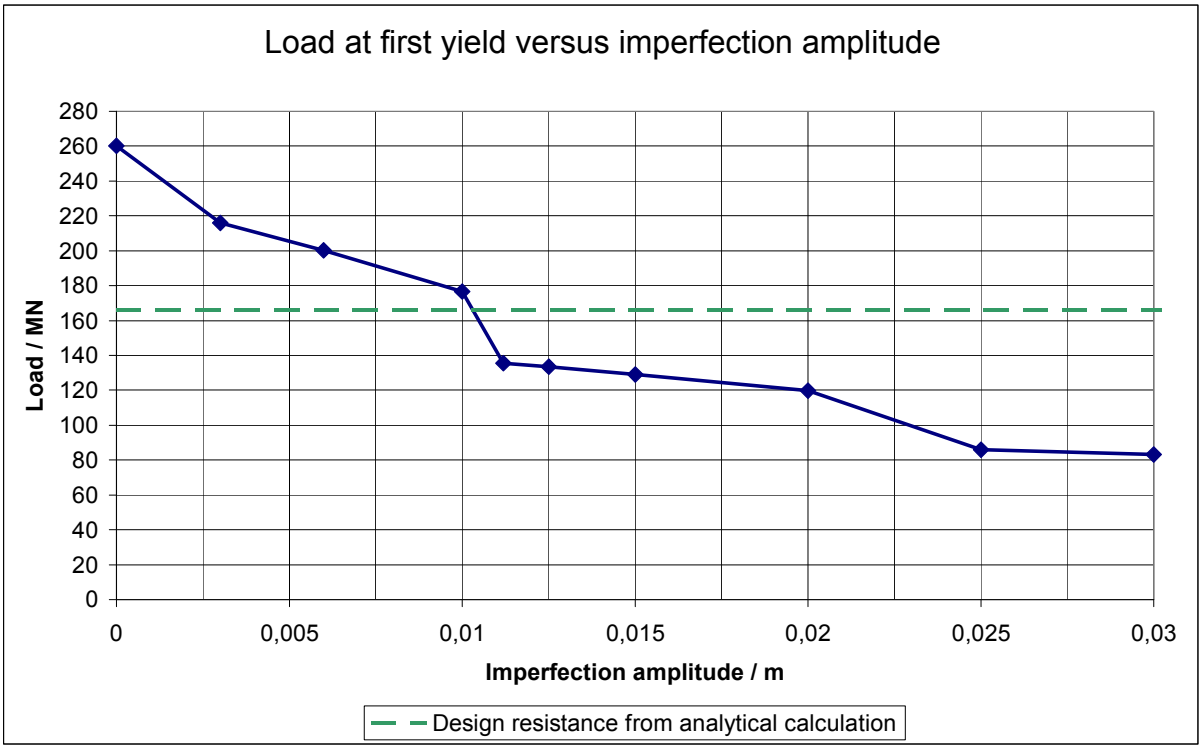

Figure 3.73: Load when the first yield occurred depending on the imperfection amplitude for steel S690 compared to the design resistance from the analytical calculation

Figure 3.74 shows the load displacement response of three selected models, the model without imperfection and the models with 33% and 42% imperfection regarding the shell thickness.
The failure mode of the structure is the same than in the previous chapter. This is reasonable because the Eigenmode of the structure is the same and with this the perturbation pattern in which the imperfection is introduced. Because of the same failure mode are no contour plots added into this chapter.

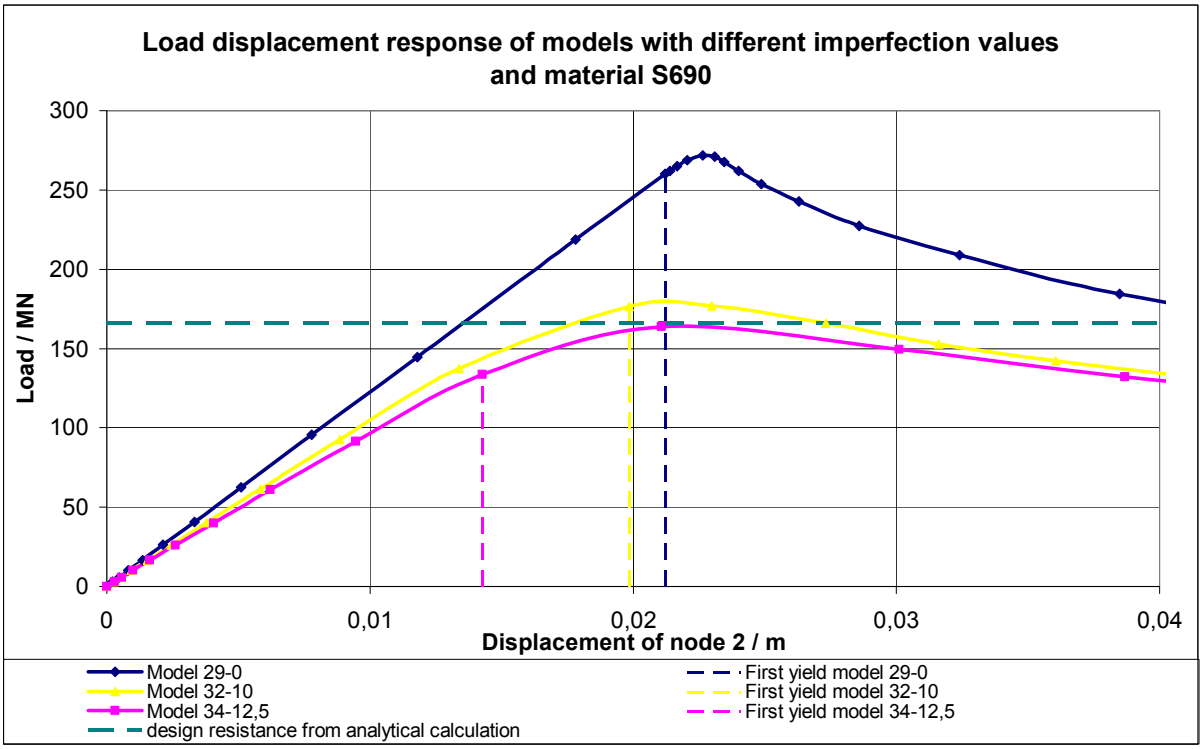

Figure 3.74: Load displacement response of the simplified FE model using steel S690 depending on the imperfection amplitude and compared to the design resistance from the analytical calculation

The imperfection amplitude of 0,01m leads to a result where the first yield occurs near to the design resistance load of the analytical calculation. The imperfection amplitude seems to be close to the elastic imperfection factor used in the analytical calculation.
As mentioned in the comparison with the lower quality steel, it is not possible to derive one imperfection value to use in every simulation.

4 Summary

The study showed that a reduction of the shell thickness with steel S355 is not possible. A reduction of the stiffener thickness is a possible option for a reduction of material. The lower tower section with reduced stiffener thickness showed resistance against failure close to the state of the art tower also when imperfection was added to the model. The limiting criterion for a stiffener reduction is the development of stress concentrations around the opening in the tower shell and on the stiffener itself.

The simulation with a change of the tower material from steel S355 to the high strength steel S690 offered the possibility to reduce the shell thickness of the tower. A reduction to two-thirds of the original shell thickness of the lower tower section is possible. The stress level was kept at a similar level compared to the original tower shell. The lower stiffness of the tower using the high strength steel, leads to expectations that the tower top has higher displacements than the original structure. With a reduction of the tower shell thickness, a noticeable cost reduction of the whole tower structure would be feasible. The cost reduction contains decreased material as well as labour costs. The thickness of weld seems is also reduced if thinner material is used. Weld seems on wind turbines need to fulfil high requirements and are because of this expensive in production.

The investigation of the influence of different imperfection amplitudes showed that the structure is not very sensitive to them. Higher imperfection amplitudes showed that the influence on the ultimate load is marginal. The development of stresses around the opening increased with higher imperfection amplitudes but the yield strength was not reached for imperfection amplitudes suggested by Eurocode.

The use of small imperfections is not conservative. The comparison between a simplified model and the analytical calculation showed that higher imperfections would lead to additional safety in the design.

4.1 Future work

Possible changes of the tower due to material reduction or material change to high strength steel needs further investigation. The influence of high strength steel on the lower part of the tower was investigated in this report. For a possible use in reality, an analysis of the complete tower structure is necessary.

This report did not take into account the influence of weld seems around the stiffener and between the sections of the tower. The welds in the structure could be the limiting factor for material reductions. An investigation of the welds, for extreme loads as for fatigue loads, need to be done.

The behaviour of the complete tower build in S690 could be different from the tower in S355. The change of the material thickness would lead to a reduction of the dead weight of the tower. A change of the dead weight would change the Eigenfrequency of the tower. Because of the dynamic circumstances of a wind turbine, this needs to be investigated in the same way than stability aspects.

A possible material reduction in the upper parts of the tower would cause a higher risk of local buckling. The influence of local buckling due to thickness changes in upper parts of the tower also needs to be investigated.

References

[4] Guideline for the certification of Wind Turbines,
Germanischer Lloyd, 2003

[5] Design approximation of wind load,
Background document of the HISTWIN project, 17.06.2008

[3] Buckling of Steel Shells, European Design Recommendations
Eurocode 3, Part 1-6, 5th Edition,
ECCS Technical Committee, Structural Stability, 2008

[4] Photos of the wind turbine and the door opening
Online photo archive of Repower
http://www.repower.de/
Accessed: 10.02.2009

Appendix A - Design example for a cylindrical shell under axial compression

Properties of the tower and values for the calculation

Geometrical properties:

$r := 2.135m$

$r_1 := 2.15m$

$t := 0.03m$

$L := 6.99m$

Radius r is used for the buckling strength verification and radius r1 for the calculation of the area under compression. The reason for two different radi is that the buckling strength verification is calculated with the middle surface of the cylinder. The real outer radius is because of this larger.

t - material thickness

L - length of the cylinder

Material properties:

$E := 210 \cdot 10^9 Pa$

$f_{yk} := 690 \cdot 10^6 Pa$

E - Youngs modulus

f_{yk} - yield strength

Partial factor:

$\gamma_{M1} := 1.1$

The partial factors γ_{M1} are defined for each application in the standards for silos, tanks, towers and masts and chimneys. For these structures, the values given there should be adopted unless the National Annex defines a different value. For other structures, no lower value than the general reference value $\gamma_{M1} = 1{,}1$ should be used.

Boundary conditions:

BC 1

therefore

$C_{xb} := 6$

With a change of the boundary conditions is a change of the C_{xb} factor necessary. This factor is only used in the calculation for long cylinders.

Load applied in axial direction of the cylindrical shell.

$P_x := 165949000N$

Standard values for the design check of cylindrical shells subjected to axial compression.

$\beta := 0.6 \qquad \eta := 1 \qquad \lambda_{x0} := 0.2$

Stress in the shell caused by axial compression

$A := r_1^2 \cdot \pi - (r_1 - t)^2 \cdot \pi$ $A = 0.402\,m^2$

$\sigma_{xEd} := \frac{P_x}{A}$ $\sigma_{xEd} = 4.124 \times 10^8\,Pa$

Procedure for the design check of cylindrical shells subject to axial compression

$\omega := \frac{L}{\sqrt{r \cdot t}}$ $\omega = 27.62$

Condition for a short cylinder

$\omega < 1.7$

$C_x := 1.36 - \frac{1.83}{\omega} + \frac{2.07}{\omega^2}$

Condition for a medium long cylinder

$1.7 \le \omega \le 0.5 \cdot \frac{r}{t}$ $0.5 \cdot \frac{r}{t} = 35.583$

$C_x := 1$

Condition for a long cylinder

$\omega > 0.5 \cdot \frac{r}{t}$ $0.5 \cdot \frac{r}{t} = 35.583$

$C_x := 1 + \frac{0.2}{C_{xb}} \cdot \left(1 - 2\omega \cdot \frac{t}{r}\right)$

Because of the condition:

$C_x := 1$

Critical buckling resistance stress

$$\sigma_{xRcr} := 0.605 \cdot E \cdot C_x \cdot \frac{t}{r} \qquad \sigma_{xRcr} = 1.785 \times 10^9 \text{ Pa}$$

Fabrication tolerance quality class Q

Class A	Excellent	40
Class B	High	25
Class C	Normal	16

Chosen value: $Q := 16$

Elastic imperfection factor

$$\alpha_x := \frac{0.62}{1 + 1.91 \cdot \left(\frac{1}{Q} \cdot \sqrt{\frac{r}{t}} \right)^{1.44}} \qquad \alpha_x = 0.352$$

Buckling strength verification for axial compression

$$\lambda_{px} := \sqrt{\frac{\alpha_x}{1-\beta}} \qquad \lambda_{px} = 0.938$$

$$\lambda_x := \sqrt{\frac{f_{yk}}{\sigma_{xRcr}}} \qquad \lambda_x = 0.622$$

$$\lambda_{x0} = 0.2$$

Case 1:
$\lambda_x \leq \lambda_{x0}$

$\chi_x := 1$

Case 2:
$\lambda_{px} \leq \lambda_x$

$$\chi_x := \frac{\alpha_x}{\lambda_x^{\,2}} \qquad \chi_x = 0.912$$

Case 3:
$\lambda_{x0} \leq \lambda_x \leq \lambda_{px}$

$$\chi_x := 1 - \beta \cdot \left(\frac{\lambda_x - \lambda_{x0}}{\lambda_{px} - \lambda_{x0}} \right)^{\eta} \qquad \chi_x = 0.657$$

Design resistance stress

$$\sigma_{xRd} := \frac{\chi_x \cdot f_{yk}}{\gamma_{M1}} \qquad \sigma_{xRd} = 4.124 \times 10^8\,\text{Pa}$$

$$k_x := 1.00 + \chi_x^{\,2} \qquad k_x = 1.432$$

Design OK for σ_n =< 1, redesign for σ_n > 1

$$\sigma_n := \left(\frac{\sigma_{xEd}}{\sigma_{xRd}} \right)^{k_x} \qquad \sigma_n = 1.00000$$

Appendix B – Procedure for the design check of cylindrical shells subjected to axial compression

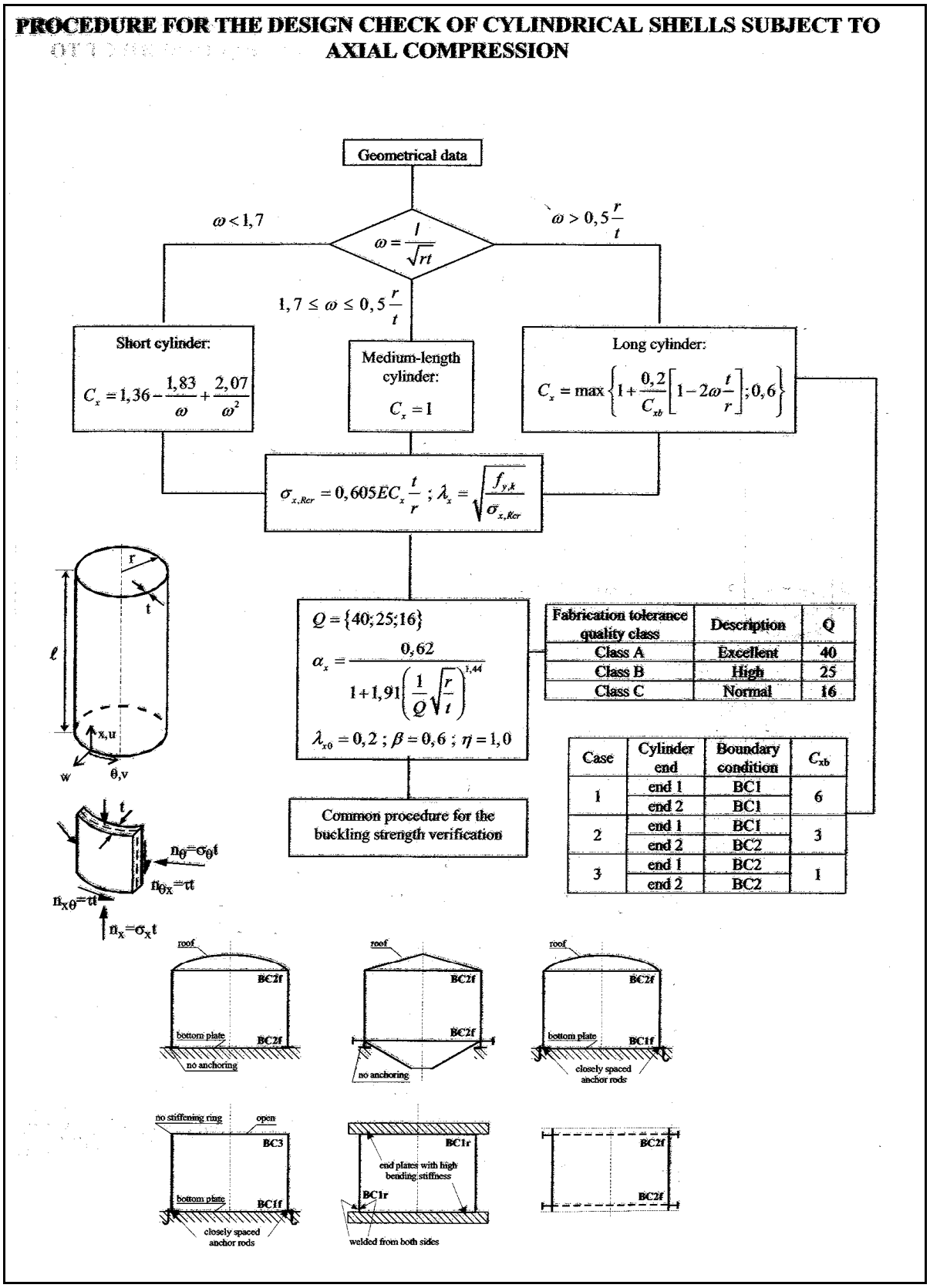

Fabrication tolerance quality class	Description	Q
Class A	Excellent	40
Class B	High	25
Class C	Normal	16

Case	Cylinder end	Boundary condition	C_{xb}
1	end 1	BC1	6
	end 2	BC1	
2	end 1	BC1	3
	end 2	BC2	
3	end 1	BC2	1
	end 2	BC2	

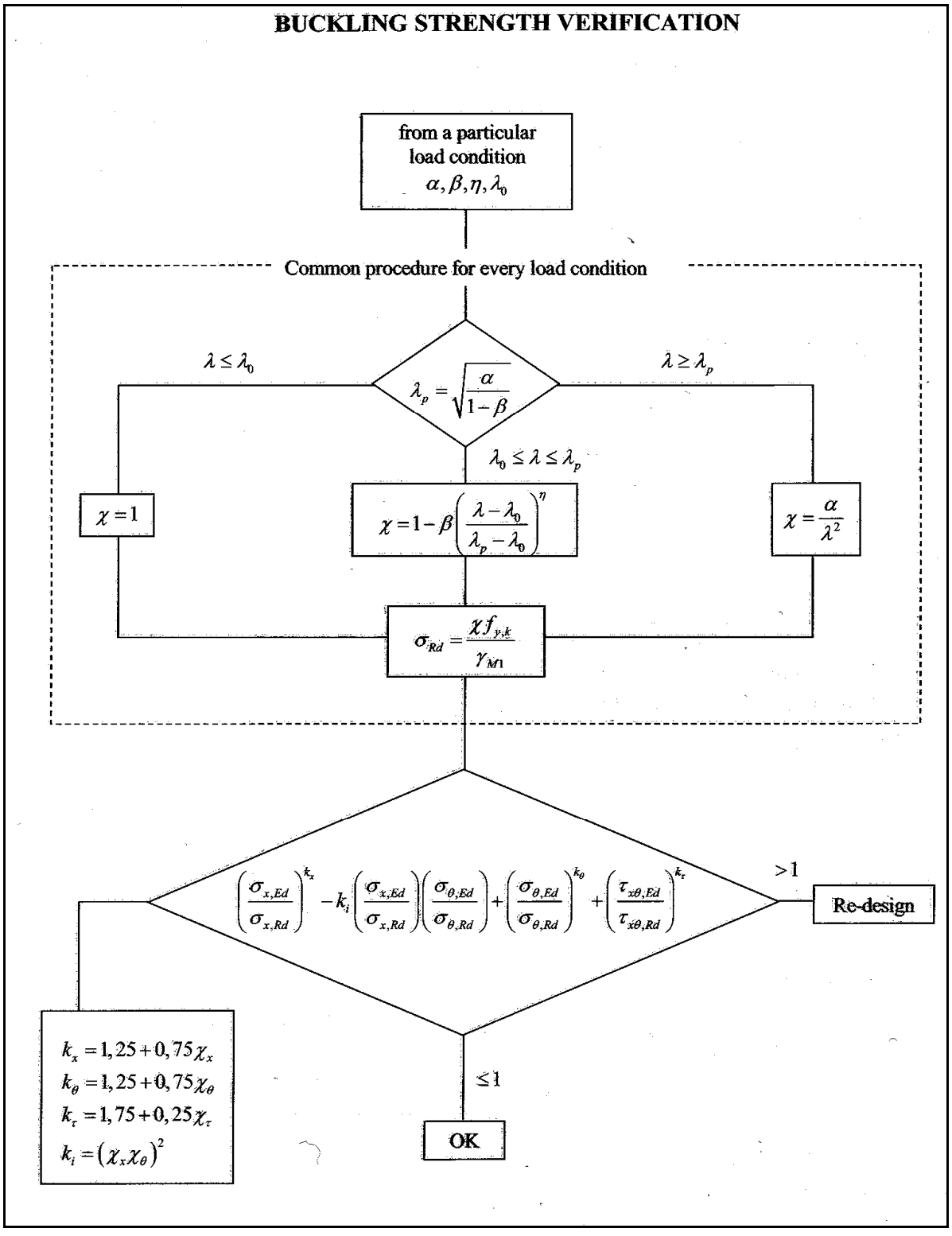
BUCKLING STRENGTH VERIFICATION
from a particular load condition
$\alpha, \beta, \eta, \lambda_0$
Common procedure for every load condition
$\lambda_p = \sqrt{\frac{\alpha}{1-\beta}}$
$\lambda \le \lambda_0$
$\lambda_0 \le \lambda \le \lambda_p$
$\lambda \ge \lambda_p$
$\chi = 1$
$\chi = 1 - \beta\left(\frac{\lambda - \lambda_0}{\lambda_p - \lambda_0}\right)^{\eta}$
$\chi = \frac{\alpha}{\lambda^2}$
$\sigma_{Rd} = \frac{\chi f_{y,k}}{\gamma_{M1}}$
$\left(\frac{\sigma_{x,Ed}}{\sigma_{x,Rd}}\right)^{k_x} - k_i\left(\frac{\sigma_{x,Ed}}{\sigma_{x,Rd}}\right)\left(\frac{\sigma_{\theta,Ed}}{\sigma_{\theta,Rd}}\right) + \left(\frac{\sigma_{\theta,Ed}}{\sigma_{\theta,Rd}}\right)^{k_\theta} + \left(\frac{\tau_{x\theta,Ed}}{\tau_{x\theta,Rd}}\right)^{k_\tau}$
>1
Re-design
≤1
OK
$k_x = 1,25 + 0,75\chi_x$
$k_\theta = 1,25 + 0,75\chi_\theta$
$k_\tau = 1,75 + 0,25\chi_\tau$
$k_i = (\chi_x \chi_\theta)^2$

Appendix D – Result of the load case simulation

Result of the simulation of different load cases and their stress distribution around the door opening.

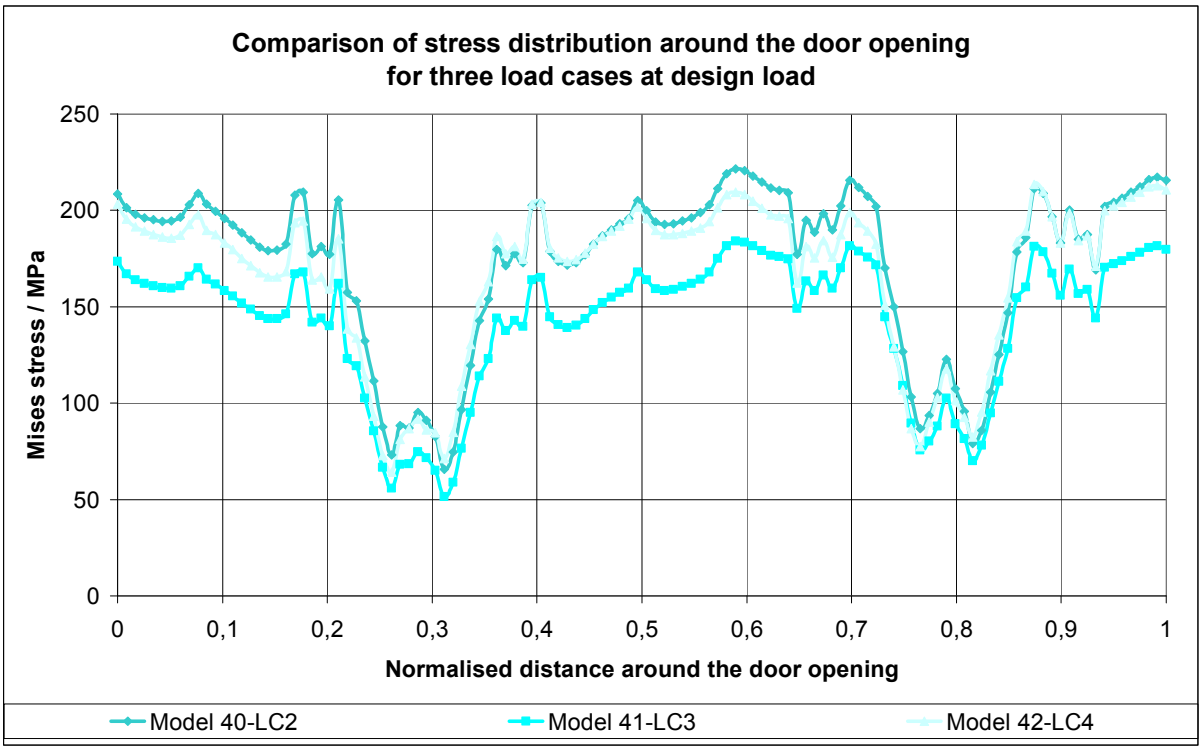

Appendix E – Contour plots of the parametric study

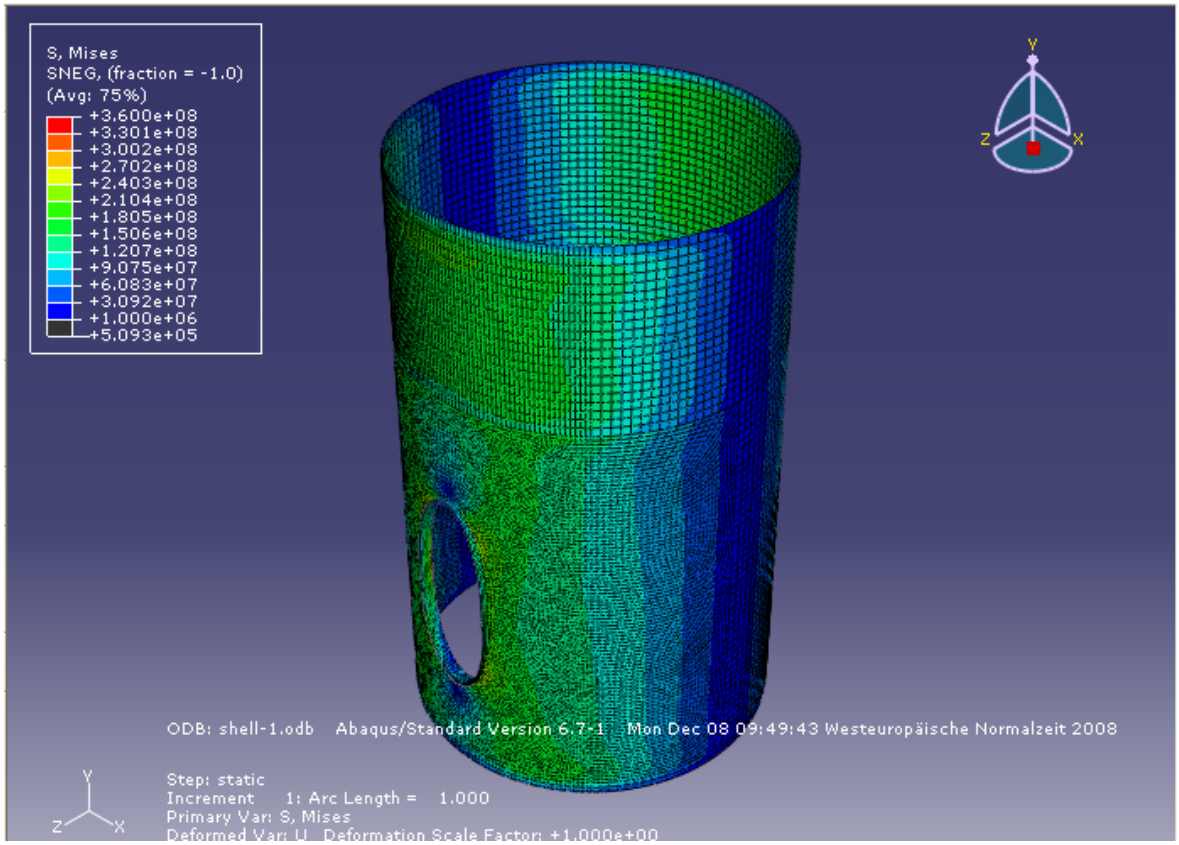

Model 1: 99,5 % Load

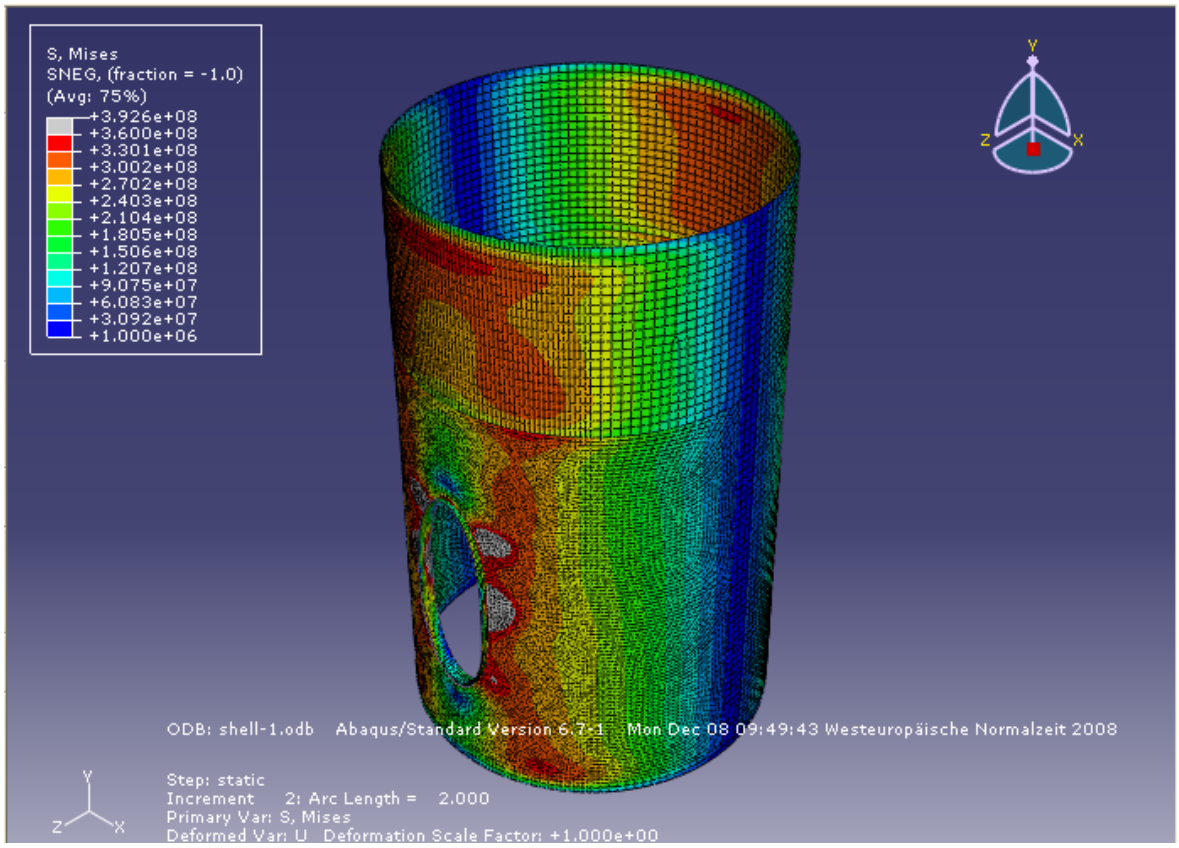

Model 1: 188 % Load

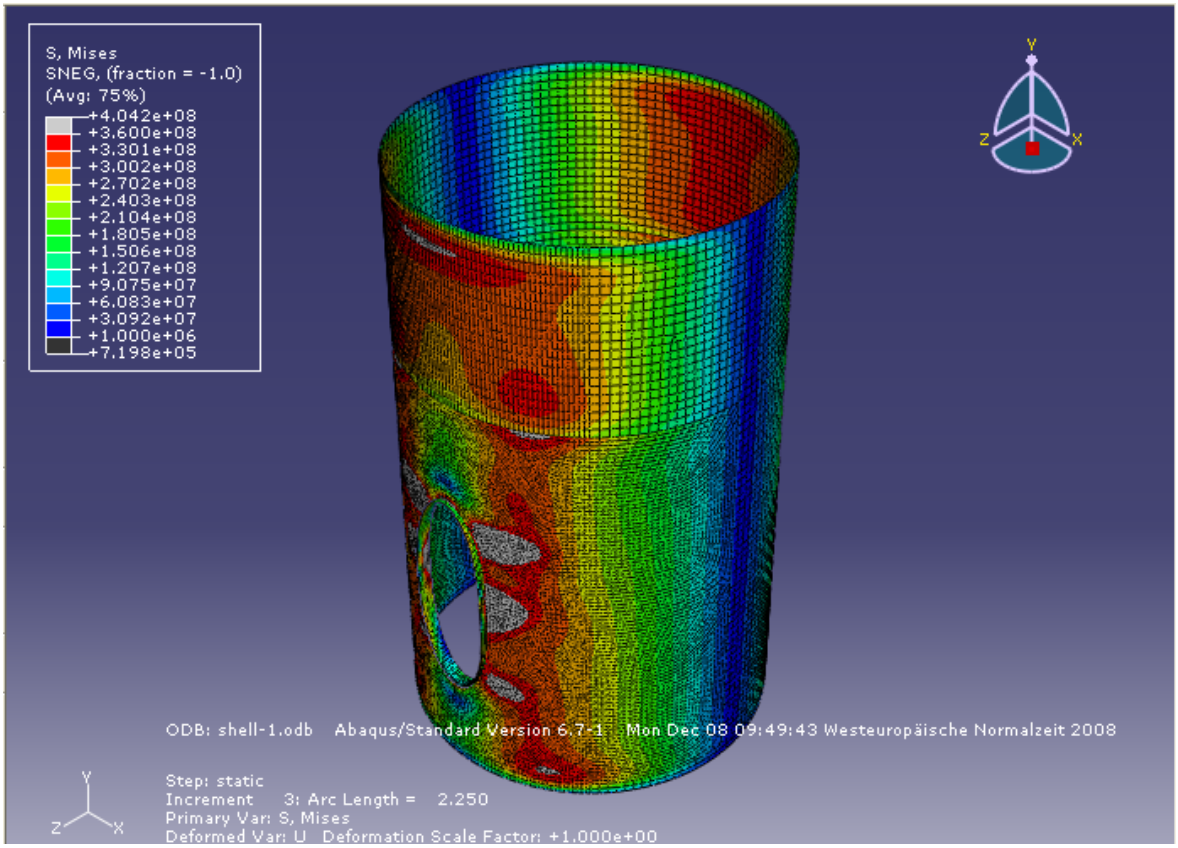

Model 1: 199,9 % Load

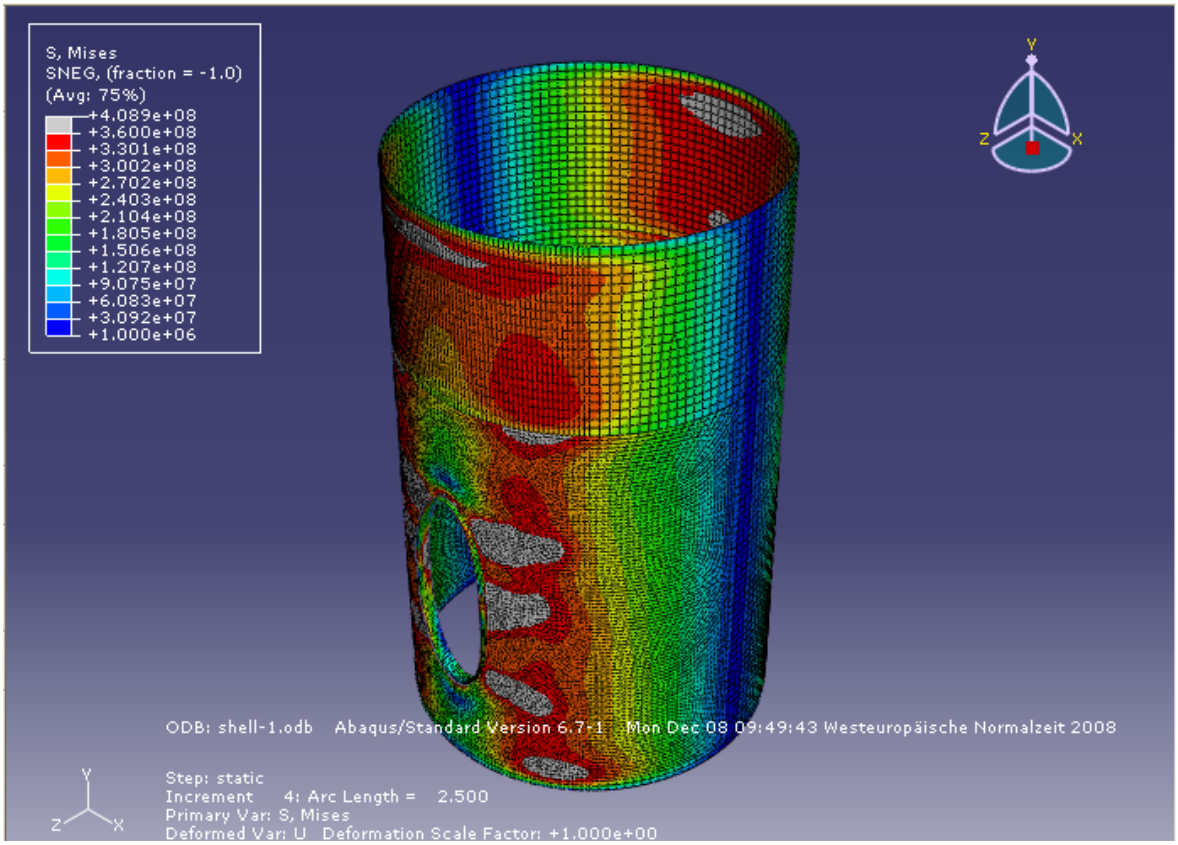

Model 1: 209,6 % Load

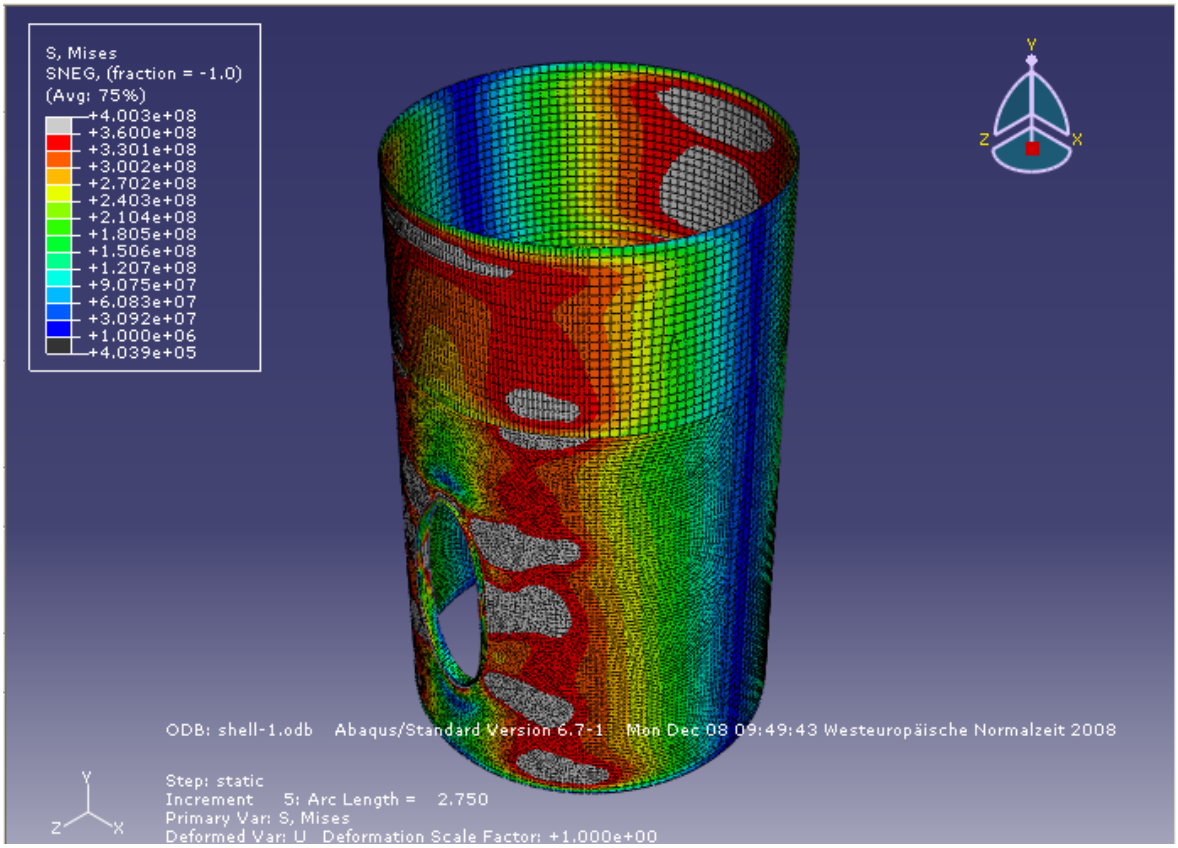

Model 1: 217,3 % Load

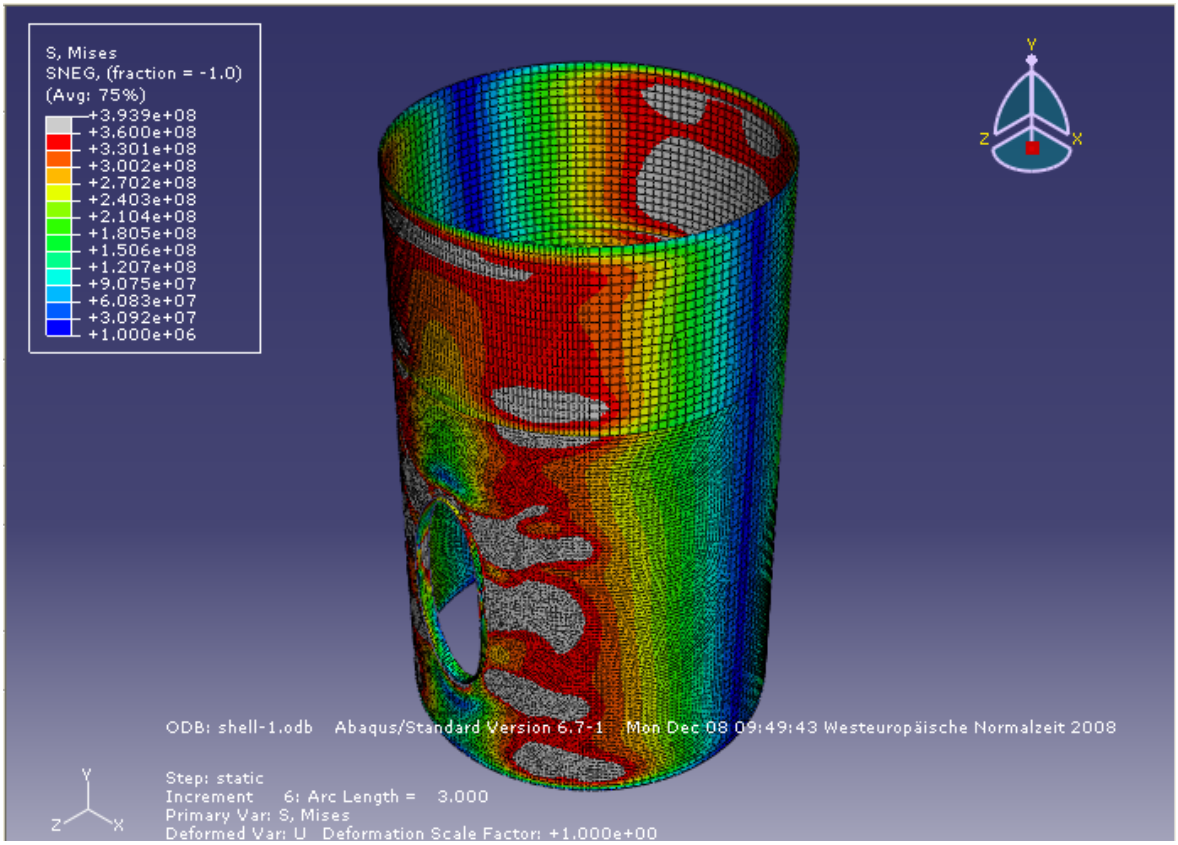

Model 1: 223,1 % Load

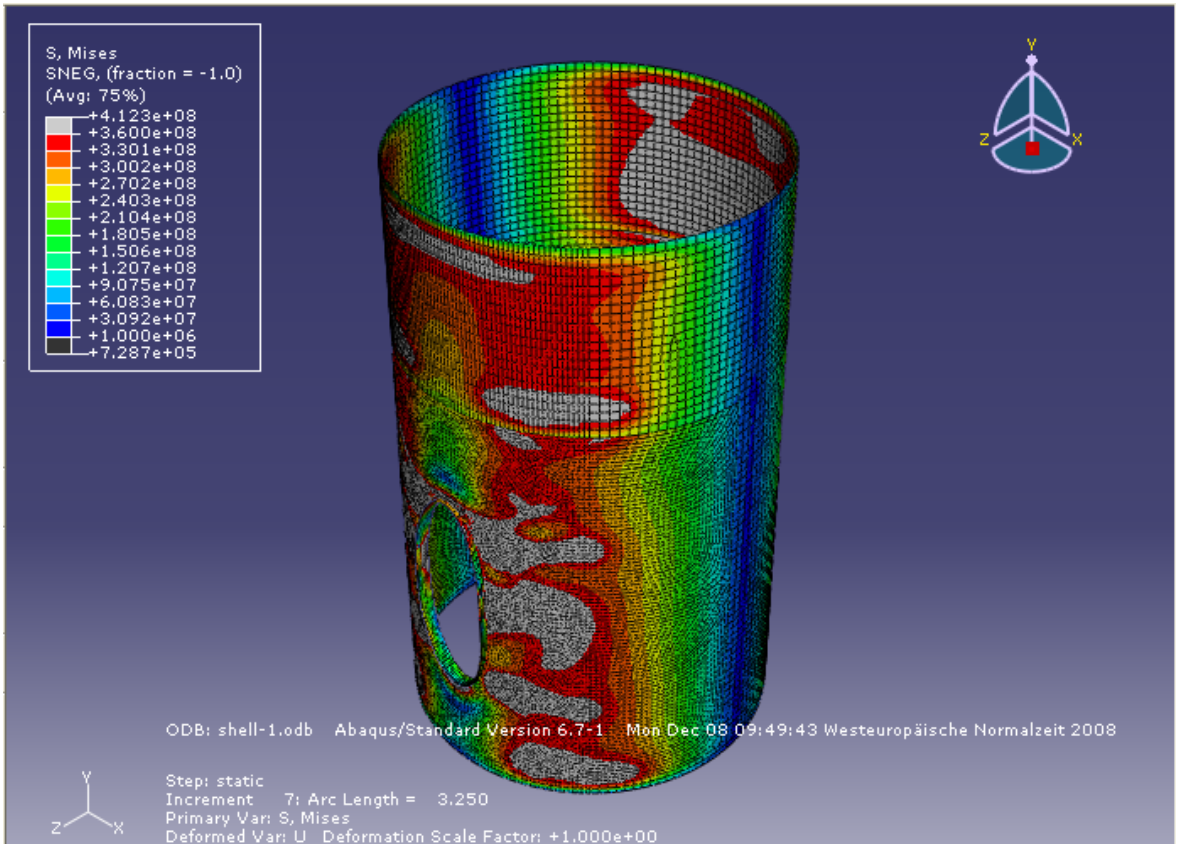

Model 1: 227,2 % Load

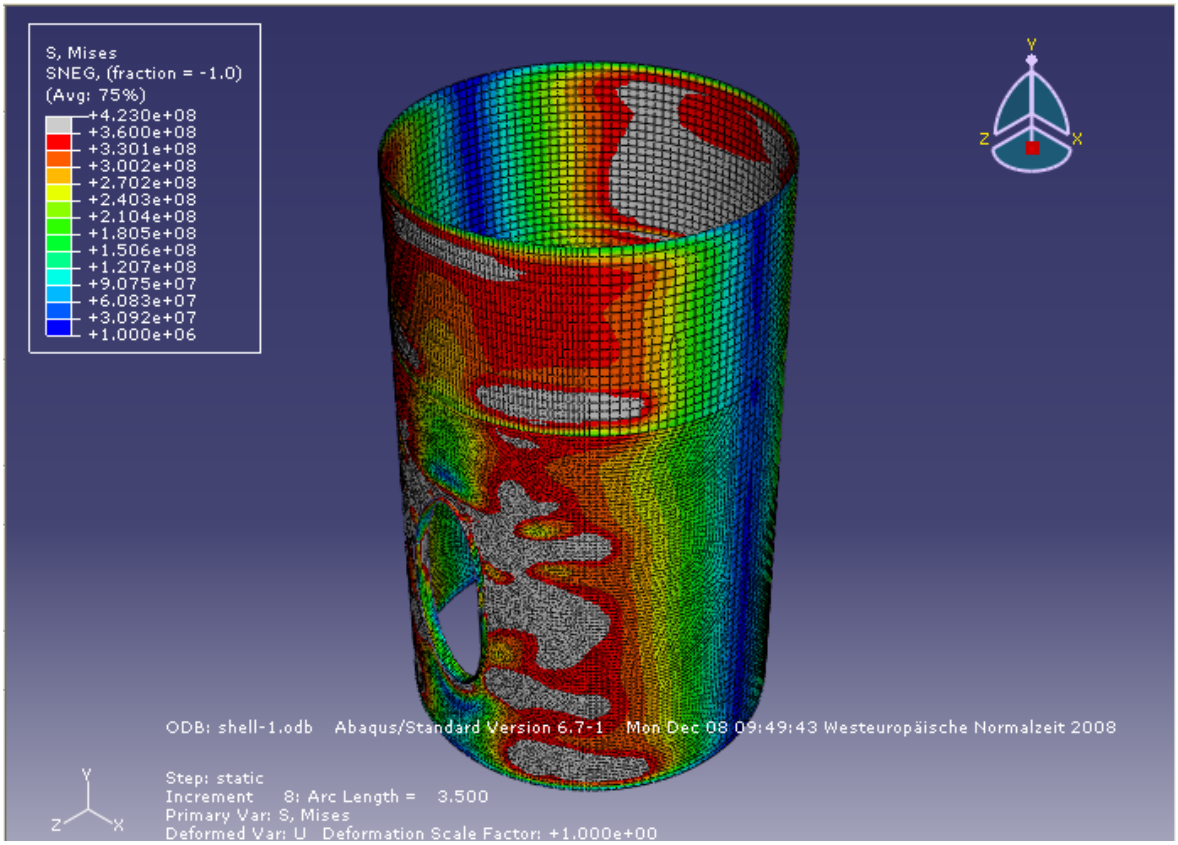

Model 1: 229,9 % Load

Appendix F – Contour plots of the stress distribution around the door in model 1

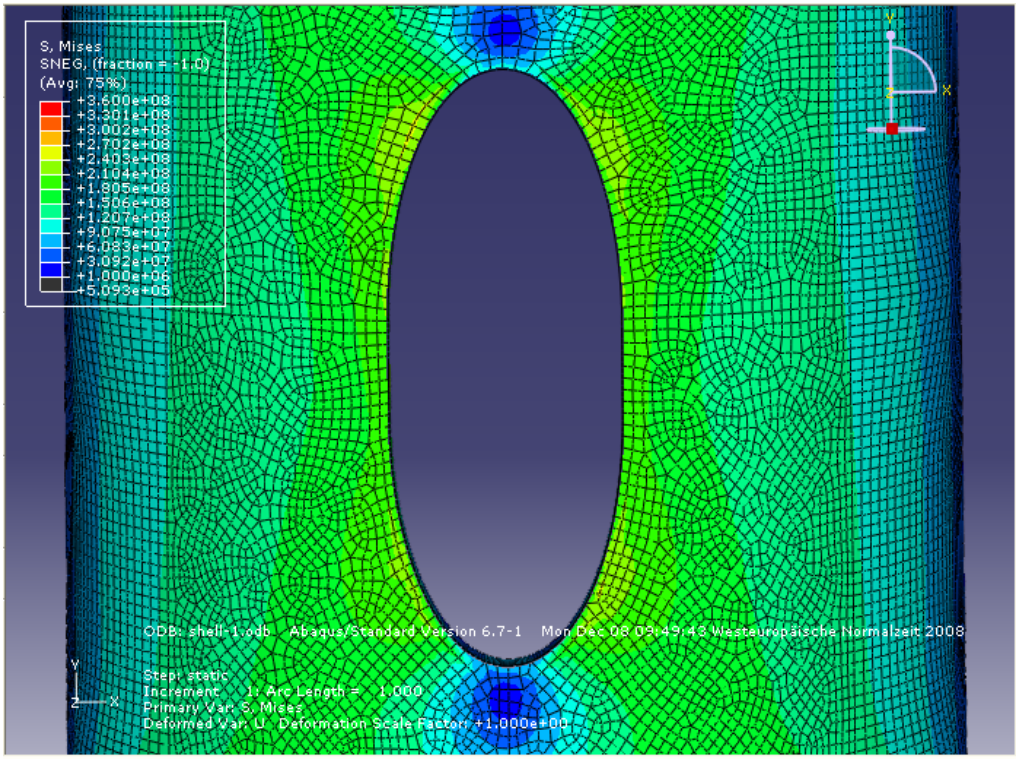

Model 1: Stress distribution at 99,5 % Load

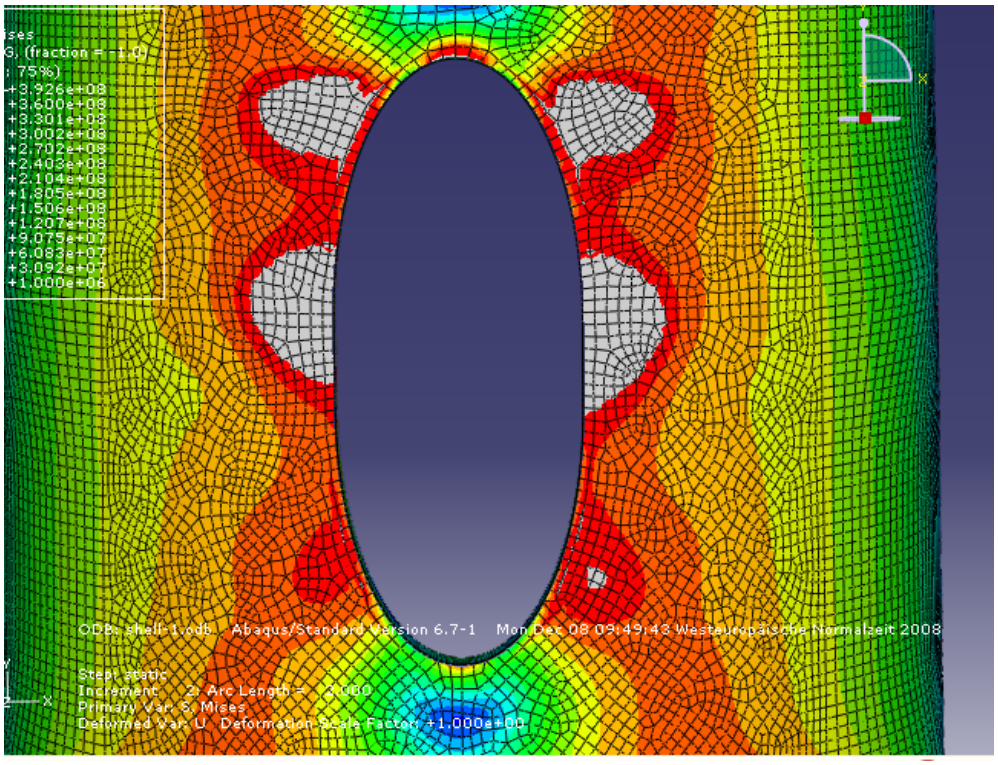

Model 1: Stress distribution at load 188,0 % Load

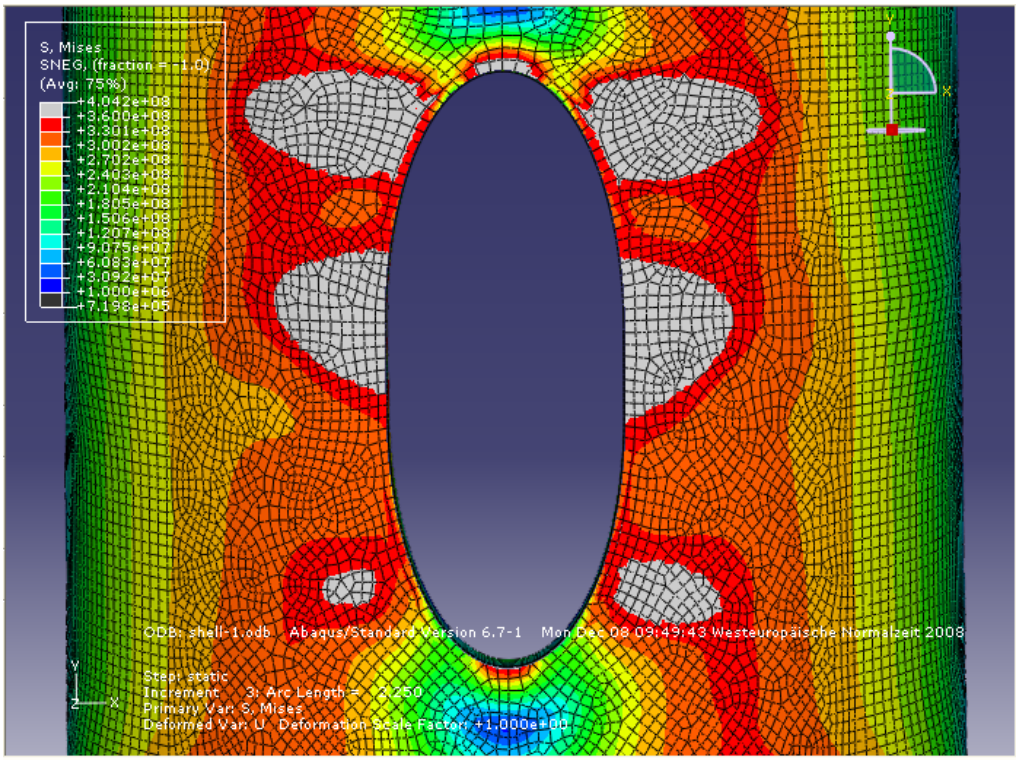

Model 1: Stress distribution at load 199,9 % Load

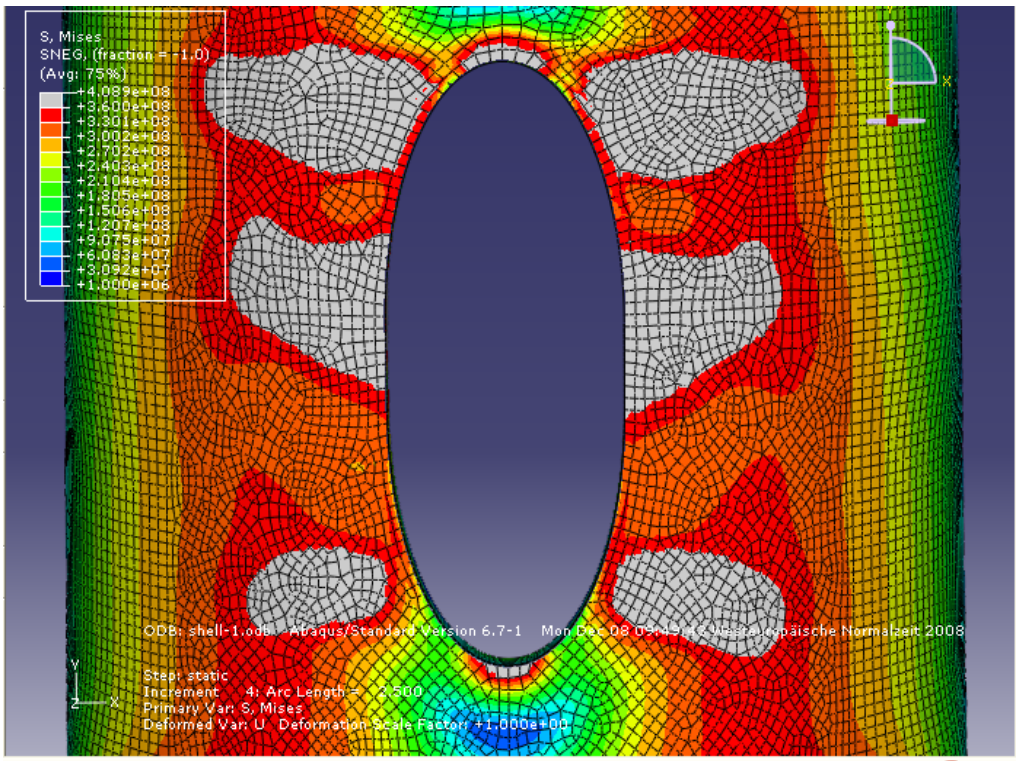

Model 1: Stress distribution at load 209,6 % Load

Appendix G – Contour plots of the buckling analysis

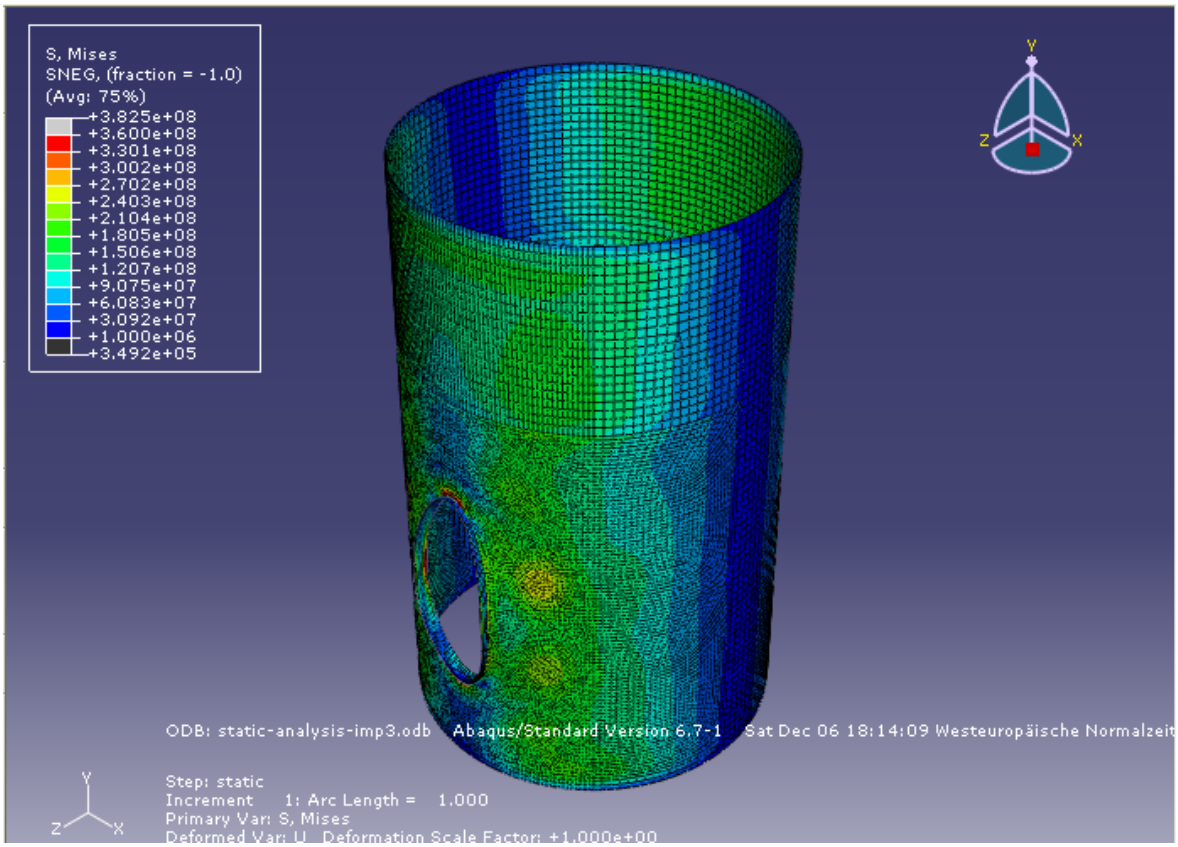

Model 11: 98,6 % load

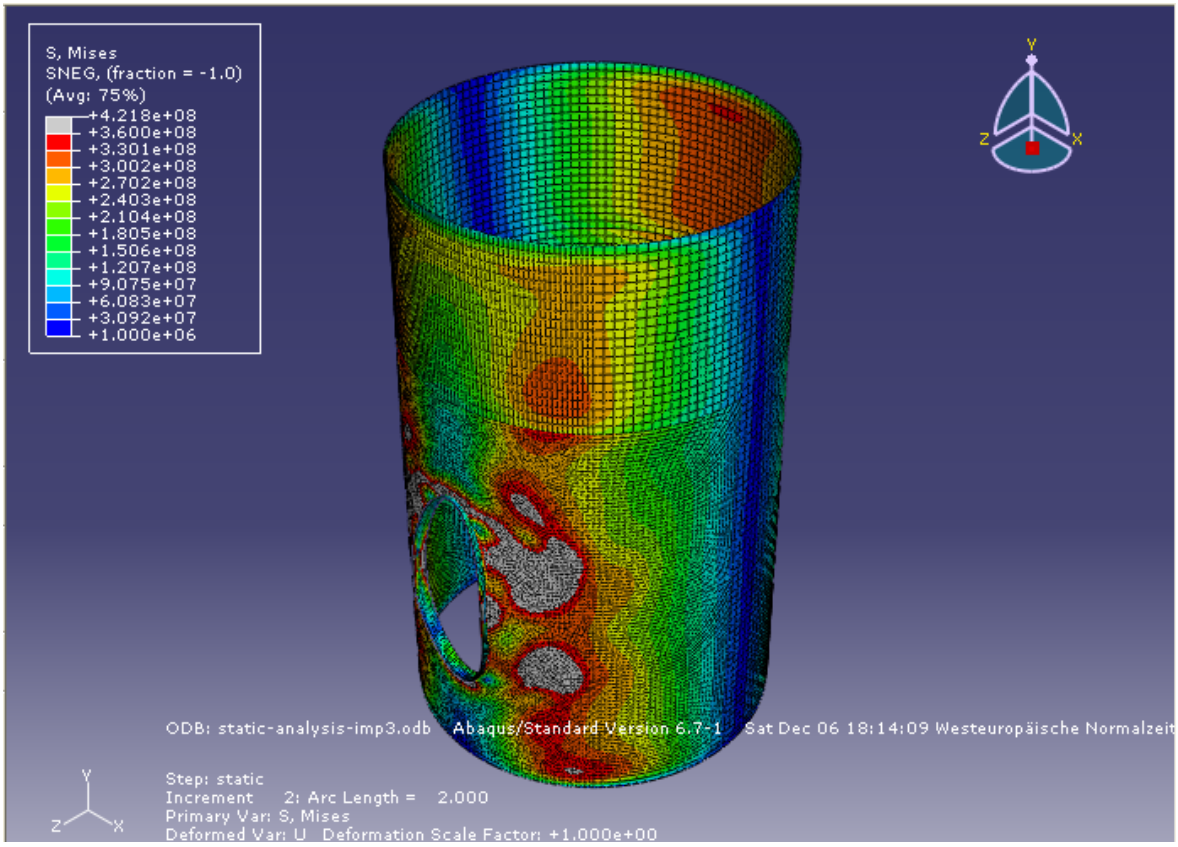

Model 11: 179,6 % load

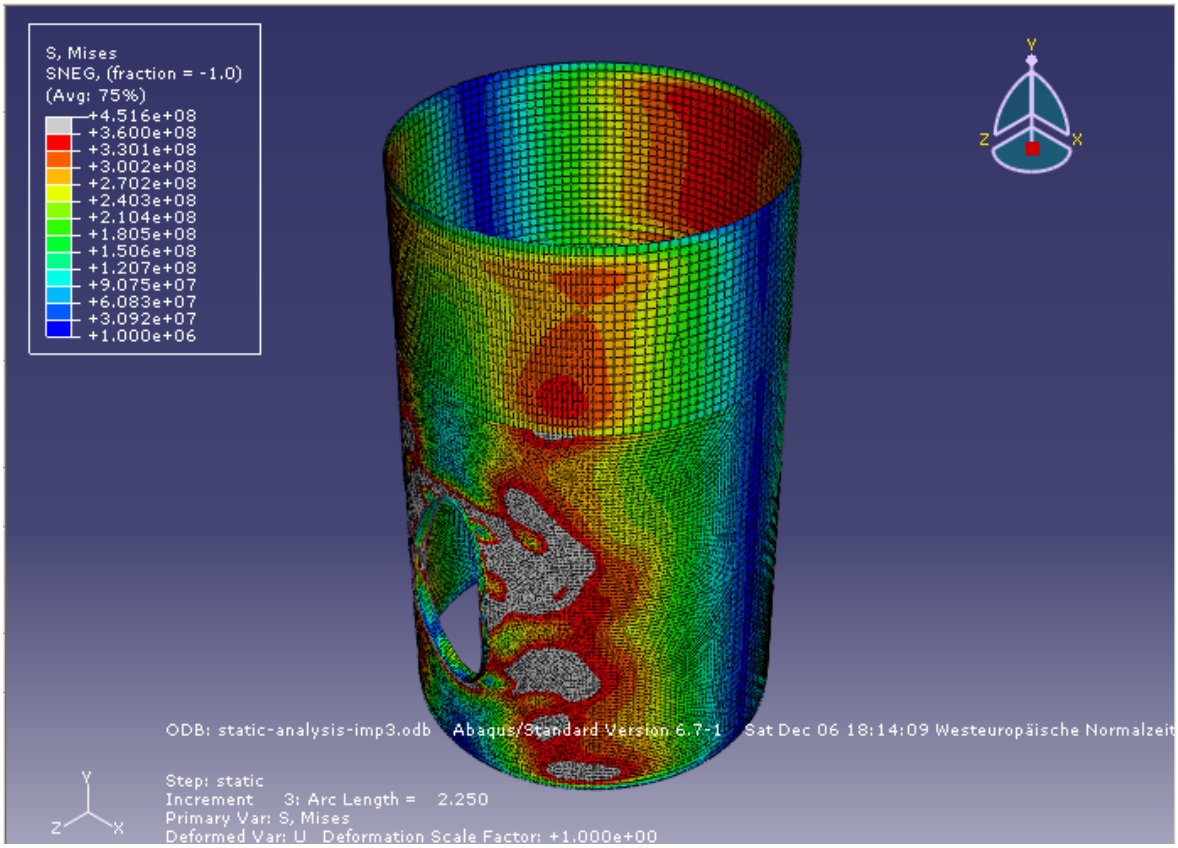

Model 11: 193,2 % load

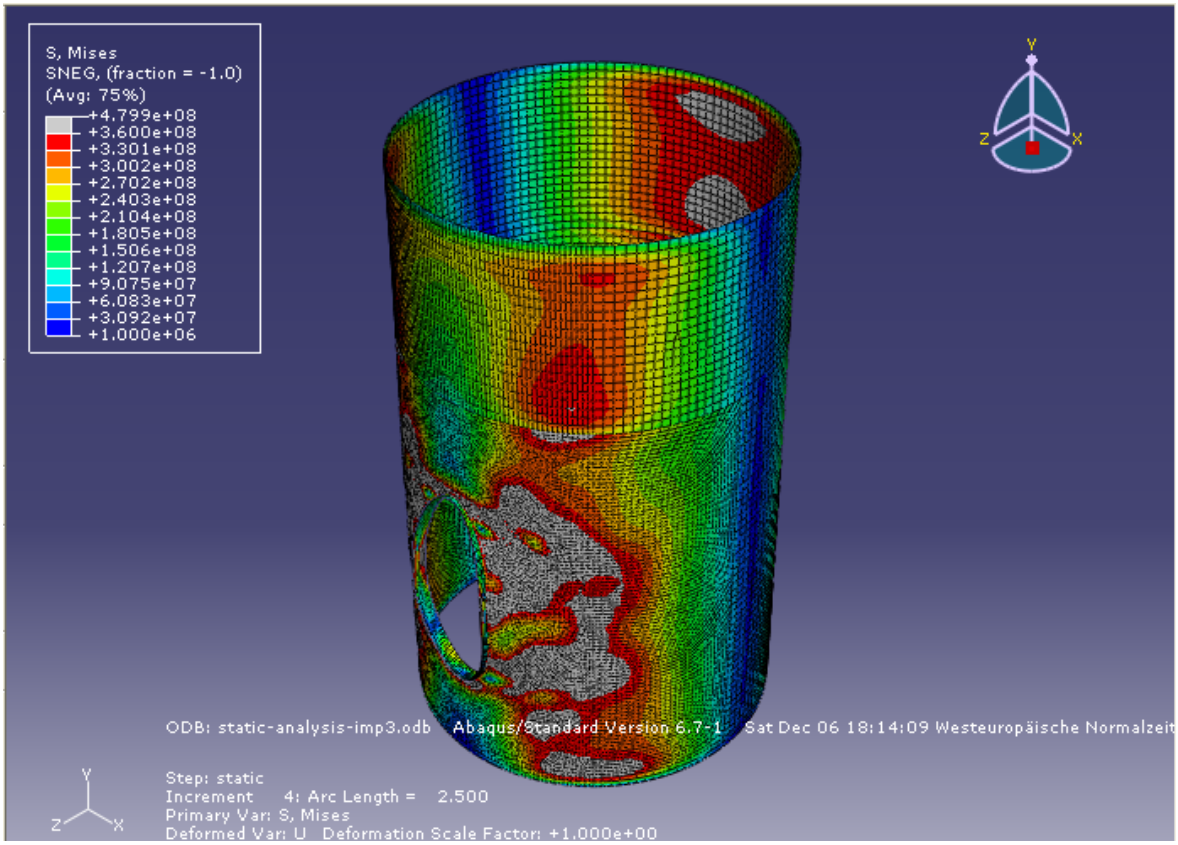

Model 11: 203,9 % load

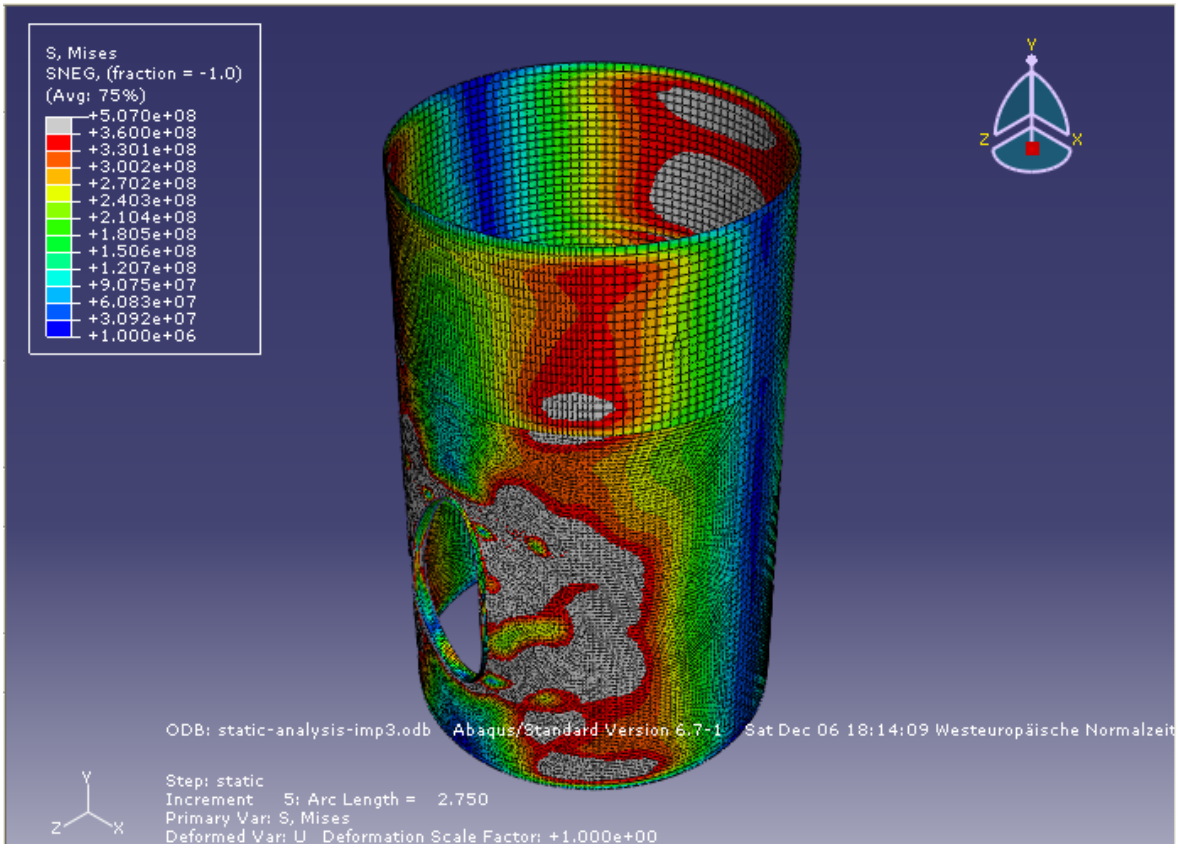

Model 11: 212,3 % load

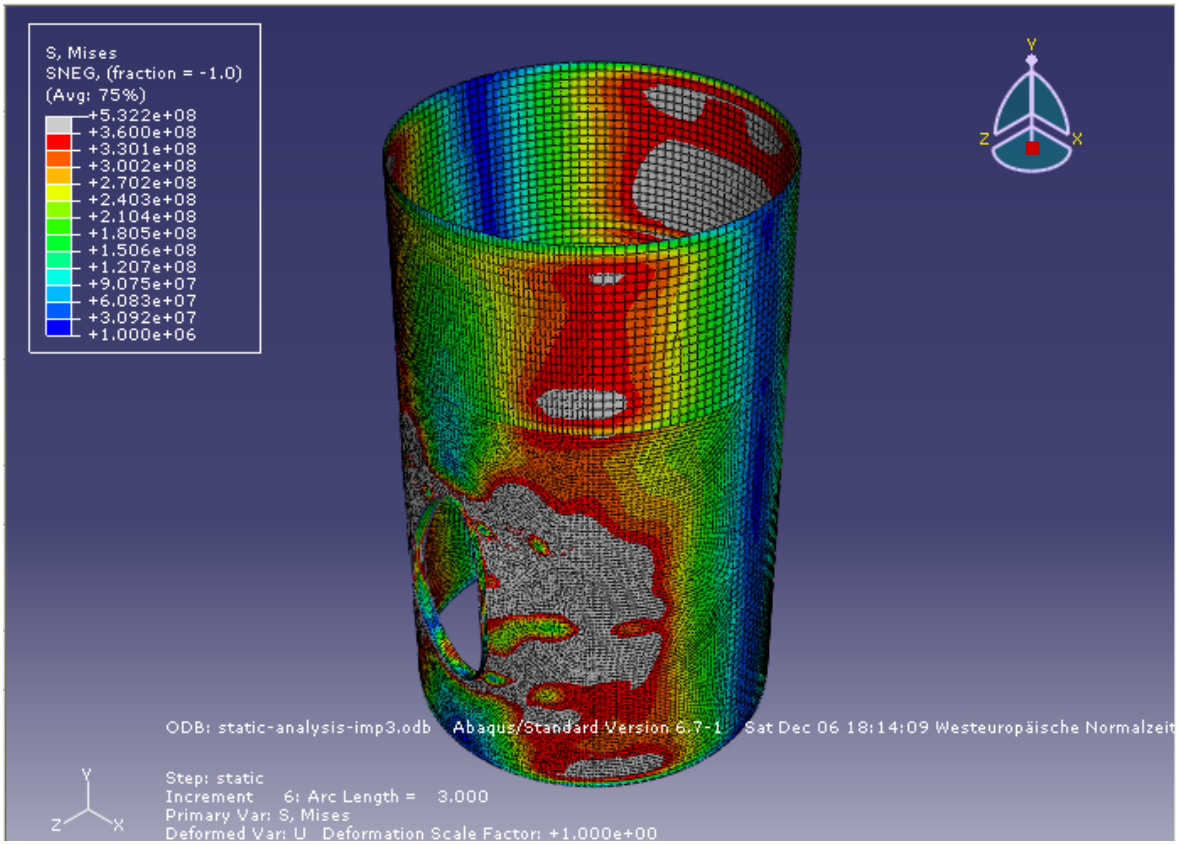

Model 11: 218,4 % load

Appendix H – Contour plots of Models 7, 15, 16

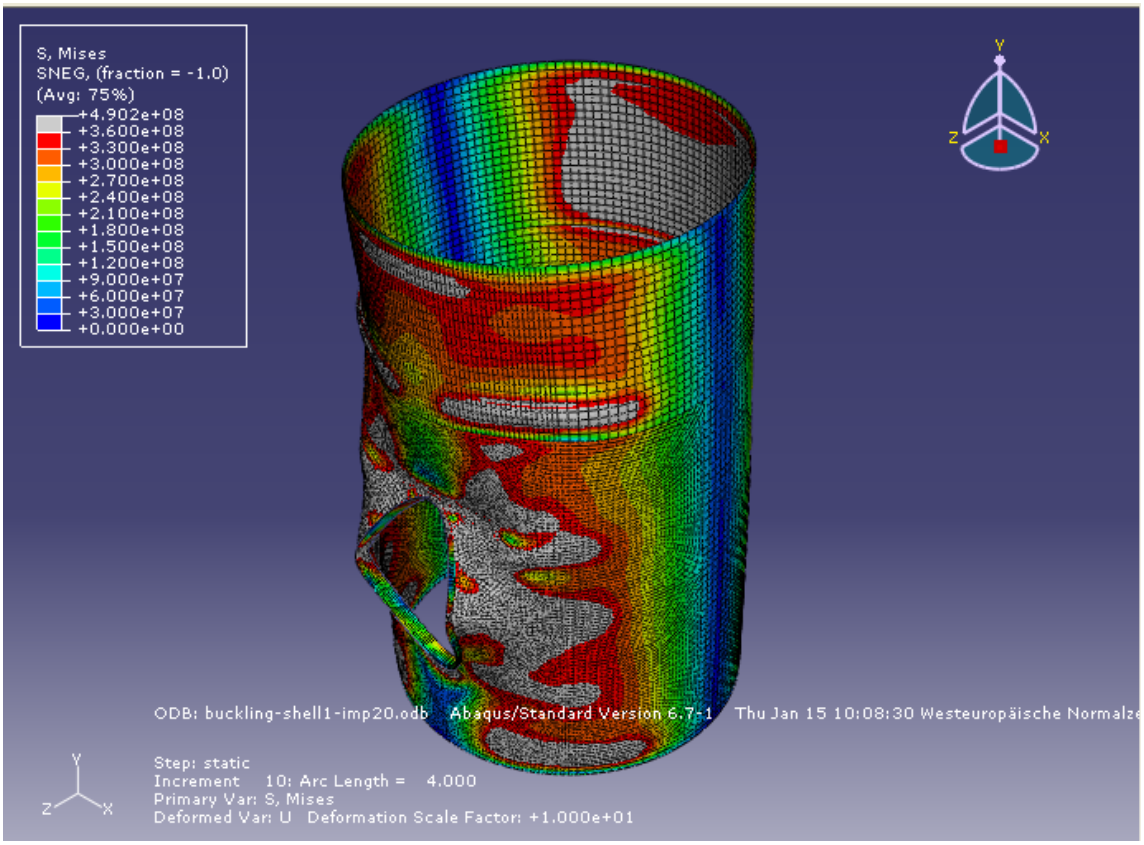

Figure 4.1: Model 7 at ultimate load

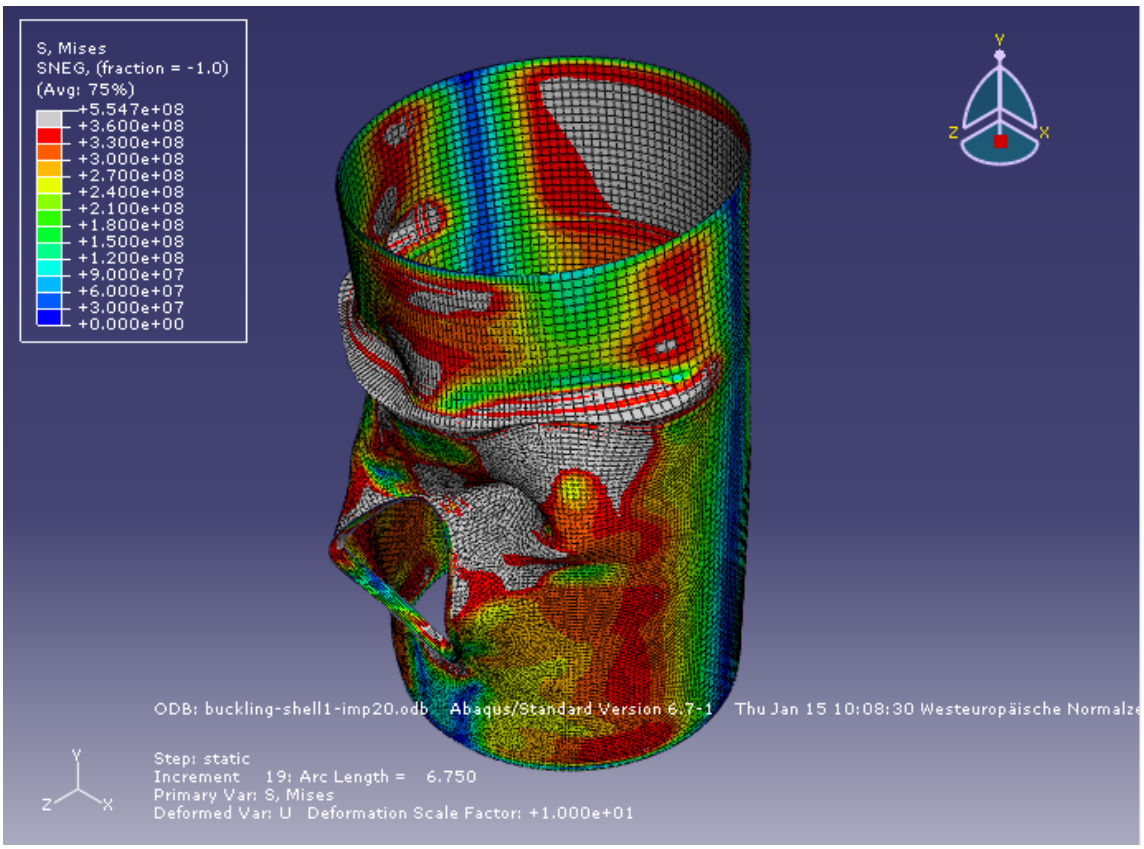

Figure 4.2: Model 7 at 197% load in the descending path

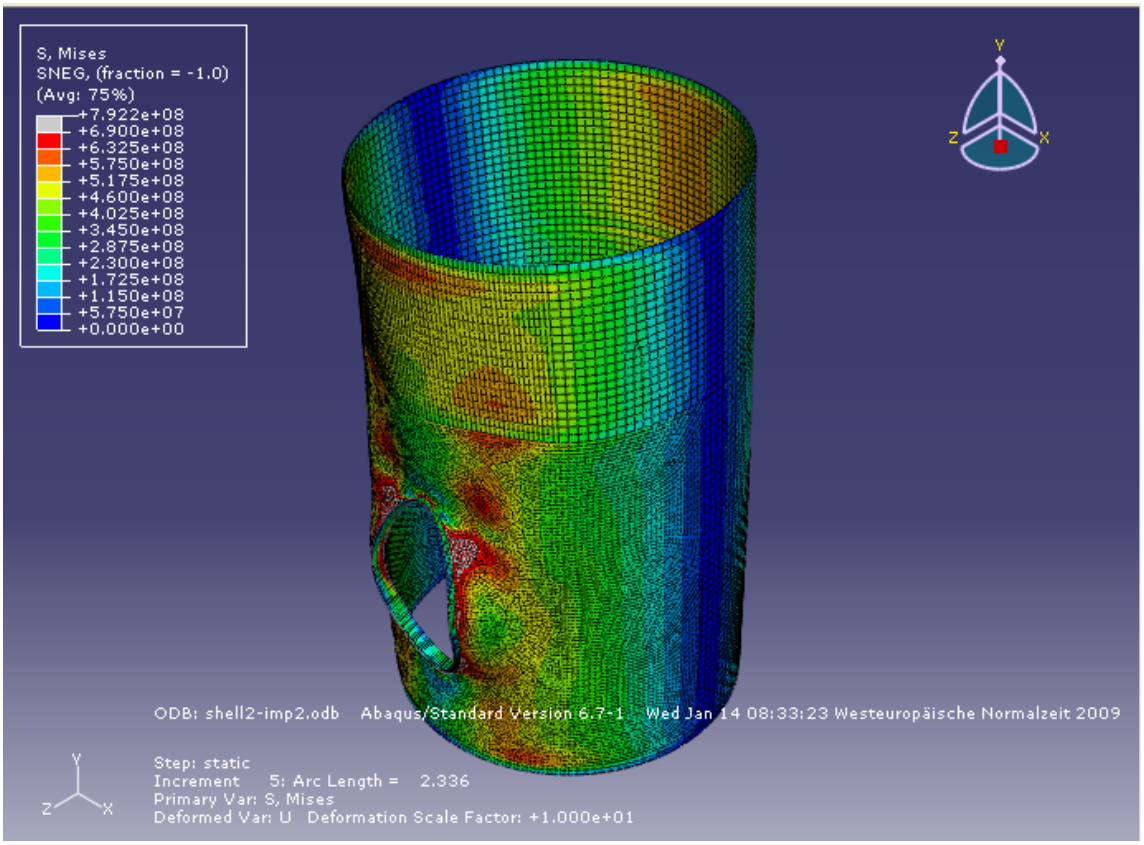

Figure 4.3: Model 15 at ultimate load

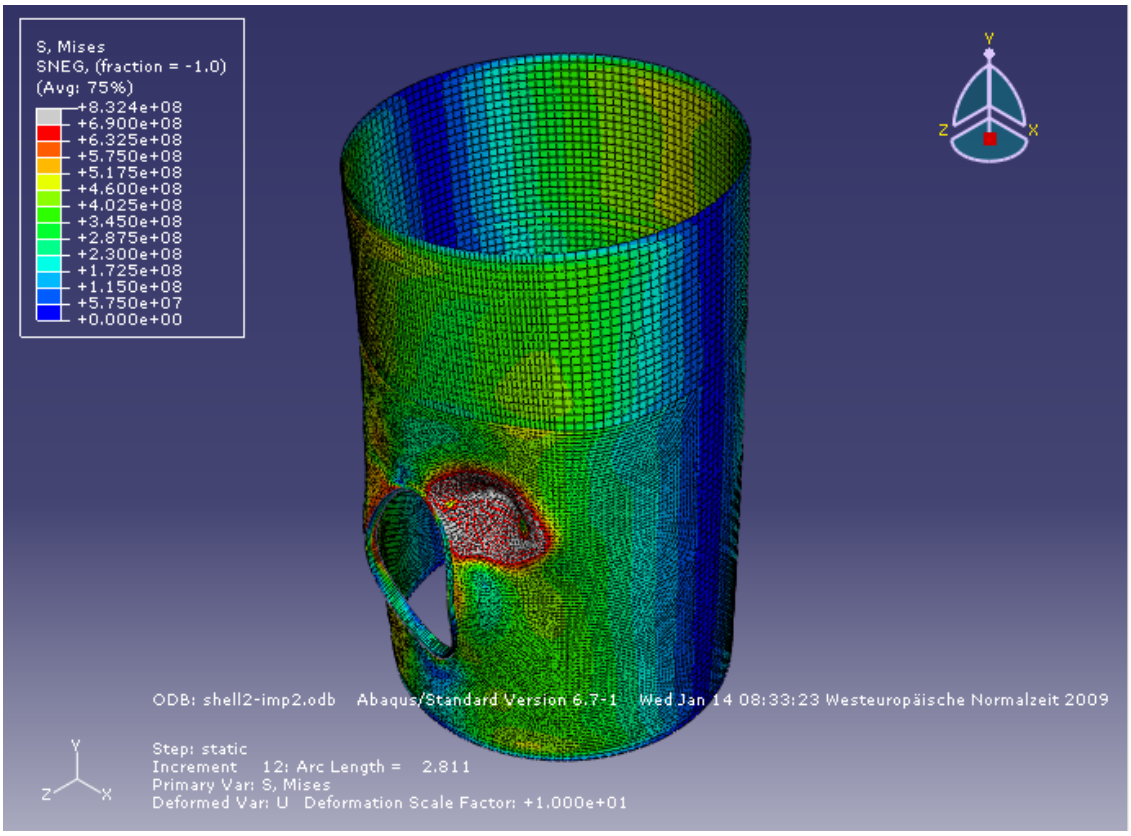

Figure 4.4: Model 15 at 175% load in the descending path

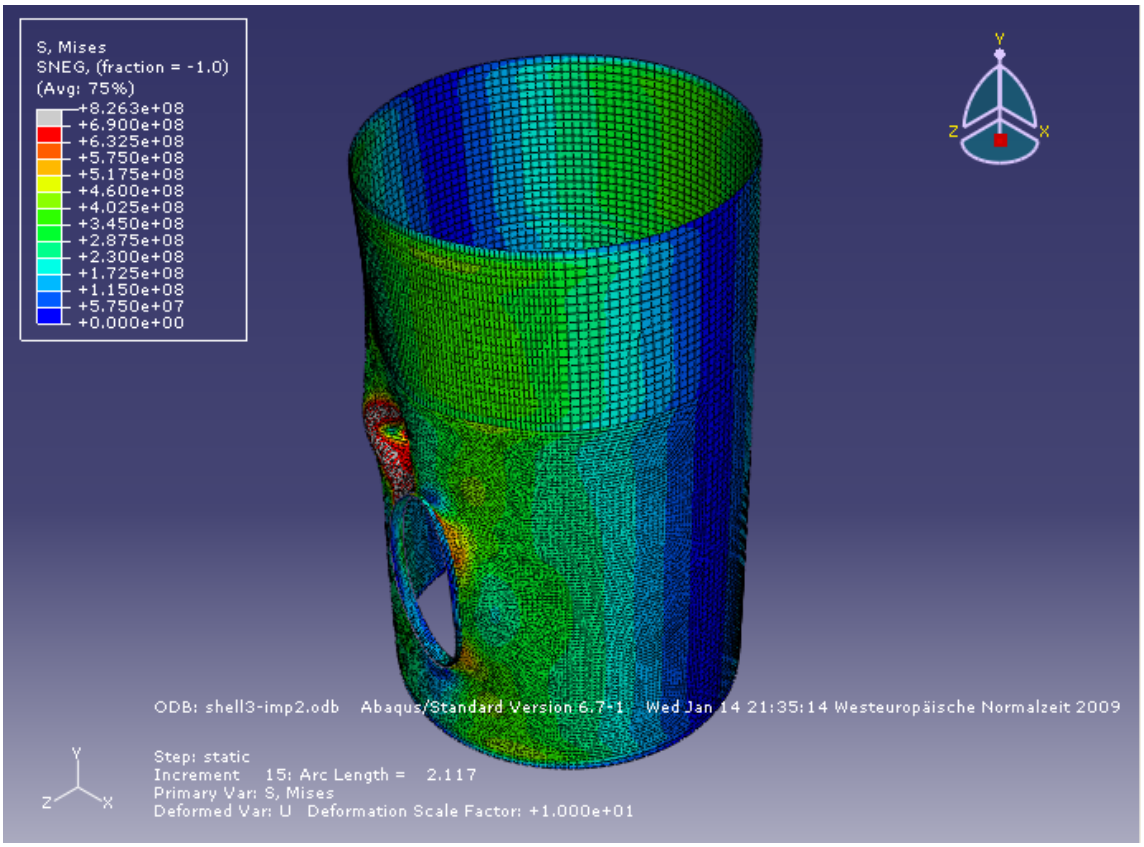

Figure 4.5: Model 16 at ultimate load

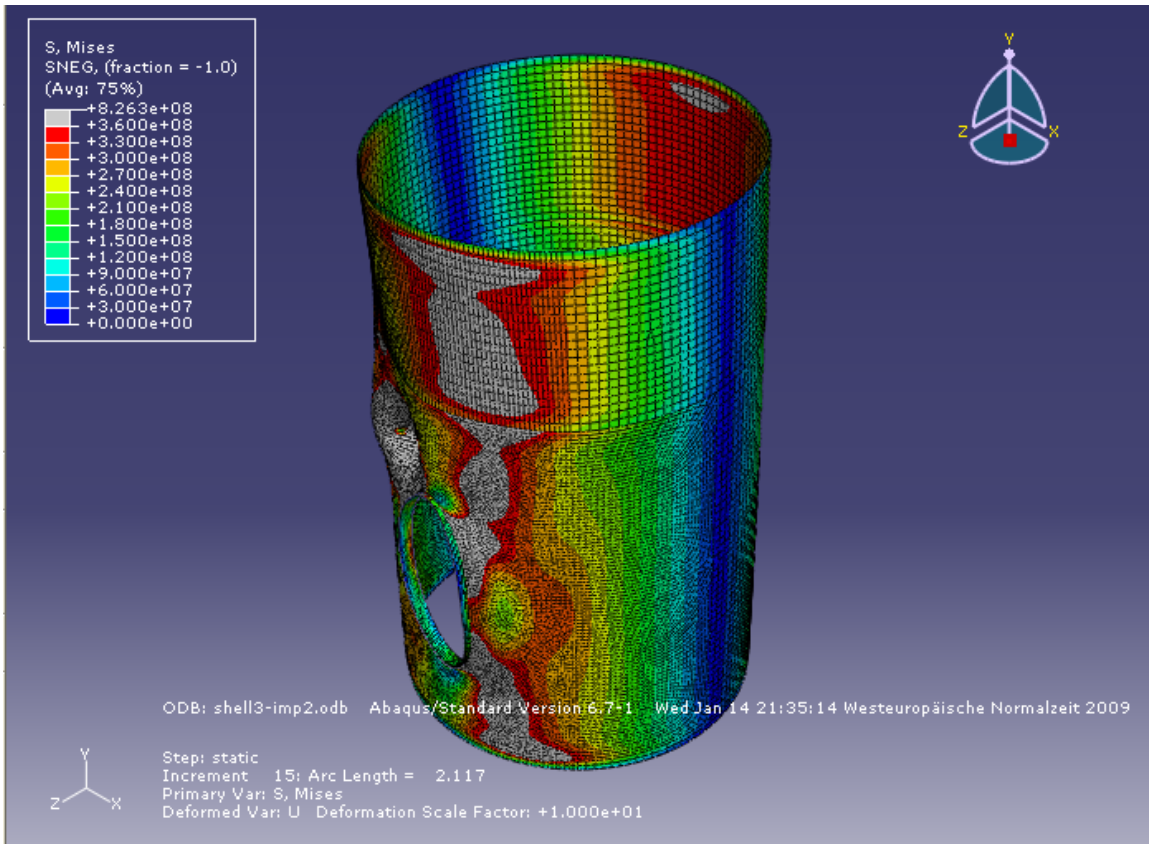

Figure 4.6: Model 16 at 103% load in the descending path

Appendix I – Contour plots of the models using S690 and high imperfection values

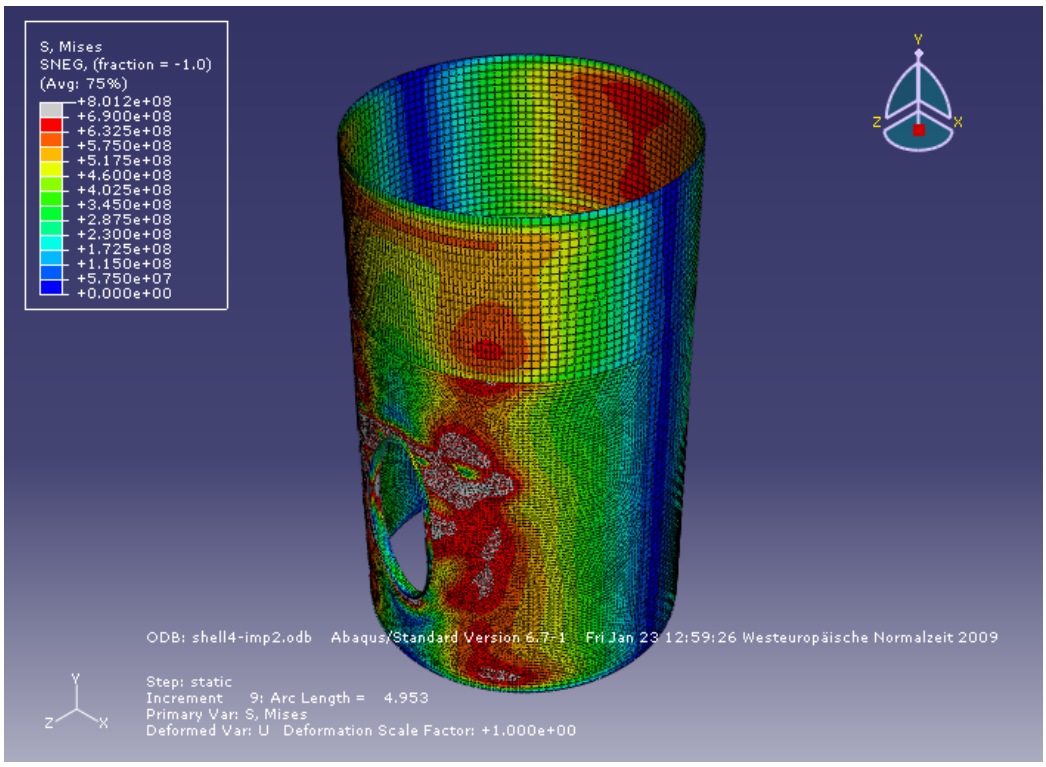

Figure 4.7: Model 14 at ultimate load

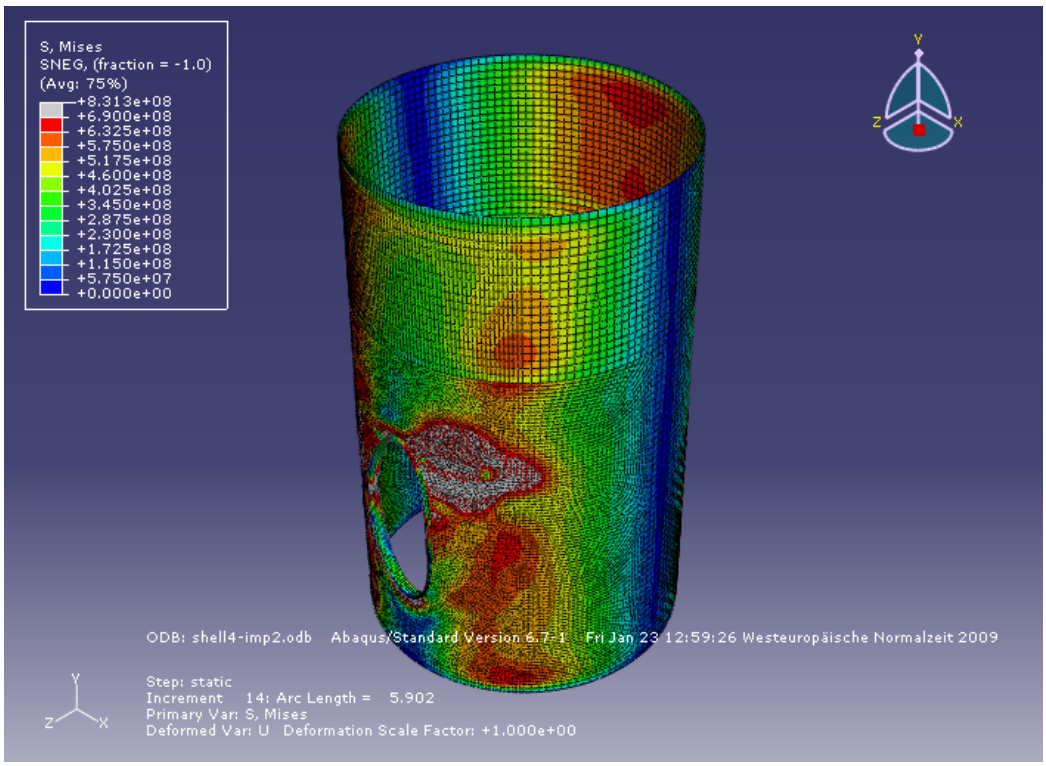

Figure 4.8: Model 14 in the descending path

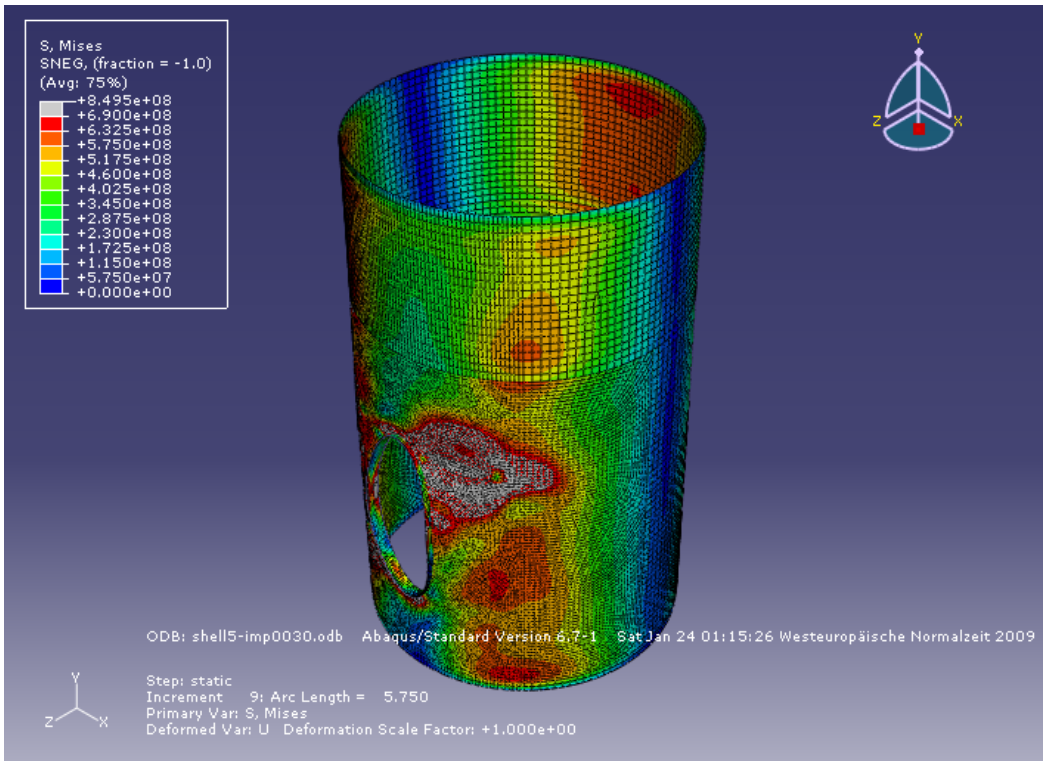

Figure 4.9: Model 17 at ultimate load

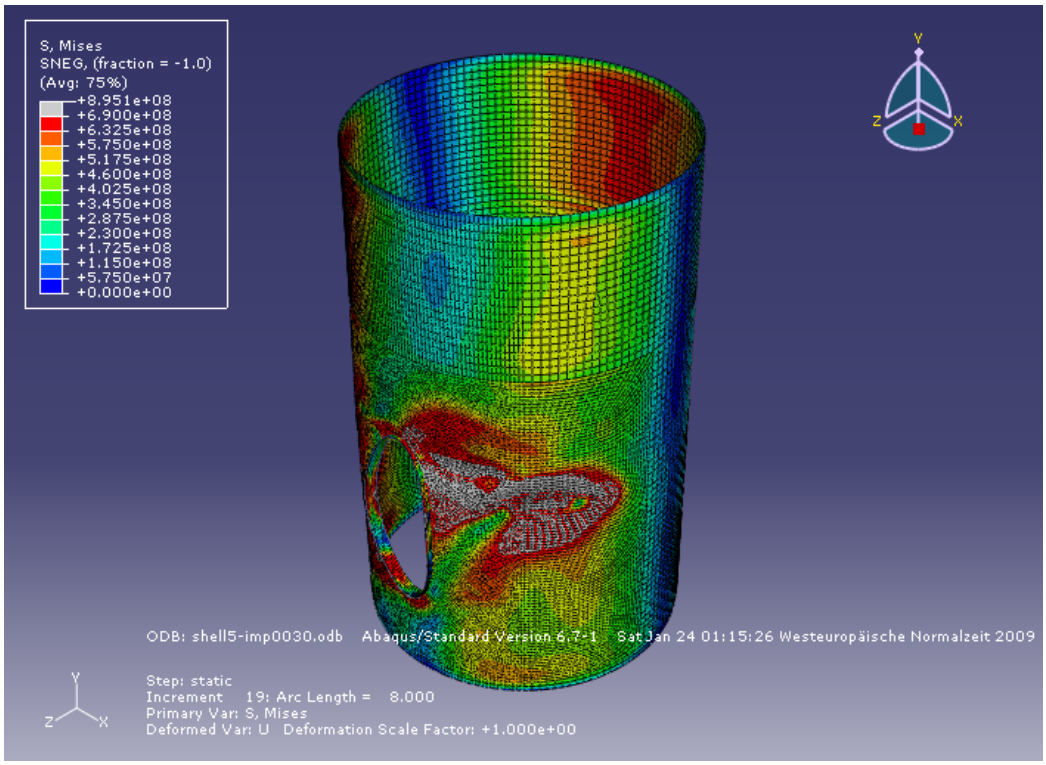

Figure 4.10: Model 17 in the descending path

Appendix J – Simulation models used for the report, properties and odb file names

Simulation model name	Thickness of the shell in Section 1 and 2 [m]	Thickness of the shell in Section 3 [m]	Stiffener thickness [m]	Yield strength [MPa]	Imperfection amplitude [m]	Name of the .odb file	Comment	Colour used for the graph
Model 1	0,03	0,026	0,07	360	0	pc-shell-1	parametric study	
Model 2	0,02	0,017	0,07	360	0	pc-shell-2	parametric study	
Model 3	0,015	0,013	0,07	360	0	pc-shell-3	parametric study	
Model 4	0,03	0,026	0,05	360	0	pc-stiffener-2	parametric study	
Model 5	0,03	0,026	0,03	360	0	pc-stiffener-3	parametric study	
Model 6	0,03	0,026	0,07	360	0	buckling-fy360-imp0	imperfection variation	
Model 7	0,03	0,026	0,07	360	0,006	buckling-fy360-imp1	imperfection variation	
Model 8	0,03	0,026	0,07	360	0,0163	buckling-fy360-imp2	imperfection variation	
Model 9	0,03	0,026	0,07	360	0,0254	buckling-fy360-imp3	imperfection variation	
Model 10	0,03	0,026	0,07	360	0,33	buckling-fy360-imp4	imperfection variation	
Model 11	0,03	0,026	0,07	360	0,09	buckling-fy360-imp5	imperfection variation	
Model 12	0,03	0,026	0,05	360	0,006	buckling-stiffener2-imp1	imperfection/stiffener variation	
Model 13	0,03	0,026	0,03	360	0,006	buckling-stiffener3-imp1	imperfection/stiffener variation	
Model 14	0,03	0,026	0,07	690	0,006	buckling-fy690-shell4-imp1	S690	
Model 15	0,02	0,017	0,07	690	0,004	buckling-fy690-shell2-imp1	S690	
Model 16	0,015	0,013	0,07	690	0,003	buckling-fy690-shell3-imp1	S690	
Model 17	0,03	0,026	0,07	690	0,03	buckling-fy690-shell5-imp0030	S690	
Model 18	0,03	0,026	0,07	690	0,06	buckling-fy690-shell6-imp0060	S690	

Simulation model name	Thickness of the shell in Section 1 and 2 [m]	Thickness of the shell in Section 3 [m]	Stiffener thickness [m]	Yield strength [MPa]	Imperfection amplitude [m]	Name of the .odb file	Comment	Colour used for the graph
Model 19	0,03	0,03	----	360	0	cmp-fy360-imp0000	Comparison FE/analytical	
Model 20	0,03	0,03	----	360	0,003	cmp-fy360-imp0003	Comparison FE/analytical	
Model 21	0,03	0,03	----	360	0,005	cmp-fy360-imp0005	Comparison FE/analytical	
Model 22	0,03	0,03	----	360	0,006	cmp-fy360-imp0006	Comparison FE/analytical	
Model 23	0,03	0,03	----	360	0,01	cmp-fy360-imp0010	Comparison FE/analytical	
Model 24	0,03	0,03	----	360	0,015	cmp-fy360-imp0015	Comparison FE/analytical	
Model 25	0,03	0,03	----	360	0,02	cmp-fy360-imp0020	Comparison FE/analytical	
Model 26	0,03	0,03	----	360	0,025	cmp-fy360-imp0025	Comparison FE/analytical	
Model 27	0,03	0,03	----	360	0,03	cmp-fy360-imp0030	Comparison FE/analytical	
Model 28	0,03	0,03	----	360	0	cmp-fy360-dooropening	door opening in cylinder	
Model 29	0,03	0,03	----	690	0	cmp-fy690-imp0000	Comparison FE/analytical	
Model 30	0,03	0,03	----	690	0,003	cmp-fy690-imp0003	Comparison FE/analytical	
Model 31	0,03	0,03	----	690	0,006	cmp-fy690-imp0006	Comparison FE/analytical	
Model 32	0,03	0,03	----	690	0,01	cmp-fy690-imp0010	Comparison FE/analytical	
Model 33	0,03	0,03	----	690	0,0112	cmp-fy690-imp00112	Comparison FE/analytical	
Model 34	0,03	0,03	----	690	0,0125	cmp-fy690-imp001125	Comparison FE/analytical	
Model 35	0,03	0,03	----	690	0,015	cmp-fy690-imp0015	Comparison FE/analytical	
Model 36	0,03	0,03	----	690	0,02	cmp-fy690-imp0020	Comparison FE/analytical	
Model 37	0,03	0,03	----	690	0,025	cmp-fy690-imp0025	Comparison FE/analytical	
Model 38	0,03	0,03	----	690	0,03	cmp-fy690-imp0030	Comparison FE/analytical	
Model 39	0,02	0,017	0,05	690	0,0207	buckling-fy690-shell2-stiffener2-imp3	higher imperfection	
Model 40	0,03	0,026	0,07	360	0	lc2-shell1	load case	
Model 41	0,03	0,026	0,07	360	0	lc3-shell1	load case	
Model 42	0,03	0,026	0,07	360	0	lc4-shell1	load case	
Model 43	0,03	0,026	0,07	360	0,006	fatigue-shell1	fatigue load	
Model 44	0,03	0,026	0,05	360	0,006	fatigue-stiffener2	fatigue load	
Model 45	0,03	0,026	0,03	360	0,006	fatigue-stiffener3	fatigue load	

Appendix K – Tutorial for Abaqus 6.7, modelling of a structure in shell elements

Tutorial for Abaqus 6.7

Modelling of a structure in shell elements

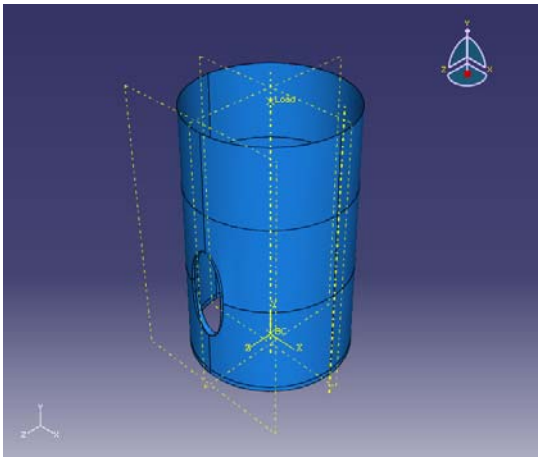

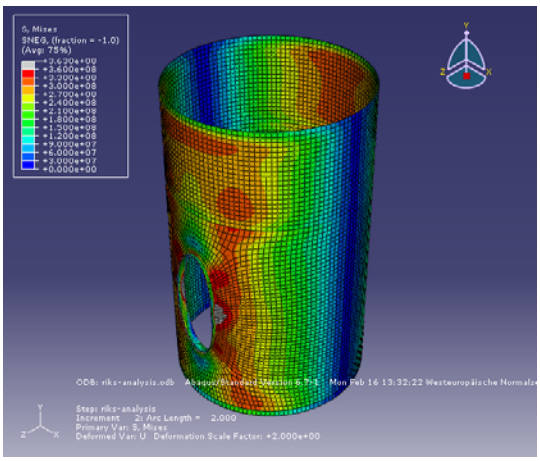

Stefan Golling

Luleå University of Technology
Dept. of Civil, Mining and Environmental Engineering
Division of Structural Engineering – Steel Structures
Luleå, March 2009

Table of contents

1. Introduction 2
   1.1. Introduction to the tutorial 2
   1.2. Modelling strategy 3
2. Installation of Abaqus 4
3. Starting Abaqus 5
   3.1. Starting Abaqus in Windows 5
   3.2. Starting Abaqus on the server of the university 5
4. Creating a simulation model 7
   4.1. The main screen 8
   4.2. Creating a model geometry 9
   4.3. Edit material properties 11
   4.4. Create sections 12
   4.5. Importing sketches 15
   4.6. Creating datum point, axis or plane 16
   4.7. Create partition 17
   4.8. Meshing the geometry 18
      4.8.1. Mesh controls 18
      4.8.2. Mesh elements 18
      4.8.3. Seeding and meshing the structure 18
      4.8.4. Mesh verification 19
   4.9. The assembly module 20
      4.9.1. Adding an instance 20
      4.9.2. Create positioning constrains 20
      4.9.3. Creating a reference point 21
   4.10. Constraints 21
      4.10.1. Tie constraint 21
      4.10.2. Coupling constraint 22
   4.11. The step module 23
   4.12. Loads and boundary conditions 23
   4.13. The key word editor 24
   4.14. The job module 25
   4.15. Submitting a job to the processor 25
5. Creating a similar model for further analysis 26
6. Analysis of the results and visualisation 28

1. Introduction

1.1. Introduction to the tutorial

The commercial available software package Abaqus is used for finite element analysis. Abaqus consists of three products, Abaqus-Standard, Abaqus-Explicit and Abaqus CAE.
Abaqus-Standard is a solver using implicit integration; Abaqus-Explicit uses an explicit integration scheme to solve finite element problems. An explicit integration scheme is used to solve highly nonlinear or quasi static problems.
Abaqus CAE is the part of the product where models can be created (pre-processing) and results can be visualized (post-processing).

This tutorial describes how to model geometry using shell elements. The tutorial was created as part of a project work. Properties which were part of the project are not mentioned here but with access to the project report it is possible to create models equal to the model used there. If no access to data of the project is possible it is still possible to create a model, values for geometry and loading etc. are provided within the tutorial.

The following chapters describe all necessary steps to create a database, to analyse it and to visualise the results. The tutorial contains basic information regarding the options used for creating the model. For further information see the user's manual.

A cae file containing the model described in this tutorial is available in the Division of Structural Engineering – Steel Structures.

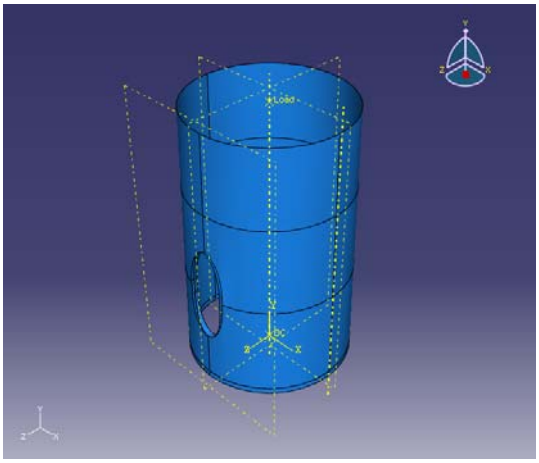

1.2. Modelling strategy

Abaqus provides the model tree as a proper tool for having an overview of the modelling process. Following the model tree from top to the bottom creates a full model database. The model tree has branches which contain further attributes. The user can select an attribute by double clicking on it in the model tree. A context will open and request information. Abaqus guides thru this context telling the user which step needs to be done next to complete the attribute.

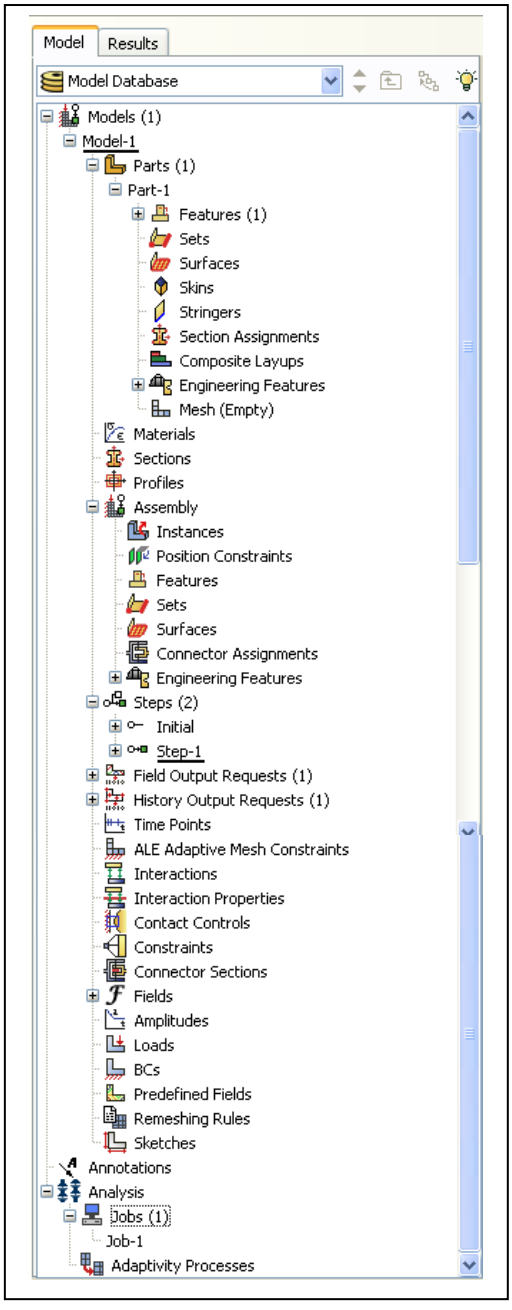

The two tabs on top allow a fast change between model and result side.

One cae file can contain several models; these models are listed in alphabetic order.
A model consists of parts. Under the heading “parts” are all parts created in the model listed. Also are in every part all necessary settings listed to define it. Important are “features” which contain the geometry, “section assignment” assigns the properties to the part and “mesh” defines the part for numerical analysis.

Following the parts are the materials. It is possible to create different materials in one model.
Sections are necessary to define a part; they include all properties of a model and are assigned to a part.

In assembly parts are added as instances. It does not matter if a simulation consists of one or several parts, adding a part in the assembly is necessary. Also positioning is performed here.

Steps contain the analysis which will be performed. It is possible to perform several steps after each other.

Constraints are necessary if two or more parts need to interact during a simulation.
Connections between parts or points are established using options from here.

Loads contain the loading of a model while BCs contain the boundary conditions used in the model.

When a model is finished an analysis can be started this is done using the Jobs option.

2. Installation of Abaqus

The installation of Abaqus 6.7 under Windows runs automatically. It is recommended to install the Abaqus html help before installing Abaqus simulation tools. The installation cd's are marked with "Abaqus 6.7 HTML help" and "Abaqus 6.7 for Windows". If the operating system of the computer differs from windows the right cd needs to be chosen. The installer supports the user during the process of the installation.
Settings which have to be done by the user during the installation are to select the way how the license for Abaqus is purchased, where the software should be installed and the work directory for the simulation process is also requested.

The setting of the installation path and the work directory can be freely chosen by the user. The path for the license depends on how the license is provided. The license for users at Luleå University of Technology is acquired from orion server. The following path needs to be added in the field for the path of the license.

orion.anl.luth.se

Abaqus will check and verify the path of the license. In some cases it happened that the license path was rejected during the first verification. If this happens the procedure of verifying the license path was repeated and solved in all cases the problem.

3. Starting Abaqus

3.1. Starting Abaqus in Windows

Abaqus is started as every other software on windows. Under “Start”, “Programmes”, “Abaqus 6.7” the start button “Abaqus CAE” is used.
Another link leads to the html documentation of Abaqus. The help opens in the standard internet browser. The use of the online help is comfortable and logic in its structure so that no explanation of it is added in the tutorial.

3.2. Starting Abaqus on the server of the university

It is additional possible to run Abaqus on the server of the university. The main advantage of using the server is the calculation time of simulations. Disadvantage is the slow graphical interface of the server, reason for this is that the server is not intended to be used for graphical displays. A logical handling of the two possibilities of running Abaqus is to create and analyse (pre- and post-processing) models local on the computer and to run the simulation (processing) on the server.
To start Abaqus on the server of the university some additional software is required on Windows based computers.

Required software:

- Putty, a terminal emulator application which can act as a client for the SSH (secure shell) network connection
- Cygwin, is a Unix-like environment and command-line interface for Microsoft Windows

The cygwin software is needed to run Abaqus on the server and to visualise it on a Windows computer is cygwin. Cygwin contains the tool x-server which allows to display Linux based software on Windows computers.
For both tools are more detailed descriptions available in the internet.

The settings in putty which are necessary to get the connection to the server are:

- Host Name (or IP address) orion.anl.luth.se
- Port 22
- Connection type SSH

- Under “SSH” → “X11” it is necessary to set a check at “enable X11 forwarding”

If one of the settings is wrong it will be not possible to establish a connection to the server.

After the settings are down a connection to the server can be established by clicking on “Open”. The window which opens then requests user name and password for the server. After the user is logged in the command “abq671 cae” starts the software. It is necessary to start x-server before the start command for Abaqus is typed.

The installation of cygwin requires the free available setup file. The file can be found in the internet by using any search engine. When the setup file is used the required components are downloaded and installed automatically. The download of the complete cygwin software package is not recommended and not helpful because of its size. To install cygwin follow the instructions of the installation manager.

The parts which are required can be found under X11 and are named “Window maker” and “Xorg-server: x.orgx servers”

The X11 Window System is a software system and network protocol that provides a graphical user interface (GUI) for computers in networks. It implements the X display protocol and provides windowing on computer displays and manages keyboard and pointing devices. Further information regarding X11 is available in the internet.

To start Abaqus on the server:

- start cygwin using the command “cygwin bash shell” from “start”, “programmes”, “cygwin”
- type in the window which is opening “X” and press enter, this command starts the x-server tool
- start putty and connect with your user name and your password to the server
- type “metacity &”, this tool creates a more user friendly surface on the screen. This setting is recommended but not necessary to run Abaqus.
- start Abaqus with the command “abq671 cae”

To disconnect from the server type in the window of putty “exit”, it is recommended to perform this logout to avoid problems with the licensing server of the university.

The use of putty and cygwin described here is only one possible way of connecting a local computer to a server. Several other ways are possible and not further mentioned here.

4. Creating a simulation model

After starting Abaqus the welcome screen is displayed. Here it is possible to choose between four options.

- Create Model Database
- Open Database
- Run Script
- Start Tutorial

To continue with the description of this tutorial it is necessary to choose “Create Model Database”. This option opens a new file and a model can be created. An existing database can be opened by using “open database”. Abaqus contains also a tutorial with example files, to open the tutorial select “Start tutorial”. The “run script” button is used if an existing python script is used. Python is a programming language and used to customize Abaqus. The scripting tool is not further mentioned in this tutorial.
The first useful, but not necessary step creating a new model is to set a work directory. This is only necessary if during the installation no work directory was created which will be used for all simulations. The default work directory is the one selected during the installation. A change of the work directory depending on the simulation project can be helpful. All data created during the simulation and the analysis is saved in this directory. The steps needed to change the work directory a shown in Figure 1.
If Abaqus runs on the server is the work directory the root folder of the user. A change of the directory is here also possible.
A change of the work directory is only valid for the actual session. If Abaqus is closed and restarted it is necessary to set the work directory again.

Note:
For the file exchange between local computer and server is a client necessary. A free available client is “Filezilla”. To connect server and local computer the same settings than in putty can be used. The client is not further described in this tutorial.

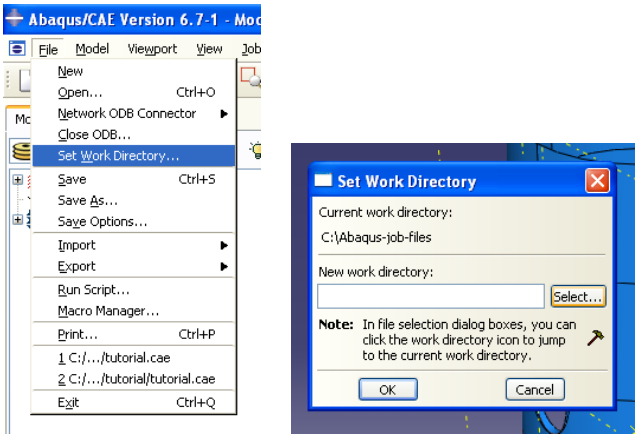

Figure 1: Change of the work directory

Change of the work directory:
Click on ”file” in the menu – select “set work directory” – click on “select” and choose the folder which will be the work directory

4.1. The main screen

The main screen of Abaqus looks always similar but changes buttons and possible actions depending on the module which is used. It is necessary to change between the modules to create a full simulation model. The change between the modules is done using the module drop down list or by clicking on the module in the model tree. Figure 2 shows the main screen, marked with a red frame the module tree and in orange the module drop down list.

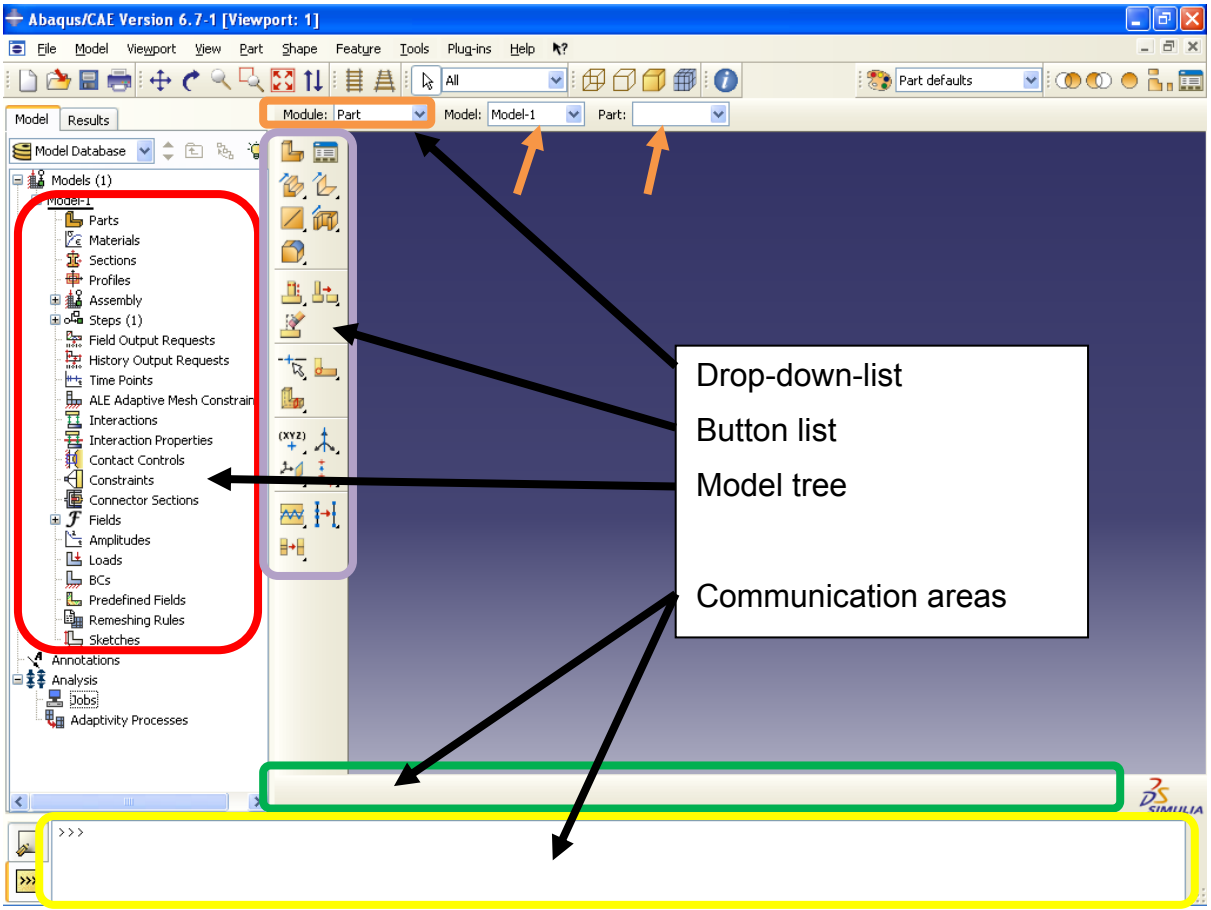

Figure 2: The main screen of Abaqus

On the right side of the module drop down list are “model” and “part” displayed, marked with orange arrows. If more parts or models are used in the same cae file are this drop down lists useful to change between different models and parts.
The green frame in Figure 2 marks the part of the screen where Abaqus communicates with the user. In every module and at every action which contains several steps until the procedure is finished Abaqus tells the user which step has to be done next. Also the confirmation of actions is done here.
The area marked with a yellow frame in Figure 2 is also a communication area. Abaqus displays here information which are requested by the user, one example for this is the use of the query which displays the results here another information provided here is the path where a model is saved..
The purple frame in Figure 2 indicates the button list.

Note:
Abaqus uses no units! The user has to take care that the units used for the creation of models match to each other.

4.2. Creating a model geometry

The first step is to create a part; the part defines the model geometry. The model geometry can be created similar to commercial CAD software. To create a part double click on “parts” in the model tree or click on the button “create part” in the button list. It is possible to give a name to the part in the dialog box; also it is possible to choose between the model space, the type of the part, the shape and the type of the part generation. Clicking on continue exits the create part dialog and to the sketching screen. Here the part can be drawn. Figure 3 visualises the create part dialog and the sketching screen.

Options in the create part list:
Modelling space → selection if the simulation space is two or three dimensional, it is up to the user to decide which one is appropriate.
Type → if a part is analysed it is necessary to choose “deformable”, in some cases of multi part simulations it is possible to create parts as rigid to simplify the model.
Base feature, shape → from this list it is possible to choose the upper-level-group of the elements which are used in the simulation.
Base feature, type → form this list it is possible to choose how the part is created. Extrusion creates a part extruded along an axis while the shape is drawn on one plane. Revolution creates parts were a lines are drawn on one plane and then revolted around an axis to create a body.
Sweep is used to draw as first step a path while the second step is to draw the cross-section which is swept along the path.
Planar is only possible for the one and two dimensional parts such as wire and shell. It is possible to create a two dimensional part in a three dimensional space.

In the sketching screen are the usual drawing tools displayed in the button list. To finish the sketch of the part a click on the “Done” button is necessary.
To add dimensions to the sketch the button “Add dimension” is to use. Dimensions can be changed afterwards so that it is possible to draw the shape without dimensions and edit them in a second step. To do this the button “Edit dimension value” is used. The described functions are mentioned in Figure 4.

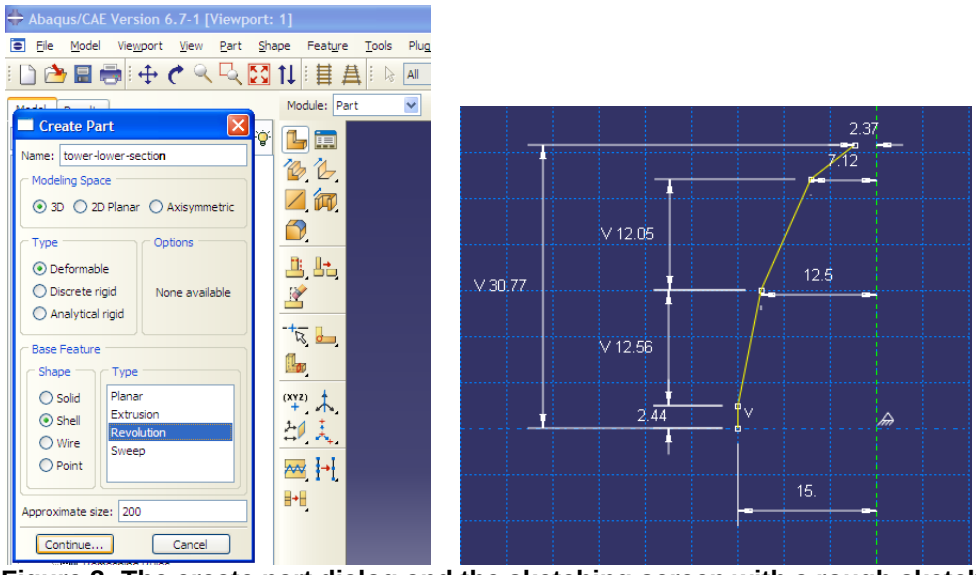

Figure 3: The create part dialog and the sketching screen with a rough sketch of the geometry

Left column	Right column
Create point	create line
Create circle	create rectangle
Create ellipsoid	create arc
Create circle with 2 points and center	create circle with 3 points
Create filet	create spline thru points
Construction lines	project edges or points
Tools for copying, moving, and cutting of lines as well as pattern tool and offset drawings	
Constrains for lines	
Add dimension tools	
Change dimension tool	parameter manager
Undo (only one action)	delete
Open sketch	save sketch
Options for changing the sketching area	

Figure 4: Drawing tools in the sketching area of the create part module

Example:

For this tutorial are shell elements used, which are revolved to a conical shape consisting of four segments. The dimensions suggested for the part are printed in Table 1. The sketch of the geometry without the suggested geometry values is plotted in Figure 3 on the right hand side. The lines one to four are counted from bottom to top.

To finish the creation of the part the button “done” is pressed and the “edit revolution” window opens. The angle of revolution can be selected; here the value 360 is to add.

Table 1: Suggested geometric properties

	Radius at bottom	Section height
Line 1	2,20	0,20
Line 2	2,20	2,40
Line 3	2,18	2,40
Line 4	2,16	3,00
	Radius at top	
Line 4	2,14	

4.3. Edit material properties

The next step in the model creation is to add material properties to the model. The access to the material properties is achieved by using the drop down list or the model tree. In the edit material dialog it is possible to set every material property required for the simulation. Material properties are not automatically assigned to a part. To add material properties it is necessary to select the main group of the property:

- General
- Mechanical
- Thermal
- Other

Access to the material properties:
Change to the property module – click in the menu on “material” and select “create” – fill in the material properties, see Figure 5 for examples

The model in the tutorial uses from the general group the density option (7850kg/m³) and form the mechanical group the elastic behaviour (Youngs modulus $2{,}1*10^{11}$MPa, v=0,3) and the option for plasticity. The window of the material properties and the values for the plasticity model are shown in Figure 5.

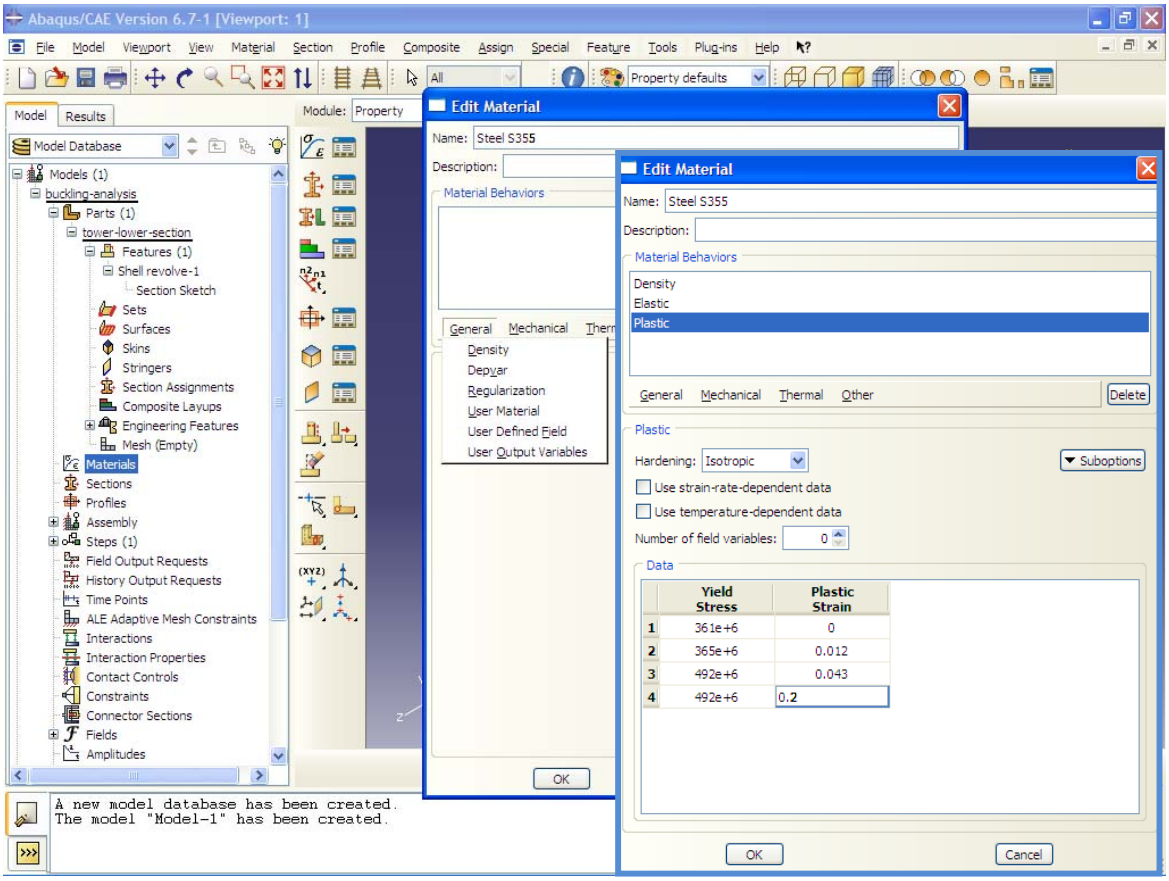

Figure 5: The material module and the plasticity model for the simulation

Example:
Add the Material properties mentioned in this chapter to the simulation model. For this use in the “edit material” window the general property “density” and from mechanical the “elastic” and the “plastic” option. Values for the plastic option are given in Figure 5

4.4. Create sections

Sections define the properties of a part. It is also possible to assign different sections to different regions of a part.

Create a section:
Change to the property module – click in the menu on “sections” and select “create” – select the type of the section and press continue – enter the requested properties to complete the section

The section is then assigned to the part or the region of the part. As an example the assignment of section 3 is shown in Figure 6.

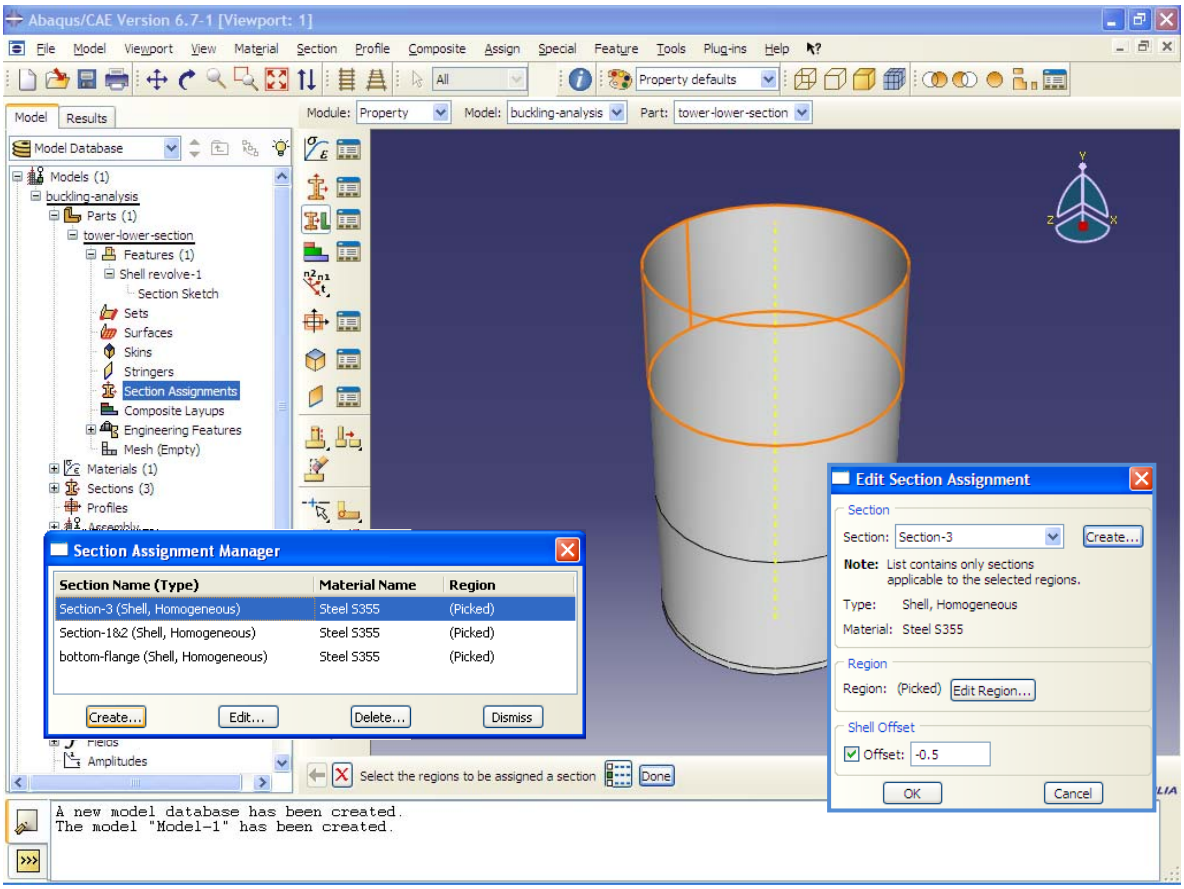

Figure 6: Section assignment on the example of section 3

Assign a section to the model geometry:
Change to the property module – click in the menu on “section” and selected “assignment manager” – click on create – select the region in the model where a section needs to be assigned – confirm the region and fill the “edit section assignment” form

Due to the use of shell elements it is possible to use an offset value. The offset defines on which side of the shell the material is orientated. By default is the offset zero which means that the material is symmetrical to the sketch of the geometry. If the outer side of the geometry is drawn it is necessary to enter an offset value.

Note:
An offset of 0,5 will generate the material thickness in positive direction of the shell normal. An offset of -0,5 will generate the material thickness in negative direction of the shell normal. Values smaller than -0,5 or bigger than 0,5 create the material thickness further away from the surface drawn in the sketch, the drawn surface becomes virtual with this. Values smaller than 0,5 or bigger than -0,5 create the material thickness proportional on both sides of the drawn surface. A value of 0 creates half of the thickness above and half of the thickness below the drawn surface.
If a surface apart from the middle surface is drawn it is necessary to know the direction of the shell normal. The shells normal direction is displayed as colour code which means that the direction of the shell normal is visualised in two different colours, how to access the shell normal is shown in Figure 7. The colour code uses brown as positive direction and purple as negative direction, due to this it is possible to set the offset value.

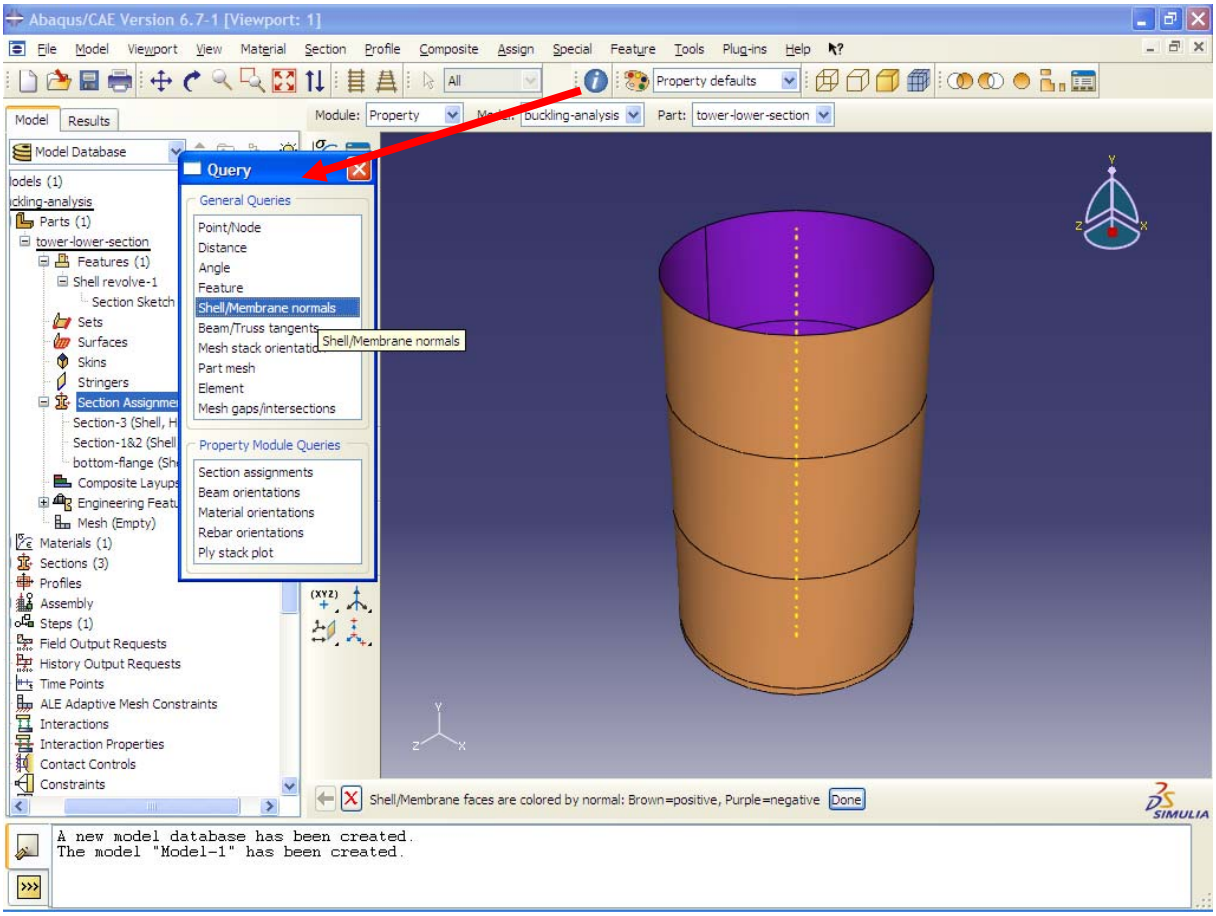

Figure 7: Displaying the shell normal

Example:
The model in the tutorial uses homogenous shell elements. The shell thickness varies in the model and due to this it is necessary to create several sections; the values for the sections are shown in Table 2

In the model for the tutorial it is necessary to create and assign two different sections. Follow the information presented in this chapter to create and assign sections to the model.

The geometry values given in a previous chapter represent the outer surface of the part, therefore it is necessary to add an offset with a value of -0,5.

Table 2: Suggested shell thickness for the tutorial model

Regions regarding to the lines used in the sketch for the geometry	Section name	Shell thickness
1 2 3	Bottom flange Section 1 Section 2	0,035
4	Section 3	0,030

4.5. Importing sketches

In some cases are CAD data available for geometries. One possibility of using them is to add them to Abaqus as a sketch. A sketch can be used for several procedures, in the model for the tutorial it was used to create a part, the stiffener, and a cut out in another part, the lower tower section. The procedure how to import a sketch is shown in Figure 8. The sketch needs to be available in a for Abaqus readable format, possible formats are sat, igs, dxf and stp. In a following step it is possible to scale the sketch, this is necessary if the units used for the model generation were not equal in Abaqus and the second party software.

Import a sketch:
Click in the menu on “file” – select “import” and “sketch” – select the directory where the sketch file is saved.

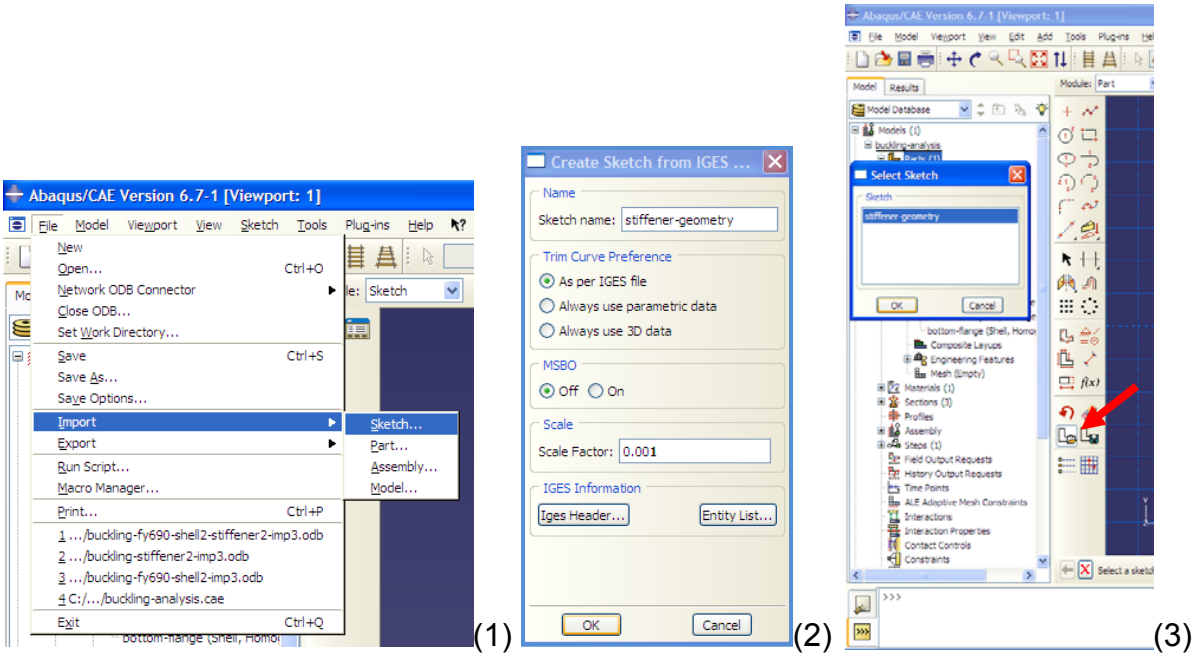

Figure 8: Import of a sketch from a native data format (1), scaling the imported sketch (2) and the import of the sketch to draw a part

The sketch is available in the part module after its import. In the part module the sketch can be imported to the screen were the sketch of the part is drawn. To do this the button “sketch” is to use marked with a red arrow in Figure 8 (3).

After this the sketch is displayed on the screen and it is possible to perform changes on it. When the work on the sketch is finished the procedure is finished with the button “done” and the window “edit base extrusion” opens where the depth of the geometry needs to be added to complete the part geometry.

Afterwards it is necessary to assign all properties to the part in the way it is shown for the lower tower section.

4.6. Creating datum point, axis or plane

For different actions in the model generation it is useful to create a datum. Examples for this are cut outs in the geometry or partitions.

Create a datum:
Change to the part module – click in the menu on “tools” and select “datum” – select the kind of datum which is needed for a following action and the type of creation which is easiest to achieve a datum – confirm by pressing enter or clicking on the done button

The model in the tutorial uses three datum planes and one datum axis. The xy- and the yz-datum plane are created by using the option “offset from principal plane” with an offset of zero. The third plane is generated with the same option but with an offset of 2,2. The datum axis is created by using the option “parallel to line, thru point”. The line is parallel the middle axis and goes thru the point at bottom of the structure. See Figure 9 to see the model after adding datum planes and axis.

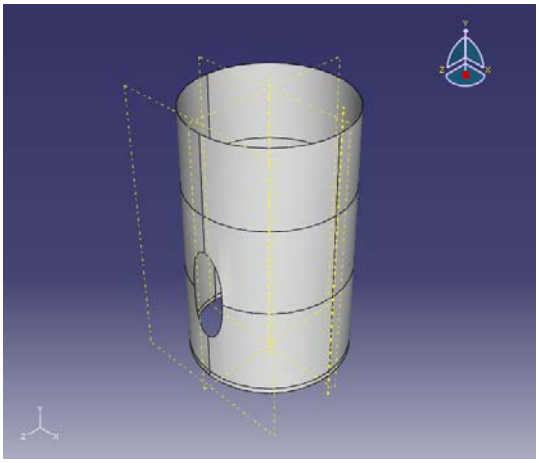

Figure 9: Model after adding datum planes and axis

To introduce the door opening into the model a cut out is necessary. This is done by using the option “create cut”. The option can be found in the button list using the part module. In Abaqus are several different options available to create cuts, the list is to see by holding the left mouse button pressed on the “create cut” field.
The cut used to create the door opening is an extruded cut. To create the cut it is necessary to choose a plane and an axis to define the orientation of the cut drawing area. If this is selected Abaqus changes to the sketch module and behaves like CAD software. In this tutorial was the geometry of the door opening added as a sketch imported from a drawing. The way to import a sketch is described in chapter 4.5 Importing sketches, how to import a sketch into the sketching area is shown in Figure 8 on the right hand side marked with(3).
To create the cut extrusion was the datum plane used which was placed with an offset outside of the geometry. The datum axis created is used as orientation for the cut extrude.
The sketch for the door opening has its own coordinate system so that it is necessary to calculate the correct position of the opening regarding to the drawing. If the original door geometry is not available freely chosen cut geometry can be used and placed in the sketch to add an opening.

The cut extrude is performed in the type “blind” therefore a value for the depth needs to be entered; the tutorial uses a value of 0.2.

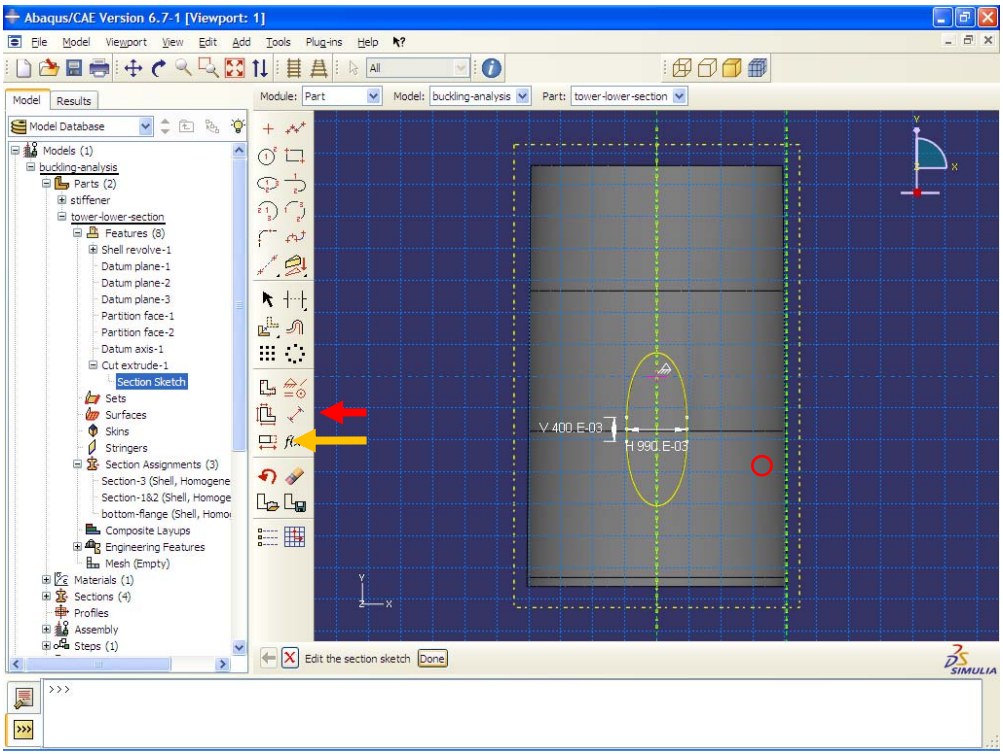

Figure 10: Adding the door opening to the model, the “add dimension” (red) and the “change dimension value” (orange) button

4.7. Create partition

Partitions allow meshing of different regions of the model with different mesh qualities, structures or elements. Changing the mesh from one partition to another can lead to a reduction of calculation time.

Create a partition:
Change to the part module – click in the menu on “tools” and select “partition” – select the type of partition and how to perform the partition – define the region which shall be partitioned – confirm the partition

Example:
The model in the tutorial uses two partitions; they are performed by using datum planes as partitioning tool. See Figure 11 to see the partitions used in the model.

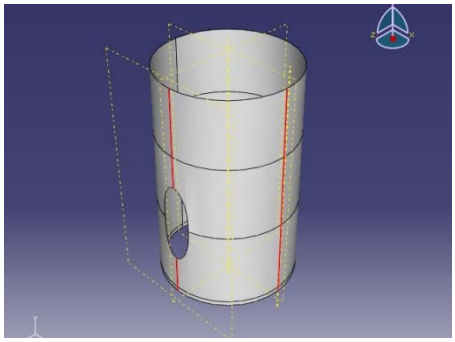

Figure 11: The partitions used in the model

4.8. Meshing the geometry

Before it is possible to calculate the structure it is necessary to divide the structure into finite elements. The elements in which the structure is divided are possible to change in some of their properties. Another aspect is the shape in which the structure is divided.

4.8.1. Mesh controls

The option of mesh controls offers the possibility to influence the shape of the elements used for the mesh. Another possibility is to change the between a free mesh with random element size and shape to a structured mesh which tries to arrange the elements to similar size and shape.

Creating mesh controls:
Change to the mesh module – click in the menu on “mesh” and select “controls” – select the region where mesh controls are desired - fill the mesh control dialog

The model in the tutorial uses structured mesh with quad-dominated structure.

4.8.2. Mesh elements

The way the processor treats the elements can be chosen in the menu “mesh elements”. It is possible to choose the geometric order of the elements and several more detailed properties. The right element type has to be chosen depending on the simulation. The elements, their different properties and their use in simulation are described in the manual of Abaqus.

Assignment of the element type:
Change to the mesh module – click on mesh in the menu and select “element type” – select the region where the element type shall be used - edit the element type dialog to achieve the necessary element properties.

Example:
The simulation in the tutorial uses S8R elements which are created by using quad elements and a quadratic geometric order.

4.8.3. Seeding and meshing the structure

The first step to divide the geometry into finite elements is to seed it. The seeds on the geometry are the start for elements created during the meshing. With the seeding it is possible to assign an element size into which the geometry is divided. Abaqus provides several different seeding tools.

To seed the complete structure in one step global seeds are used. This kind of seeding tries to create elements in similar size.

Global seeding:
Change to the mesh module – click in the menu on “seed” and select “part” – select the region which needs to be seeded – type the approximate global size of the elements

It is also possible to assign different mesh sizes to a region:
Change to the mesh module – click in the menu on “seed” and select “edge by size” – select the region which needs to be seeded – type the size of the element in the dialog

The model in the tutorial uses a global seed size of 0,1. The edge around the door opening is meshed with elements of a size of 0,05.

To mesh the part:
Change to the mesh module – click in the menu on “mesh” and select “part” – press enter or click on yes to confirm the meshing procedure

Note:
The procedure for other seeding tools is similar to the described methods.
It is possible to mesh on part or on instance. The decision if a part is meshed on instance or part is up to the user. If a part is used several times in an assembly and it is not necessary to mesh all of them in the same quality a mesh on instance is a possibility to avoid the use of another part.

4.8.4. Mesh verification

After the mesh is created it is possible to request mesh verification. The mesh verification analyses the quality of the mesh. If elements have a shape outside of defined boundaries they are marked in the model and it is up to the user to decide if a re-mesh is done.

Mesh verification:
Change to the mesh module – click in the menu on “mesh” and select “verify” – select the region for the mesh verification – press enter or the done button to confirm the selection – press “highlight” to display warnings or errors in the mesh.

4.9. The assembly module

4.9.1. Adding an instance

The parts which were created in a previous chapter need now to be assembled. Parts are added to the assembly as instances.

Add an instance to an assembly:
Change to the assembly module – click in the menu on instance and select create or double click on instance in the model tree – add the part from the list which needs be added

Note:
If it is the first part in the assembly the screen will be empty before a part is added.
It is possible to use an auto-offset form other instances, this is useful if all parts are drawn at the origin of part coordinate system.
A suggestion for the case of more instances is that one instance after another is added to the assembly.

4.9.2. Create positioning constrains

Positioning constraints are used to position parts to each other. The position constraint has just an optical influence on the model and no influence on the result. By default Abaqus displays the part which, is added as instance to assembly, at the position where it is positioned in the part coordinate system. For the displaying of the model and for the visualisation of the results it is recommended that the parts are positioned.
The positioning constraints are similar to the options offered in CAD software.

Positioning of an instance:
Change to the assembly module – click in the menu on constraint and select the constraint which shall be used

In the model for the tutorial the stiffener is positioned by using the coincident point option. See Figure 12 for the positioning of the stiffener in the model.

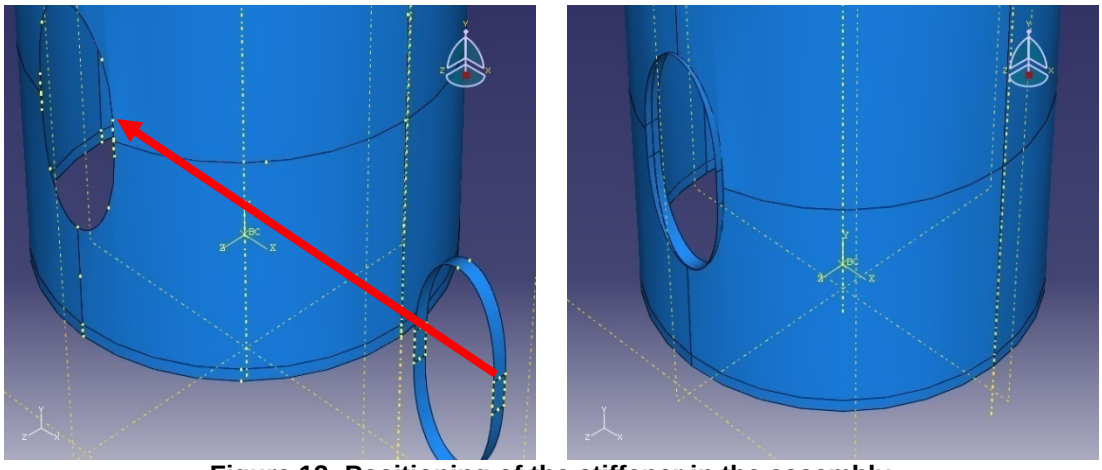

Figure 12: Positioning of the stiffener in the assembly

4.9.3. Creating a reference point

It is possible to add reference points in the part and in the assembly. Limitation is that in the part module it is only possible to place one reference point whereas in the assembly module it is possible to create more points. Reference points can be used for several different actions.

Creating a reference point:
Change to the assembly module – select from the menu “tools” and click on reference point – select a reference point by clicking on an existing point or enter coordinates for a point

The model in the tutorial uses two reference points, one on the top and one at the bottom of the structure. The coordinates suggested for the reference points are printed in Table 3.

Table 3: Coordinates for the reference points

Name of the RP	Position of the RP in the model	x-coordinate	y-coordinate	z-coordinate
Load	Top of the structure	0	8	0
BC	Bottom of the structure	0	0	0

4.10. Constraints

4.10.1. Tie constraint

The tie constraint connects two surfaces of two different parts with each other. The connection is performed by tying nodes of the mesh. For further details regarding tie constraints the chapter in the manual of Abaqus is recommended.

Create a tie constraint:
Select the interaction module and select create from the constraint menu or double click on constraints in the model tree – select coupling from the list and click on continue – select master and slave surface in the order Abaqus requests them – fill out the edit constraint dialog

The model for the tutorial uses the edge on the tower shell as master surface and the stiffener surface as slave. The slave surface is not adjusted to the initial position; the check has to be removed. See the tie constrain in Figure 13.

Note:
The mesh of the surface which is selected as slave surface needs to have a finer mesh than the master surface. If this is not observed a message will be written in the monitor and in the message file. The reason for the finer mesh on the slave surface is the position tolerance. Nodes which are outside the position tolerance are not tied to the master surface therefore a finer mesh on the slave surface is necessary. This will be noted in the monitor as warning but is not influencing the result of the simulation. It is in the responsibility of the model creator that necessary nodes are within the position tolerance to achieve interaction between the parts.

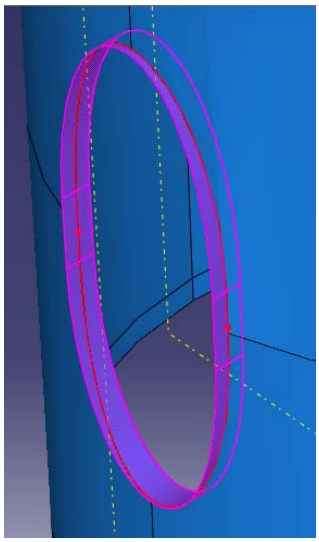

Figure 13: The tie constraint

4.10.2. Coupling constraint

The coupling constraint is used between the reference points where later on the loads and boundary conditions are applied. The coupling constraint connects reference point and the selected surface rigid with each other.

Create a coupling constraint:
Select the interaction module and select create from the constraint menu or double click on constraints in the model tree – select coupling and click continue – select a reference point and a surface to which it is connected – fill out the edit constraint dialog – press ok

Example:
The model for the tutorial uses two coupling constrains, one for the load and one for the boundary condition. Therefore, it is necessary to do the procedure twice. See Figure 14 for the finished coupling constrain on the bottom of the model.

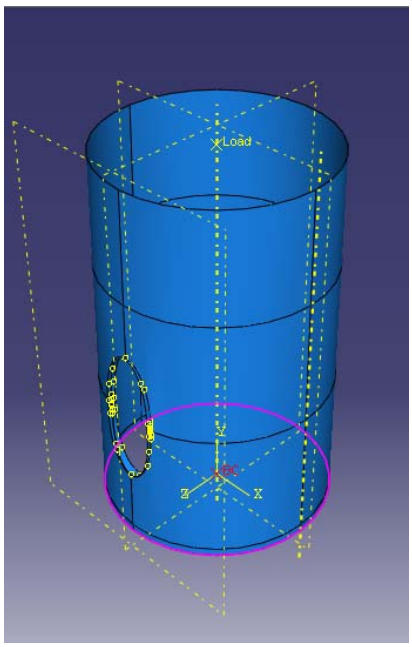

Figure 14: Finished coupling constrain at the bottom of the model

4.11. The step module

The step module describes which kind of analysis is performed. A step is necessary to create loads and boundary conditions.

Create a step:
Change to the step module – click in the menu on step and then on create or double click on step in the model tree – select the analysing step in the window which opens and continue – settings depending on the step can be done – click on ok to accept the settings, the step is created and listed in the model tree

Example:
The model in the tutorial uses two steps; the first step is a buckling analysis of the structure. To create a buckling analysis select in the create step window under procedure type “linear perturbation” select then “buckle”.
In the edit step window the number of requested eigenvalues can be selected, also the type of solver can be chosen. The model for the tutorial requests four eigenvalues and uses the Lanczos solver.

Note:
For the case that a solver in a buckling analysis is not able to find a solution, a change of the solver can help to get results.

4.12. Loads and boundary conditions

To add loads and boundary conditions to the model change to the load module.

Adding a load to the model:
Select load in the menu – create load – select the type of the load and in which step it is applied onto the model – click continue – select a point/edge/surface on which the load is applied – fill out the “edit load” form

Adding a boundary condition to the model:
Select BC in the menu – select the type of the boundary condition – selected the region of the boundary condition – fill out the “edit boundary condition” dialog

The model in the tutorial uses three forces and two moments which are applied in the upper reference point, see suggested values in Table 4. The boundary condition is applied in the second reference point at the bottom of the model and uses the “ENCASTRE” condition to lock all degrees of freedom.

Table 4: Suggested values for load of the model in the tutorial

Axis	Force [kN]
1-direction	30
2-direction	-3000
3-direction	800
	Moment [Nm]
1-direction	60000
2-direction	1500

4.13. The key word editor

The key word editor displays in text form the model properties. Changes in the keyword editor are therefore easily and fast realised.

Some commands are not supported in Abaqus CAE. Because of this it is necessary to add them through the keyword editor.

To access the keyword editor click in the menu on “model”, “edit keywords” and select the model where changes or additional lines are necessary.

The model in the tutorial needs an additional line. The fact that the analysis of the model is performed in two separate analyses makes it necessary to write the result of the buckling analysis to a text file. The output of a buckling analysis is normalised displacement of the eigenmode shape.

The displacement of every node is written into a text file using the command:
**nodefile*
U

The letter U stands here for the displacement of nodes. Several more commands are available and described in the user’s manual of Abaqus.

The line is added at the end of the keyword editor, see Figure 15

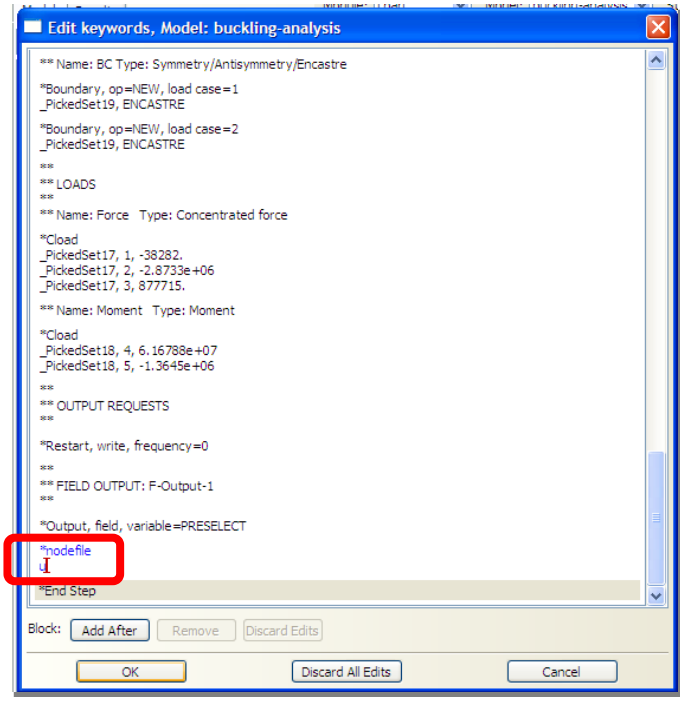

Figure 15: Keyword editor window with added command

More changes in the keyword editor are necessary in the second analysis step which is described later in the tutorial.

For more information regarding the keyword editor and possible additional command lines check the user’s manual.

4.14. The job module

The creation and analyses of a job are done in the job module. It is possible to create a job by selecting “create job” from the menu or by double clicking on job in the model tree.

To create a job it is necessary to select the source. The source can be a model which is listed above in the model tree or an input file. The job name will be used for the naming of all files Abaqus is creating during the calculation process.

In the “edit job” window settings regarding the submission and the memory can be selected. In the field submission the time when Abaqus starts to run the analysis can be set. This option is useful if simulations are performed while the user is not available. If several simulations shall start after another it is necessary to know how long one calculation takes.

Depending on the size of the simulation model it is recommended to allow Abaqus to use more memory than the standard value. If the memory is too small Abaqus cannot perform simulations and aborts the process.

Example:
The simulation in this tutorial uses 1024MB of the memory.

4.15. Submitting a job to the processor

To submit a job to the processor two ways are possible. One is to click with the right mouse button on the job name in the model tree and to select “submit” from the list. Another way is to go through the menu, click on “job” and then on “submit”, choose the job which shall be analysed.

In the same way it is possible to select the option “monitor”. The monitor displays the progress of the simulation, prints warning and error messages.

Another possibility which is interesting is, if Abaqus is used on a local computer to create the model but a server is used to run the calculation. It is possible to create input files which contain all model information. The “write input” is also accessed through the job menu or by clicking on the job name in the model tree. In this case all data are written to the input file but no analysis starts. The input file is possible to transfer to another computer where the analysis is performed. If the graphical interface of Abaqus CAE is used it is necessary to create a job which reads the data from the input file. The procedure for this is described in the chapter 4.14.

5. Creating a similar model for further analysis

The following chapter describes how to change an existing model to a model with the same properties but with changed analysing steps and with an edit in the keyword editor. This is done for an example continuing the analysis presented in the previous part of the tutorial. The buckling analysis presented delivers not the results usually requested therefore it is necessary to continue with a second step.

The first step is to copy the existing model to a new model. To do this click with the right mouse button on the model and select “copy model”. The command opens a window, which requests a model name. After confirming the new model name a second model with equal properties is generated.

After a buckling analysis it is possible to continue with different steps. If the ultimate load of the structure is requested it is necessary to continue with a “static, riks” analysis. This analysis type uses the load entered in the load model as a start point for the simulation and loads the structure above this load. Also a decrease of the load beyond the maximum is possible so that an ultimate load of the structure can be found. This analysis is shown in the tutorial. Another possible step is the “static, general” analysis, here the load entered in the load module is applied on the structure and results are provided. If the load entered in the load module is higher than the load the structure can bear the simulation will abort.
For further information about steps and their use see the description in the manual.

To replace an analysing step:
Change to the step module – click in the menu on “step” and select “replace” – if a model uses several steps selected the step to replace – select the step to perform in the analysis – edit the requested information in the edit step dialog – confirm with clicking on ok

Example:
The model in the tutorial replaces the “buckle” step with a “general, riks” step. The option “nlgeom” is activated and in the field incrementation the maximum number of increments is set to 30.

Because of the change of the step an edit in the keyword editor is necessary. The command added in the buckling analysis is not available in this analysing step and causes a conflict error. This error is marked in the keywords but no notice in another way is given to the user. For the case that a job is submitted without removing the conflict error message the job will abort and no specific message is delivered what can be done to avoid the abort.

To remove the wrong parts open the keyword editor and delete the lines marked on the left side in Figure 16.

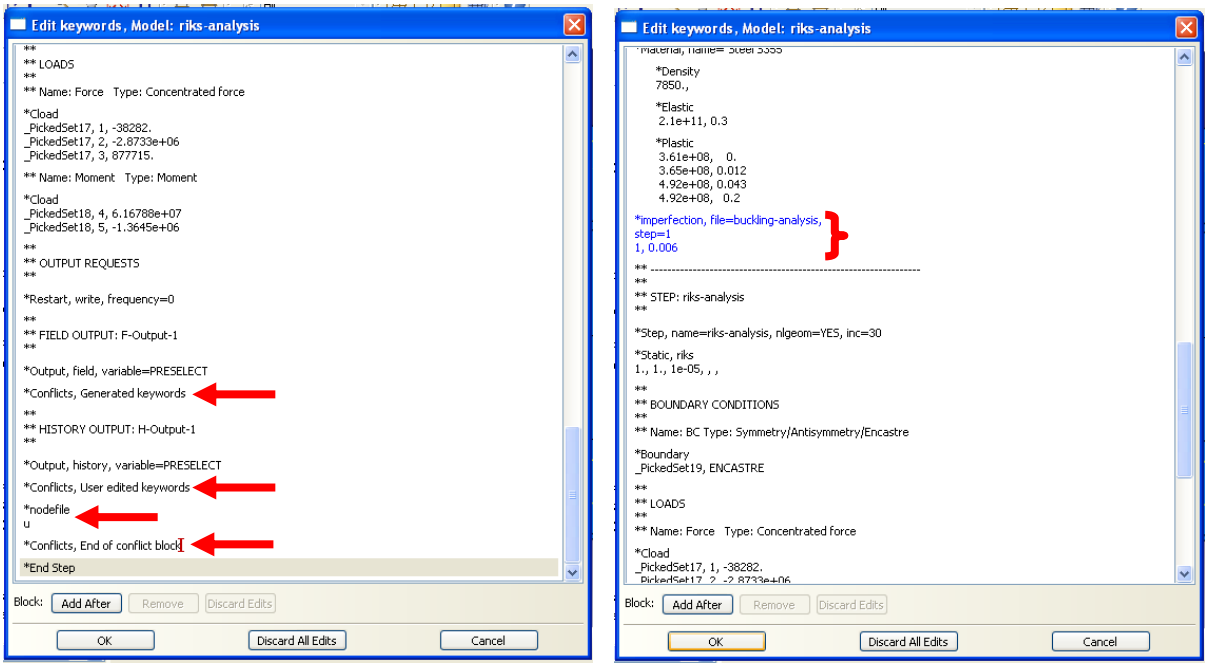

Figure 16: Lines to delete in the keyword editor are marked in the left picture and the position of the imperfection command is marked in the picture on the right

Abaqus offers the possibility to use the deformed shape calculated in the buckling analysis to introduce imperfections into the simulation. The necessary lines to introduce imperfections are marked on the right side in Figure 16.

The place where the lines are added is before the step starts. A placement at another position can cause an abort of the simulation.

The denotation of the introduced lines:

**imperfection*	Command used in Abaqus to introduce imperfection
file=……,	Indicates the file name which includes the result from the previous buckling analysis. The file name is the job name used in the simulation before
step=1	Indicates the step number where the results for of the buckling analysis were achieved. The initial step is not counted.
1,	Indicates the eigenmode used to achieve the deformed shape.
0,006	Imperfection scaling factor. The value entered here is proportional to the maximum deformation in the eigenmode shape, all other values from the eigenmode shape follow proportional to it.

6. Analysis of the results and visualisation

In the visualization module it is possible to access all results and to get print-outs of the model in deformed shape. Some basic commands are explained in this chapter. The presented commands are used to achieve the data extraction needed for the evaluation shown in the report.
The results can be accessed by opening the odb file in the common way of opening a file like in any other software. A second way is to click with the right mouse button on the job from which the results are requested and then select “results” in the list. The second way is only possible if the files are located in the working directory. The odb file (output database) contains all results requested by the user. By default is the output database opened in the read only mode. If the odb file is opened thru “file”, “open” in the menu it is possible to select the read and write mode. In this mode it is possible to save created paths or coordinate systems to the file.
Figure 17 shows the visualisation screen and the window for changing the deformation scale factor.

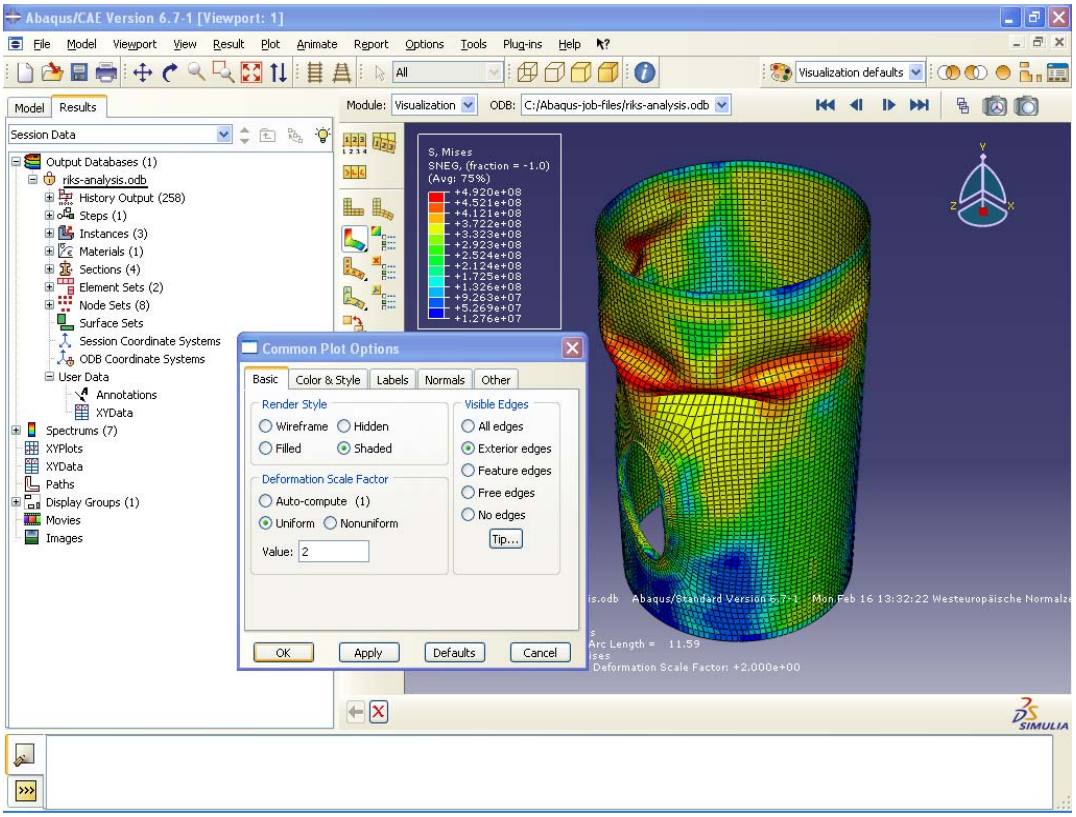

Figure 17: Visualisation screen with opened window for changing the deformation scale factor

<u>The deformation scale factor:</u>
Change to the visualisation module – click on options and select common – in the field basic it is possible to choose between the auto-computed and a self selected deformation scale factor

<u>Changing the colour code:</u>
Change to the visualisation module – click on options and select contour – go to the field “limits”, here it is possible to specify the limits for the colour code. Also it is possible to get information at which node the maximum or minimum value of the requested variable is achieved, the position is marked in the viewport.

To access the applied load in every step:
In the model tree click on history output – select lpf (load proportionality factor), right click on “save as“ to add it in the xy-data list
All xy-data are listed in the model tree and can be accessed by double clicking on them.

Create a path for data extraction:
Change to the visualisation module – click on tools and select path – create path – create from node list – selected the instance on which the path is created and add the nodes by entering their number or by picking them from the viewport.

Request data values from the odb file:
Change to the visualisation module – click on tools and select xy-data – create – source odb-field output – continue – choose under Variables “position – unique nodal” and select the spatial displacement in 3 direction - change to Elements/Nodes and click here under methods on “node sets”, in the box right of it is possible to select the reference point for the load.

Change to the visualisation module – click on tools and select xy-data – create – source path – in the field data extraction select the path from which the data shall be extracted – select the value which will be plotted on the x-axis in the field x-values – in the field y-values it is possible to select the output variable and the step or frame from which the data will be extracted.

Print the requested data into a report file:
Change to the visualisation module – click on report and select xy-data – in the field xy-data select the xy-data which shall be added to the report file – change to the setup field, here it is possible to change the name of the report file and to change the output format of it – by clicking on ok the report file will be saved into the working directory – the report file is a text file which can by imported to second party software
Note: Abaqus exports the data in American/British style (dot and comma have the oppositional denotation). This fact makes it necessary to add this information while transferring the data to European standards.